Institut für Medizinische Genetik und Humangenetik

der Medizinischen Fakultät Charité – Universitätsmedizin Berlin

DISSERTATION

A recurrent homozygous mutation affects the *BUD13* gene whose residual expression correlates with the severity of a novel human progeroid disorder

zur Erlangung des akademischen Grades

Doctor of Philosophy (PhD)

vorgelegt der Medizinischen Fakultät

Charité – Universitätsmedizin Berlin

von

Namrata Saha

aus New Delhi

Datum der Promotion: 03.12.2021

Foreword

The experimental procedures and results included in the given thesis report have had valuable contributions from several contributors. The author of this thesis report, Namrata Saha, gratefully acknowledges the efforts of all the contributors.

Currently, a journal paper is underway summarising the findings from this thesis report. Namrata Saha is a first co-author who contributed equally to the work-

Uwe Kornak, Namrata Saha, Boris Keren, Alexander Neumann, Ana Lisa Taylor Tavares, Juliette Piard, João Guilherme Rodrigues Alves, Ana Berta Sousa, Miguel Rodriguez De Los Santos, Marten Jäger, Jean T. Pantel, Thatjana Gardeichik, Naji El Choubassi, Beatrix Fauler, Thorsten Mielke, Jochen Hecht, David Meierhofer, Tim M. Strom, Lars Wittler, Malte Spielmann, Alexis Brice, Stefan Mundlos, Aida Bertoli-Avella, Peter Bauer, Florian Heyd, Odile Boute, Juliette Dupont, Christel Depienne, Lionel van Maldergem and Björn Fischer-Zirnsak. **Alternative splicing of *BUD13* determines the severity of a progeroid lipodystrophy syndrome.**

Additionally, the findings from this thesis report have been presented as a part of conference appearances as poster/ talk as also outlined in the statutory declaration-

Namrata Saha, Björn Fischer- Zirnsak, Boris Keren, Michael Thelen, Mohammed Al-Bughaili, Claire Schlack, Ulrike Krüger, Jochen Hecht, Malte Spielmann ,Lionel Van Maldergem, Christel Depienne, Uwe Kornak. **Corrective alternative splicing events in a novel segmental progeroid disorder.**

Table of Contents

List of Figures and Tables

List of Abbreviations

RT-PCR	Reverse transcription-Polymerase chain reaction
qPCR	Quantitative polymerase chain reaction
IF	Immunofluorescence
IR	Intronic Retention
IDP	Intrinsically Disordered Protein
RES	pre-mRNA REtention and Splicing Complex
HGPS	Hutchinson-Gilford Progeria Syndrome
mESC	Mouse Embryonic Stem Cell
MEF	Mouse embryonic fibroblast
RP	Retinitis Pigmentosa
PBS	Phosphate Buffered Saline
DDR	DNA Damage Repair
ROS	Reactive Oxygen Species
BSA	Bovine Serum Albumin
DNA	Deoxyribonucleic Acid
cDNA	Complementary DNA
RNA	Ribonucleic Acid
TEM	Transmission Electron Microscopy
GAPDH	Glyceraldehyde 3-phosphate dehydrogenase
ATP	Adenosine triphosphate
SDS	Sodium dodecyl sulphate
SA-βgal	Senescence-Associated β-galactosidase
snRNP	Small Nuclear ribonucleoprotein

Abstract

Human progeroid disorders tend to mimic aspects of physiological ageing seen in humans that include disruption of various cellular functions. Amongst molecular processes, alternative splicing events generating truncated pathogenic variants are previously implicated in progeroid disorders such as Hutchinson-Gilford Progeria syndrome. In eukaryotic spliceosome, correct splicing is ensured by the interplay of splicing factor proteins. The retention and splicing (RES) complex is a heterotrimer involved in splicing processes that prevents nuclear pre-mRNA leakage and is highly conserved from yeast to other higher organisms. However, the function of its components are poorly understood in mammalian development.

In this study, we identified a homozygous nonsense mutation affecting a RES component BUD13 in five individuals diagnosed with a complex progeroid disorder. The disease is characterised by growth restriction, lipoatrophy and early demise in three individuals of an unidentified cause. The C- terminal region of BUD13 is specifically associated with splicing activity. Upon investigation of human adult fibroblasts from patients, the pathogenic variant was observed to induce alternative splicing of the *BUD13* pre-mRNA, producing a truncated but stable protein carrying an in-frame deletion at the N-terminal. A lower expression level of the truncated variant correlated with shorter life expectancy of the individuals and also with a higher degree of mitochondrial perturbation, nuclear aberration, impaired proteostasis and early cellular senescence. However, upon whole transcriptome analysis of fibroblasts from affected individuals, very few pre-mRNA or nascent transcripts were found to be misspliced. Modeling of the exact human mutation in mice using CRISPR/Cas9 also caused alternative splicing to produce an in-frame deleted Bud13 variant (Bud13-106del). A second mouse model carrying frame shift mutation at the N-terminus also led to the generation of an alternatively spliced out product (Bud13-113del). The Bud13-113del variant interestingly gave rise to viable chimeric mice that eventually displayed some major aspects of the human disease including progressive lipoatrophy and early demise. In both the mouse models, reduced expression of the Bud13 protein caused early embryonic lethality as has also been shown previously for loss-of-function of Bud13 in zebrafish.

Altogether, the N-terminus of BUD13, not present in yeast, truncated by the variant detected in the affected individuals is much less conserved than the C-terminus, suggesting that this part of the protein could have acquired additional functions during evolution. Our findings indicate that the protein and its N-terminus, governing various cellular functions and senescence, are critical candidates for future studies to understand physiological ageing in humans.

Zusammenfassung

Humane progeroide Erkrankungen ahmen Facetten des physiologischen Alterns des Menschen nach und häufig treten dabei Beeinträchtigungen zellulärer Strukturen. Bisher wurden bezüglich zugrundeliegender molekularer Prozesse insbesondere alternative Spleißvorgänge, die verkürzte pathogene Varianten erzeugen, bei progeroiden Störungen wie dem Hutchinson-Gilford-Syndrom in Betracht gezogen. Für ein korrektes Spleißen im eukaryotischen Spleißosom sorgt das Zusammenspiel einer Vielzahl Spleißfaktoren bezeichnet werden. Der Retentions- und Spleißkomplex (RES) ist ein Heterotrimer, welches an Spleißprozessen beteiligt ist und von Hefen bis zu anderen höherentwickelten Organismen hoch konserviert ist. Die Funktion seiner Komponenten sind jedoch bei der Entwicklung von Säugetieren nur unzureichend verstanden.

In dieser Studie haben wir bei fünf Personen, bei denen eine komplexe progeroide Störung diagnostiziert wurde, eine homozygote Nonsense-Mutation identifiziert, die eine RES-Komponente BUD13 betrifft. Diese ist gekennzeichnet durch Wachstumseinschränkungen, einer Lipoatrophie und dem frühen Ableben von drei der fünf Individuen. Die C-Terminalvon BUD13 ist von entscheidender Bedeutung für die Spleißaktivität. Bei der Untersuchung der menschlichen, reifen Fibroblasten der Patienten wurde beobachtet, dass die pathogene Variante ein alternatives Spleißen der BUD13-prä-mRNA induziert und ein verkürztes, aber stabiles Protein mit einer in-frame-Deletion am N-Terminus produziert. Ein niedrigeres Expressionsniveau der verkürzten Variante korrelierte mit einer kürzeren Lebenserwartung der Individuen und auch mit einem höheren Grad an mitochondrialen Störungen, nuklearen Aberrationen, gestörter Proteostase und früher zellulärer Seneszenz. Allerdings wurde bei der Analyse des gesamten Transkriptoms der Fibroblasten der Betroffenen festgestellt, dass nur sehr wenige die prä-mRNA oder die naszierenden Transkripte falsch gespleißt wurden. Die Imitation der humanen Mutation mit CRISPR/Cas9 führte auch zu alternativem Spleißen und zwei in-Frame-deletierten Bud13-Varianten (Bud13-106del und Bud13-113del) im Mausmodell. Die Bud13-113del Variante brachte interessanterweise Maus-Chimären, die letztendlich einige wichtige Aspekte der menschlichen Krankheit zeigten, darunter fortschreitende Lipoatrophie. In beiden Mausmodellen verursachte die verminderte

Expression des Bud13-Proteins eine frühe embryonale Letalität, wie zuvor auch für den Funktionsverlust von Bud13 bei Zebrafischen gezeigt wurde.

Alles in allem, die N-terminale Region von BUD13, die in Hefen nicht vorhanden ist und die von der in den betroffenen Individuen entdeckten Variante verkürzt wird, ist viel weniger konserviert als die C-terminale Region. Unsere Ergebnisse deuten darauf hin, dass das Protein und sein N-Terminus, die verschiedene Zellfunktionen und die Seneszenz steuern, entscheidende Kandidaten für zukünftige Studien zum Verständnis des physiologischen Alterns beim Humanen sind.

Chapter 1: Introduction

1.1. The Inevitable Course of Physiological Ageing

Ageing, as the time-dependent process of progressive waning of one's physiological being, is accompanied by an increased frailty and vulnerability to death in most living organisms. The pace & shape of ageing displayed throughout various species across the tree of life (Darwin, 1859) have been of immense interest to mankind for centuries. Variability in the same owing to confounders ranging from genetic & environmental backgrounds to organismal complexity are not unheard of. Lifespans can be of the order of a few minutes in the simplest prokaryotes up to hundreds of years as seen in a mammalian species such as the bowhead whale (Johnson A et al., 2019). For human lifespan, at large, the average life expectancy with the availability of better health systems has witnessed an increase over the last centuries (Folgueras et al., 2018) drawing a larger focus on its genetic/biological bases.

At the very macroscopic level in humans, ageing is typically recognised by the gradual loss of muscle mass & agility, progressive decline in hearing ability, loss of vision, development of wrinkles, loss and greying of hair, and arthritic inflammation and a marked higher risk of developing cancer, heart diseases, and neurodegeneration. Hence, it does not come as a revelation that at the microscopic cellular level or the more complex molecular level, physiological ageing is governed by an amalgam of processes underlying the vast plethora of tissue level signs and symptoms as previously described.

Growing evidence has repeatedly indicated ageing as the primary risk factor for the development of complex disorders such as cardiovascular diseases, diabetes, cancers, and neurodegenerative diseases (Lopez- Otin et al., 2013). As a result, elucidating the pathologies underlying these diseases has become an important aspect of ageing and its associated investigations.

1.2. Cellular manifestations of physiological ageing

A prominent representation of cellular ageing include various layers of progressively decelerating operative mechanisms at the genetic and molecular level. While the genomic integrity and stability are continually challenged by exogenous physical, chemical and biological agents, endogenous threats such as faulty DNA replication, defective repair mechanisms, perturbed nuclear architecture and a buildup of mitochondrial stress also contribute towards cellular stress.

1.2.1. Accumulation of cellular damage

The accumulation of cellular damage is a common factor governing chronological ageing with DNA damage and mutation accumulation as primary drivers of the process (Somatic Mutation theory of Ageing, Szilárd, 1959). The accumulation of genetic lesions such as point mutations, translocations, and gene disruptions arising from extrinsic or intrinsic damage tend to be minimised by a complex network of DNA repair mechanisms working to recover nuclear DNA from damage. However, an accumulation of such damage over a timeline of physiological ageing is inevitably capable of affecting essential genes and transcriptional pathways resulting in dysfunctional cells, ultimately jeopardizing tissue and organismal homeostasis. Indeed, deficiencies in repair mechanisms have shown to lead to accelerated ageing or progeroid syndromes such as Cockayne syndrome and Werner syndrome, discussed in subsequent sections.

Additionally, as organisms age with due course of time, the diminishing efficiency of the mitochondrial respiratory chain leads to reducing ATP generation and an increased production of reactive oxygen species. The process forms a continuous cycle of events that only further deteriorates the mitochondria causing extensive global cellular damage (Free radical theory of ageing, Harman, 1956).

1.2.2. Cellular senescence

Cellular senescence describes as an irreversible state of permanent cell cycle arrest often brought about because of genotoxic stress (Loaiza and Demaria, 2016). Hayflick using human fibroblasts under serial passaging in culture (Hayflcik and Moorhead, 1961) first described the phenomenon. Marked by both phenotypic and transcriptional

heterogeneity, transcriptome programs underlying senescence vary depending on cell type and the kind of stress it undergoes (Hernandez-Segura, A et al., 2017). For instance, a diminishing production of immune cells responsible for adaptive immunity causing immunosenescence are attributed to myeloid malignancies (Shaw et al., 2010).
Several non-exclusive markers of senescence include constitutive DNA damage response signaling, senescence-associated β-galactosidase (SA-βgal) activity, and increased expression of cyclin-dependent kinase inhibitors p16INK4A (CDKN2A) and p21CIP1 (CDKN1A) amongst others (Loaiza and Demaria, 2016).

1.2.3. Telomere attrition

Terminal ends of linear DNA molecules can undergo replication only in the presence of a special DNA polymerase called telomerase. However, most mammalian somatic cells do not express the enzyme due to which telomeric regions are susceptible to age-related deterioration from chromosome ends (Blasco, 2007), a process called as telomere exhaustion or telomere attrition. It explains the limited proliferative ability of cells cultured in-vitro that tend to undergo replicative senescence or in other words, attain the Hayflick limit (Hayflcik and Moorhead, 1961). Additionally, nucleoprotein complexes called shelterins (Palm and de Lange, 2008) conceal telomeres. Rightly called so as they shield telomeres from repair machineries, shelterins result in recurrent DNA damage to telomeric ends causing detrimental results including senescence (Fumagalli et al., 2012). Hence, telomere shortening occurs concomitantly with cellular ageing, both as a cause and effect simultaneously, and as a result forms an important factor for stem cell decline in ageing tissues.

Both cellular senescence and telomere attrition reflect components of a larger machinery of cellular ageing where impaired stem cell division is an integrative consequence of multiple types of damage.

1.3. Human Progeroid Disorders: Accelerated ageing

A major challenge in the domain of mammalian ageing research, at the molecular level, has been the dissection of interconnectedness between various hallmarks of ageing and their relative contributions. The availability of animal models emulating the ageing process in humans has only been partly instrumental in bridging the research gap due to evolutionary inter-species differences. In this light, placed at nearly the opposite end of the spectrum of physiological ageing, are the **'Human Progeroid Disorders'**. They tend to recapitulate hallmarks of physiological ageing (figure1, Carrero et al., 2016), thereby offering alternatives to study isolated hallmarks of ageing by shedding light on the mechanisms underlying the pathogenesis of these diseases.

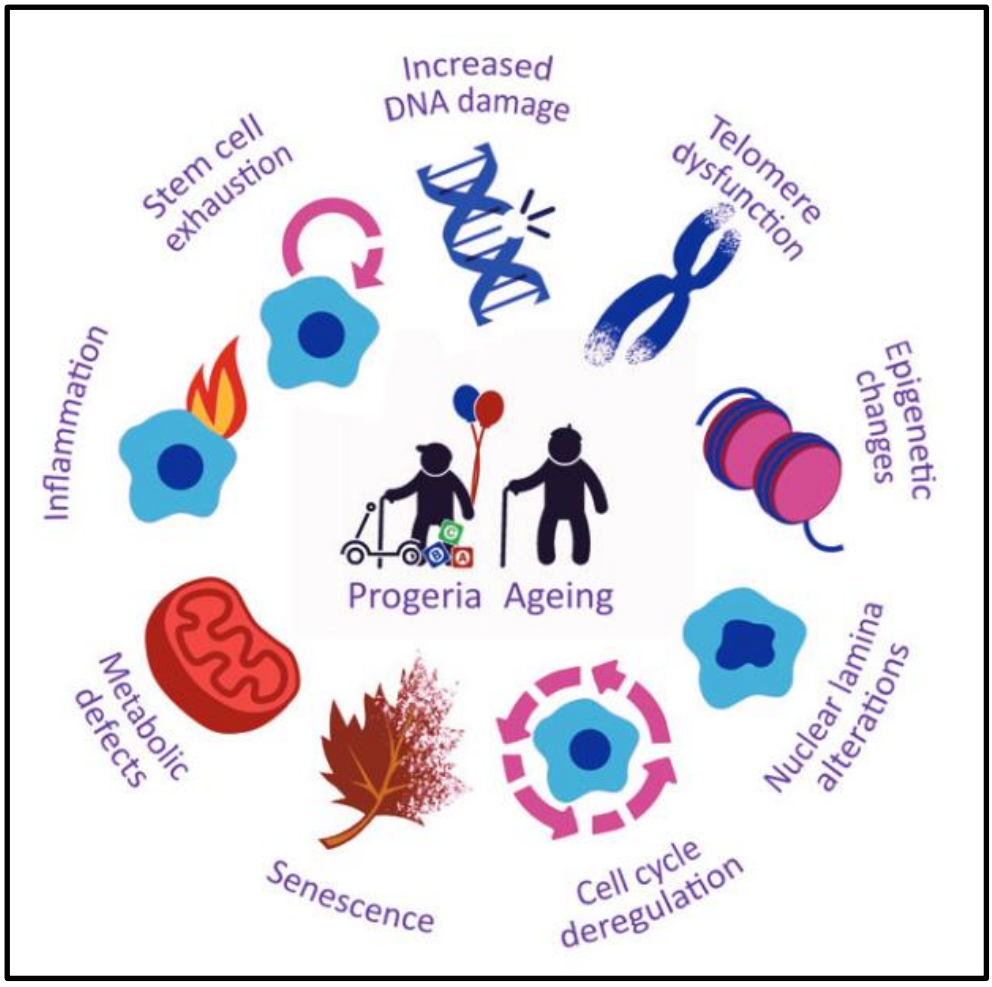

Fig.1. Various molecular and cellular hallmarks of human progeroid syndromes that tend to represent signs often visible in physiological ageing. Adopted from Carrero et al., 2016.

Progeroid or progeria-like disorders may be prudently referred to as premature ageing diseases. They represent diseases that tend to mimic, in part, but may differ from normative ageing as seen in the general human population. Individuals suffering from such a disease seemingly exhibit, to a certain degree, complications typical of old age at a very early stage in life. Investigations aimed at probing such accelerated ageing are instrumental towards understandings of natural models of more specific isolated hallmarks of ageing. Thus, explicating the molecular details and associated patho-mechanisms of novel progeroid disorders becomes interesting in the light of understanding better the rather complex process of ageing. This thesis aims to uncover the molecular anomalies underlying one such novel and complex progeroid disorder.

Human progeroid disorders are often classified into two categories: **Segmental** disorders that represent multisystemic diseases affecting several organs and tissues. Some well-studied examples are Hutchinson-Gilford Progeria syndrome (HGPS or Classical Progeria), various types of cutis laxa (Kornak,U. 2009), Cockayne syndrome (Batenburg et al., 2015) and Werner syndrome (Martin, G.M.et al., 2000). Unimodal disorders, on the other hand, primarily affect a single organ or tissue (Martin and Oshima., 2000) , such as monogenic Alzheimer type dementias.

Fig.2. Image of a girl (17-year-old) with Hutchinson-Gilford Progeria Syndrome (HGPS). Adopted from Miyamoto, M.I. et al, 2014.

A more recent classification categorises the progeroid diseases into two separate sets depending on the underlying molecular pathway: the first group consists of those progeroid diseases, which are recognised by anomalies in the components of the nuclear envelope (eg. HGPS) and the second one is characterised by defects in genes involved in the DNA damage repair pathway (eg. Cockayne Syndrome) (Carrero et al., 2016). Although a vast number of progeroid disorders do exhibit these hallmarks of ageing as the fundamental pathologies, it is noteworthy that such a classification system tends to exclude progeroid disorders recognised by antagonistic hallmarks (*Carlos Lopez- Otin et al., 2013)* of ageing and do not display either of the pathologies. The cutis laxa disease spectrum, for instance, includes a number of syndromes with varying underlying genetic mutations affecting other subcellular organelles and processes, such as the retrograde Golgi trafficking (Kornak U et al., 2008, Fischer B et al., 2012) and the mitochondrial structure (Ehmke et al., 2017).

1.4. General Mechanisms of Progeroid Disorders

1.4.1. Irregular Nuclear Architecture

A common feature of several progeroid disorders has been irregularities in nuclear organisation and unstable nuclear envelope, in turn causing genome instability (Dechat et al., 2008). A well understood example is the Classical, HGPS, most cases of which are characterised by a recurrent heterozygous silent mutation in *LMNA* causing the aberrant splicing of lamin A and leading to the production of a toxic protein called progerin; the association of progerin with the inner nuclear membrane is detrimental for nuclear shape and function (Goldman R et al., 2004). Interestingly, progerin has also reportedly been detected in healthy ageing individuals (Righolt et al., 2011; Scaffidi and Misteli, 2006) owing to the sporadic occurrence of the same splicing event as seen in the *LMNA* gene in HGPS and therefore has been of immense interest to ageing researchers. In addition, such profound morphological abnormalities in the nuclear envelope have also been observed in Nestor-Guillermo progeria syndrome (NGPS) (Loi et al., 2016), restrictive dermopathy (RD) (Columbaro et al., 2010) and atypical progeria such as mandibuloacral dysplasia type A & B (Barthelemy et al., 2015). The mutations are not necessarily contained within *LMNA* in case of such a nuclear aberration, like in NGPS and RD. In NGPS, a homozygous mutation causing reduced BANF1 protein levels, affects nuclear assembly, chromatin organisation and regulation of gene expression (Cabanillas et al., 2011). Cells from such individuals display nuclear blebbing and altered subcellular distribution of emerin (Puente et al., 2011). RD, on the other hand, can arise from mutations affecting either Lamin A/C (Navarro et al., 2004) or ZMPSTE24, affecting the proteolytic function of the metalloprotease of removing the three C-terminal residues of farnesylated Lamin A/C (Moulson et al., 2005; Navarro et al., 2005). Cultured cells from affected individuals show an aggregation of unprocessed, toxic lamin A in nuclei reflecting the defective processing of lamin A (Moulson et al., 2005).

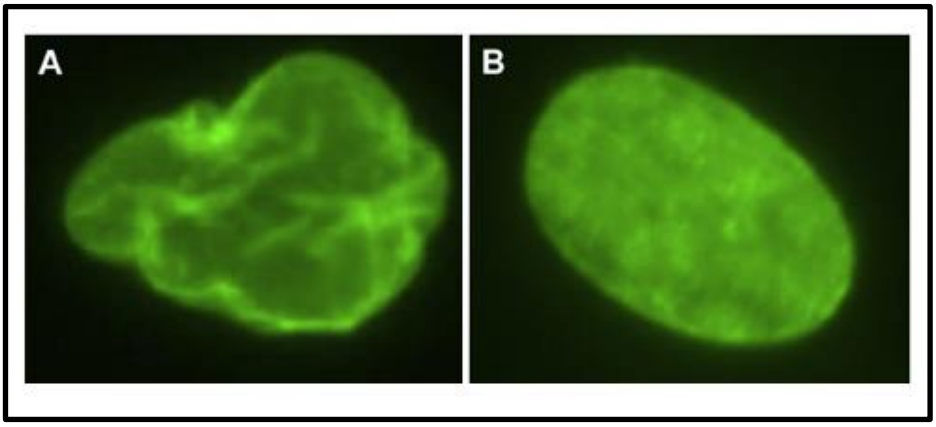

Fig.3. Irregular nuclear architecture and the presence of progerin in Hutchinson-Gilford Progeria Syndrome (A) and (B) physiological ageing- Fibroblasts are stained for anti-lamin A antibody. HGPS fibroblasts show an irregular blebbed appearance due to the production of permanently farnesylated, toxic prelamin A (progerin).

1.4.2. The delay in cutting the chase: Deficits in DNA Damage Repair

Nuclear DNA damage is a direct cause of ageing and accumulation of DNA damage due to progressive decline in efficacy of repair mechanisms as a part of both premature and physiological ageing has been elucidated (Vijg and Suh, 2013).

Individuals with Cockayne syndrome (CS), carrying mutations in either *CSA* or *CSB*, undergo devastating physical and neurological debilitation while those with Xeroderma Pigementosum (XP) show increased cancer susceptibility. Individuals with CS and with XP show a high photosensitivity to UV light. CS cells have been shown to be hypersensitive to ionising radiations known to induce not only double strand breaks (DSBs) (Leadon & Cooper, 2003), but also oxidative damage (Batenburg NL et al., 2015). Specifically, the detection of such DSBs followed by the recruitment of the damage signaling and repair proteins is attributed to the marker protein, γH2AX, also called as repair ‘’foci’’ (Lukas et al., 2011; Chapman et al., 2012). Defects in nucleotide excision repair have also been reported to result in these progeroid phenotypes (Marteijn et al., 2014).

Mutations in the RecQ helicase family of proteins, integral to the processes of DNA replication and genome maintenance, have been implicated in progeroid conditions such as Rothmund Thomson syndrome and Werner syndrome (Crabbe et al., 2006). Cells from individuals carrying *WRN* mutations have typically shown chromosomal instability, telomere dysfunction and senescent phenotype (Crabbe et al., 2007) resulting in accelerated ageing symptoms and high susceptibility to cancer.

1.4.3. How much is too much: ROS generation and Mitochondrial Stress

The free radical theory of ageing (Harman D. 1965) correlates progressive dysfunction of the ATP producing sub-cellular organelle with an increased production of reactive oxygen species (ROS). Although a re-evaluation of the theory proposes that ROS may actually prolong lifespan in lower organisms such as yeast (Mesquita et al., 2010), the findings from human progeroid disorders and their corresponding mouse models have consistently shown to support the initial theory for more complex organisms.

De Novo SLC25A24 mutations affecting the inner mitochondrial membrane carrier of the respiratory chain and subsequent oxidative stress in the Gorlin-Chaudhry-Moss Syndrome have shown to result in a rare progeroid phenotype characterised by skeletal and connective tissue anomalies (Ehmke et al., 2017). The autosomal-recessive cutis laxa type 3 (ARCL3) spectrum of diseases caused by mutations in either *PYCR1* or *ALDH18A1*, which encode enzymes of the mitochondrial proline cycle, cause a multisystem disorder with pronounced progeroid appearance and marked by a typical facial gestalt, lax & wrinkly skin, cataract and profound intellectual disability (Fischer, B et al., 2012).

Rothmund-Thomson syndrome caused by mutations in *RECQL4,* coding for a helicase enzyme localised at the mitochondria as well as telomeres, causes a growth deficiency alongside skin abnormalities arising from oxidative stress leading to inefficient DNA damage repair and ultimately growth arrest (Croteau at el., 2012; Puzianowska-Kuznicka and Kuznicki, 2005; Werner et al., 2006). The pathogenesis of disorders such as Hutchinson-Gilford Progeria Syndrome (arising from mutations affecting the nuclear envelope) and Cockayne Syndrome (caused by impaired DNA damage repair proteins)

has also been linked to a marked downregulation of mitochondrial oxidative phosphorylation proteins and increased ROS production (Rivera-Torres et al., 2013; Scheibye-Knudsen et al., 2013).

1.4.4. Golgi Apparatus Malfunction

Progeroid disorders arising from impaired Golgi complex function have also been described influencing retrograde trafficking and its transport & secretory functions. They have furthered the developing class of hereditary congenital disorders of glycosylation owing to delayed transport and damaged posttranslational modification in the Golgi complex (Kornak, U et al., 2007; Egerer, J et al., 2015; Chan W.L. et al., 2018).

Mutations in the *ATP6V0A2* gene encoding the α2 subunit of the V-type H^+ -ATPase, influencing proton translocation and possibly vesicular fusion with the ER, have been reported in individuals with autosomal recessive cutis laxa type 2 of the Debré type (ARCL2) or wrinkly skin syndrome (Wu, X et al., 2004; Morava, E et al., 2005; Kornak, U et al., 2007). The mutations, causing elevated TGF-β signaling (Fischer, B et al., 2012), have shown to perturb the normal glycosylation of serum proteins and affecting Golgi trafficking in fibroblasts from the affected individuals.

Additionally, the condition of gerodermia osteodysplastica (GO), a progeroid phenotype affecting both skin and bone, has also been attributable to loss-of-function mutations in a golgin called GORAB. The mutations affect either GORAB localisation within the Golgi or its interaction with small GTPases, ultimately disrupting Golgi targeting and secretion (Egerer, J et al., 2015). Furthermore, Chan, W.L. et al. in 2018 uncovered impaired proteoglycan glycosylation and elevated TGF- β signaling for a mouse model for GO.

1.4.5. Defects in Nutrient Sensing and Proteostasis

Homozygous knockout mice for *Zmpste24*, associated with accelerated ageing and a reliable model of HGPS, reportedly exhibit profound transcriptional alterations in levels of

circulating GH and IGF-1 (Marino et al., 2010). The glucose-sensing, insulin and IGF-1 signaling pathway or the IIS and its upstream regulator, growth hormone (GH, released by the pituitary gland) and downstream targets, such as autophagy and protein translation regulating mTOR, have been shown to play an essential role of nutrient and energy handling on longevity (Barzilai et al., 2012, Fontana et al., 2010). In addition, the interconnected nutrient-sensing systems of AMP-activated protein kinase (AMPK) and sirtuins, with their respective roles of sensing high AMP levels and NAD^+ levels, have also been shown as positive regulators of longevity. Compounds such as metformin and resveratrol inducing activation of AMPK were uncovered to beneficially alter the splicing pattern of *LMNA* gene in patient-derived HGPS cells and lower progerin levels, thereby alleviating the pathological defects (Finley J, 2014, 2018). Recently, Monnerat et al., 2019, using non-targeted and targeted metabolomics for biomarker validation in HGPS, revealed several globally changed metabolic pathways including those of fatty acid oxidation, glucose, amino acids, and sphingolipids, among others. Interestingly, *Zmpste24*-null mice show an extensive basal autophagic activation that is associated with a series of changes in lipid and glucose metabolism (Marino et al., 2010).

Ageing associated studies have repeatedly reiterated the gradual accumulation of improperly processed proteins in ageing and related diseases such as Alzheimer's and Parkinson's disease. These damaged/misfolded proteins result from the general failure of protein homeostasis (Powers et al., 2009), also referred to as proteostasis. It comprises of quality control mechanisms for correct protein folding and degradation of proteins by the lysosome-autophagy systems, which are critical to maintain the proteome as functional and stable. However, contrary to this well-established concept for chronological ageing, progeroid diseases caused by nuclear lamina mutations or DNA damage repair defects were shown to exhibit a marked activation of autophagic proteolysis in progeroid mice (Marino et al., 2010). Since the accumulation of such damaged proteins underlies the pathology of various progeroid disorders, it possibly hints towards a general measure of accelerated catabolism as a pro-survival strategy.

Although the mechanisms regulating such proteins underlying progeroid phenotypes is largely obscure, a growing body of research is attempting possible therapeutic interventions to promote the autophagic clearance of defective proteins. Studies in HGPS have shown that regulatory molecules, such as SMURF2 and Rapamycin, can promote

a high turnover of lysosomal breakdown and rapid clearance of progerin, the mutant and toxic form of lamin A underlying HGPS. SMURF2 was shown to negatively regulate lamin A and progerin expression in a SMURF2-dose and E3 ligase-dependent manner, with its overexpression leading to a significant reduction in nuclear distortion (Borroni, AP et al., 2018). MTOR inhibitor, rapamycin, was also shown to selectively and efficiently clear farnesylated progerin via autophagy bringing about correction of aberrant genome organisation and decreased DNA damage respectively (Graziotto, JJ et al., 2012; Bikkul M.U. et al., 2018).

1.5. Splicing: in Ageing and Progeria

Pre-mRNA alternative splicing presents a crucial event of the *"*Central Dogma of molecular biology" (Crick FH, 1958) in the genetic flow of information that also apparently regulates the complex process of ageing.

1.5.1. Out you go: The process of Splicing

More than 90% of the pre-mRNA generated by the process of transcription is removed as introns, and only about 10% of the average pre-mRNA is eventually joined to form the protein-coding exonic sequence. This process, called as pre-mRNA splicing, is carried out within the nucleus prior to the transport of the mature mRNA to the cytosol for subsequent translation into proteins (Tazi J et al., 2009). However, the use of exon is alternative, meaning, the cell takes the decision on which part of the pre-mRNA ultimately goes on to become an exon and which one is excluded as intron. As a result, the process of alternative splicing generates plentiful transcripts or proteins from a single protein-coding gene, thereby increasing the use of genetic information (Lander ES et al., 2001; Ben-Dov C et al., 2008; Tazi J et al., 2009).

The DNA sequences that define exons, introns and regulatory sequences essential for correct splicing are referred to as consensus splice site sequences. These include classical signals or *cis*-elements, which are donor (5') & acceptor (3') splice sites, branch point and polypyrimidine tract sequences, as well as auxiliary elements (or *cis*-acting regulatory elements) such as exonic and intronic splicing enhancers (ESE and ISE

respectively) and silencers (ESS and ISS respectively) (Abramowicz and Gos, 2018). The process of splicing is catalysed by a part of the proteome called as the **Spliceosome,** which is a protein-RNA complex. The machinery of *trans*-acting factors contains more than 300 different proteins besides five small ribonucleoproteins (snRNPs-U1, U2, U4-U6) that have small nuclear RNA entities, which identify the specific splice sites by the spliceosome forming complementary RNA-RNA complexes (Faustino and Cooper 2003). The *trans*-acting factors regulate the process of alternative splicing by their association with the *cis*-elements. The splice sites are mostly recognised at the exon-intron boundaries by sequences containing GT and AG motifs at the 5' and 3' respective ends of the intron.

The proper identification of the splice sites is extremely crucial as errors leading to improper removal of introns may lead to changes in the open reading frame (ORF) or even result in the formation of unstable proteins that can be potentially detrimental to the cell.

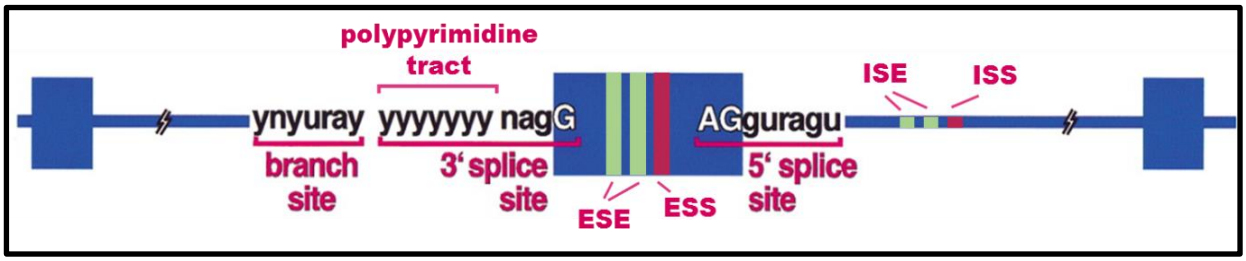

Fig.4. Schematic diagram showing the prerequisites of splicing: Consensus splice site sequences or *cis*-acting elements include classical signals (donor, acceptor, & branch sites and polypyrimidine tract) and auxiliary splicing elements including enhancers (ESE and ISE) and silencers (ESS and ISS). Adapted from Faustino and Cooper, 2003.

The process of splicing consists of the formation of four complexes between the pre-mRNA and the spliceosome spanning two major events, the first one being the identification of the splice sites at intron/ exon junctions and the second one includes the removal of introns and joining of the exon ends-

i. Early Complex 'E' - The snRNP U1 identifies and binds to the complementary AG-GU sequence at the 5' splice site or the donor site of the intron accompanied simultaneously by the binding of SF1 and followed by U2AF65 to SF1 at the

branchpoint sequence. The U2AF65 is also bound to the polypyrimidine tract situated between the 3' end of the intron and the branch point.

ii. ATP-dependent Complex 'A' – Upon the displacement of SF1 protein by U2 snRNP, complex A is formed. The RNA helicases Prp5 and Sub2 stabilise the interaction between the U2 snRNP and the branchpoint, which then marks the recruitment of the tri-snRNP U4/ U6.U5.

iii. Complex 'B' – The recruitment of the tri-snRNP gives rise to complex B formation, which is also called as the pre-catalytic spliceosome.

iv. Complex ' B* ' – Additional helicases bring about changes in the conformation of complex B that leads to the dissociation of U1 & U4, and eventually the formation of complex B*.

v. Complex 'C' – The action of such specific helicases also brings about additional interactions between snRNPs, U2 and U6 leading to the formation of a pre-mRNA loop typical of complex C formation. The complex is characterised to undergo two transesterification reactions that bring about the release of the loop, a step called as the lariat formation and the final steps of intron removal and exon end joining resulting in spliced mRNA.

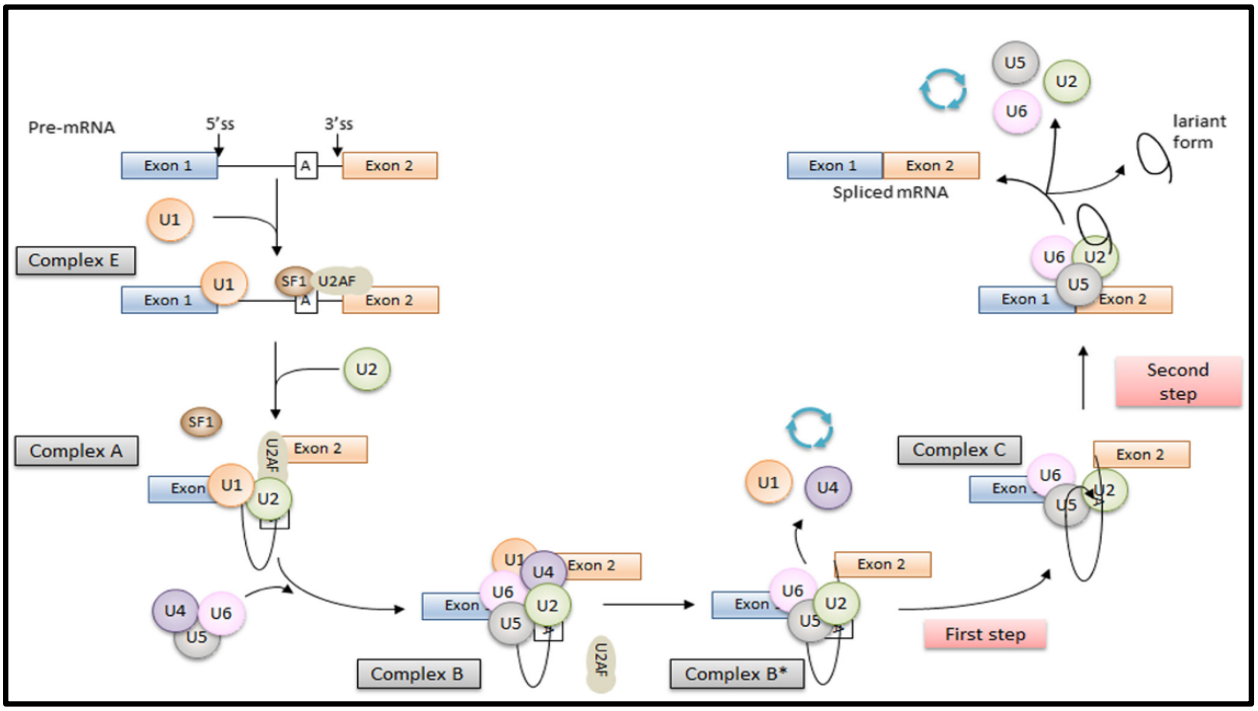

Fig.5. Schematic diagram showing the splicing process consisting of the formation of four complexes between the pre-mRNA and the spliceosome. Adopted from Abramowicz and Gos, 2003.

The consensus sequences so involved in the process are often very short and there tend to be very many similar sequences existent elsewhere in the genome. These sequences are named as noncanonical or cryptic splice sites and are generally not used in the splicing process due to the lack of *cis*-regulatory elements (Cartegini et al., 2002; Abramowicz and Gos, 2018), assuring pre-mRNA splicing being executed at a high fidelity (Fox-Walsh and Hertel, 2009). However, in the presence of a point mutation altering canonical sites, cryptic splice sites can come into use generating a truncated protein that may or may not undergo nonsense-mediated decay (NMD) depending on whether a premature termination codon (PTC) is introduced (owing to a shift in the ORF) or if the deletion is in-frame. In case of NMD, the effect is comparable to a gene deletion (Sterne-Weiler and Sanford, 2014). Splicing mutations may also potentially create new splice sites other than the canonical or the cryptic sites.

1.5.2. To splice or not to splice: Human Disorders with Splicing Alterations

Defects in pre-mRNA splicing can arise from either mutations affecting a splicing *cis*-element or mutations that result in an effect in *trans* (Faustino and Cooper, 2003). The latter involves components of the splicing machinery and hence are potentially deleterious to multiple genes resulting in spliceosomopathies. Thus, categorically, human disease caused by disrupted alternative splicing can arise from-

(i) *Cis* effects- mutations disrupt either the use of constitutive or alternative splice sites

Mutations present in either exons or introns can result in splicing pattern modifications causing genetic disorders. When present in canonical splice sites, the mutations generally lead to exon skipping; one to several exons may be excluded accompanied by the generation of distinct mRNA splice isoforms. For e.g. a variant in the *COL5A1* gene causing Ehlers-Danlos syndrome leads to the production of several transcripts (Takahara et al., 2002). A *de novo* donor splice site mutation in the *FBN1* gene causing a neonatal progeroid variant of Marfan syndrome with congenital lipodystrophy reportedly led to the skipping of one entire exon and the subsequent production of a truncated yet stable protein with an altered C-terminal (Jacquinet A et al., 2014).

Amongst the well-understood progeroid disorders, Hutchinson-Gilford Progeria Syndrome (HGPS, OMIM: 176670), as stated elsewhere, is caused due to the missplicing of the *LMNA* gene encoding lamin A and lamin C proteins. About 80% of the cases arise from a *de novo* point mutation causing a heterozygous base substitution (C->T) that result in the activation of a cryptic splice site within exon 11 of the gene affecting mature lamin A production. The use of the cryptic splice for alternative splicing site results in a truncation of 50 amino acids at the carboxy terminus of prelamin A protein that is permanently farnesylated (LA∆50) and cannot undergo further processing to render mature lamin A (Eriksson et al., 2003, Young, S et al., 2006). LA∆50 is associated with the aberrant nuclear changes as seen in cultured patient-derived HGPS fibroblasts (Goldman R.D. et al., 2004).

(ii) *Trans* effects- mutations either affect the constitutive / basal splicing machinery or affect the regulators of alternative splicing

Human diseases resulting from defects in spliceosome components have also been described for diseases such as retinitis pigmentosa (RP) and spinal muscular atrophy (SMA).

RP is characterised by progressive retinal degeneration, night blindness, loss of peripheral vision, eventually resulting in complete blindness that may be inherited as an autosomal dominant, autosomal recessive, or X-linked disorder. One of the genes implicated in autosomal dominant RP includes *PRPF31* whose functions are best defined. The PRPF31 is a U4/U6 snRNP-associated protein that via direct interactions with a U5-specific protein, promotes the association of U4/U6 snRNP with the U5 snRNP. The association of tri-snRNP U4/ U6.U5 is critical to complex B or pre-catalytic spliceosome formation and reportedly, the depletion of PRPF31 prevents the assembly of the active spliceosome (Makarov et al., 2002). Additionally, *PRPC8* mutations cause a very severe type of RP inherited in an autosomal dominant fashion (McKie et al., 2001). The PRP8 protein reportedly establishes direct contact with the 5' & 3' splice sites and with U6 and U5 snRNAs, providing overall structural integrity to the catalytic core and regulating the RNA helicase activity, which in turn modulates the extensive RNA: RNA base-pairing rearrangements essential for the spliceosome activation (Faustino and Cooper, 2003, Collins and Guthrie, 2000).

Spinal muscular atrophy is diagnosed with a progressive loss of motor neurons of the spinal cord and is inherited in an autosomal recessive fashion. This results in skeletal muscle denervation, consequentially leading to subsequent weakness, atrophy and paralysis of voluntary muscles. Majority of the cases for SMA are attributed to homozygous mutations in complex components of the survivor of motor neuron gene (SMN) complex, best described for its role in the cytoplasmic assembly of U1, U2, U4, and U5 snRNPs that contain a common set of seven Sm proteins as well as respective unique sets of proteins for each snRNP (Will and Lührmann 2001). Depletion of SMN in *Xenopus* oocytes correlated with prevention of U1 snRNP assembly; remarkably, overexpression of an N-terminal truncation mutant of SMN was shown to result in cytoplasmic accumulation of Sm proteins, SMN, and U snRNAs (Meister et al., 2001, Pellizzoni et al., 1998)

1.5.3. The Inevitable Effects of Alternative Splicing on Senescence and Ageing

Increasingly available literature indicates an intimate association of pre-mRNA splicing dynamics with cellular senescence and organismal ageing. Notably, more than 50% of age-related alternative splicing alterations are estimated due to changes in the expression of splicing factors (Mazin et al., 2013). For instance, differential splicing of the *ENG* gene, encoding for the glycoprotein endoglin, regulates vascular ageing and cellular senescence depending on the production of the long or short variant (L-endoglin or S-endoglin). L-endoglin has a proliferative and pro-angiogenic effect on endothelial cells while S-endoglin has been shown to contribute to cellular senescence and lower the proliferation of endothelial cells of transgenic mice overexpressing S-endoglin (Blanco et al., 2008). During normal ageing, a gradual shift towards the S-form occurs in the endothelial cells (Blanco et al., 2008, Blanco and Bernabeu, 2011).

Progerin, the misspliced lamin A protein synthesised in HGPS is detected in trace amounts in healthy ageing individuals and senescent cells lacking HGPS mutations. This indicates that lamins, including progerin, as possible regulators of senescence pathways in both HGPS and healthy individuals via alternative splicing. (Wood et al., 2014, Freund et al., 2012).

1.6. Discovery of the RES complex in Yeast: Bud13 function in *S. cerevisiae*

The structure and function of the Bud13 protein were initially elucidated in the yeast model *Saccharomyces cerevisiae* with the discovery of a new trimeric complex. Proteomic analysis revealed the protein as part of a novel heterotrimeric protein complex composed of, besides Bud13, the Snu17 and Pml1 proteins and is present in the nucleus/spliceosome.

The complex was reportedly important for efficient splicing, both in-vitro and in-vivo and the downstream effect of its inactivation was discovered to be nuclear pre-mRNA leakage. This complex was named as the pre-mRNA REtention and Splicing or the RES complex (Dziembowski A et al., 2004). Interestingly, the subunits were found not to be essential for viability.

1.6.1. Structure

Brooks M et al. in 2009 followed up the structural investigation of the yeast complex and its functional consequences using serial truncations and mutagenesis of the complex subunits. Mutation of the putative binding site of the Pml1 subunit revealed no effect on the RES complex assembly or its downstream function of pre-mRNA splicing. Tripsianes et al. in 2014 combined structural and biochemical analysis to unravel a novel RNA-recognition motif (RRM) - protein surface formed by the Snu17p-Bud13p interaction. Additionally, Wysoczanski P et al., in 2014, presented the dynamics of cooperative folding within the three-dimensional structure of the RES core complex. An intricate folding of the sub-factors was shown to stabilise the RRM of the Snu17p, thereby strengthening the RNA-binding efficiency within the spliceosome.

1.6.2. Function

RES complex in yeast was found to be a crucial facilitator for enhanced splicing. Although the subunits were discovered not to be critical for the overall viability of the organism, yeast cells disrupted for the respective RES subunits have shown to display growth

defects that are aggravated at higher temperatures (Dziembowski A et al., 2004), as well as alterations in the budding pattern (Ni and Snyder, 2001). Deletion of Snu17 or Bud13 has particularly shown to be correlated with a greater accumulation of unspliced, intron-containing pre-mRNAs while that of Pml1 has been concluded to be majorly influential in the pre-mRNA retention function of the RES (Dziembowski A et al., 2004, Zhou Y et al. 2017).

However, experimental approaches involving pre-mRNA co-immunoprecipitation and splicing assays uncovered that the interaction of the RES with the spliceosome is rather transient. This implied that the complex may not be absolutely vital for splicing (Dziembowski A et al., 2004) and its function is more like that of an enhancer. The action of RES was eventually shown to occur before the first catalytic step of the splicing process in the efficient transformation of the pre-catalytic B spliceosome into an activated B^{act} complex (Bao P et al., 2017). As an enhancer, its function was speculated to be of particular significance to the processing of weak introns typically characterised to have a poor 5' splice site that do not conform to the consensus sequence (Dziembowski A et al., 2004; Spingola M et al., 2004; Frederick W et al., 2006). But advanced studies have shown otherwise in that RES-regulated transcripts can also include those harbouring consensus 5' splice sites (Schmidlin T et al., 2008; Tuo S et al., 2012; Zhou Y et al., 2013)

A number of dependents since then have been described in yeast that require one or more of the complex components for efficient splicing and nuclear retention of unspliced pre-mRNA, including a subset of Mer1-dependent introns crucial for meiosis (Frederick W et al., 2006), Tan1 expression regulating tRNA maturation (Zhou Y et al., 2013), and Med20 expression that co-regulates RNA polymerase II transcription via the Mediator complex (Zhou Y et al., 2017).

1.7. BUD13 Function in Vertebrates

1.7.1. Findings from the Zebrafish Model

In 2018, Fernandez et al. uncovered the role of the RES complex during vertebrate development using the zebrafish model. Generation of loss-of-function mutants for the three components of the splicing complex revealed their role during early development. The mutants displayed an increased cell death in the brain and decrease in differentiated neurons. Transcriptomic analysis of the complex components in the mutants further revealed a global defect in intron splicing, with a strong missplicing of short, GC-rich introns via intronic retenetion (IR) in the knockout studies.

1.7.2. Insights into Mammalian BUD13 function

Frankiw et al. followed this in early 2019, displaying the role of BUD13 in mouse-bone-marrow- derived macrophages. Using RNA antisense purification-mass spectrometry (RAP-MS), which employs antisense biotin-containing single-stranded DNAs complementary to exonic regions of the target gene revealing both mRNAs associated with its total pool of transcripts, BUD13 was identified as a splicing modulator of intron 4 of the *IRF7 gene* intron (figure 2), regulating the type I interferon response in macrophages upon viral infection.

Additionally, they assessed global splicing differences owing to BUD13 knockdown and revealed an increased IR and affected gene expression of a special subset of genes having short, GC-rich introns with non-consensus splice donor sites. The mode of action for BUD13 was concluded to be that of an antagonist to IR in the general alternative splicing dynamics. Notably, however, BUD13 depletion and subsequent assessment of differential alternative splicing events in multiple datasets revealed very few of such differential events and even fewer events specifically for intronic retention.

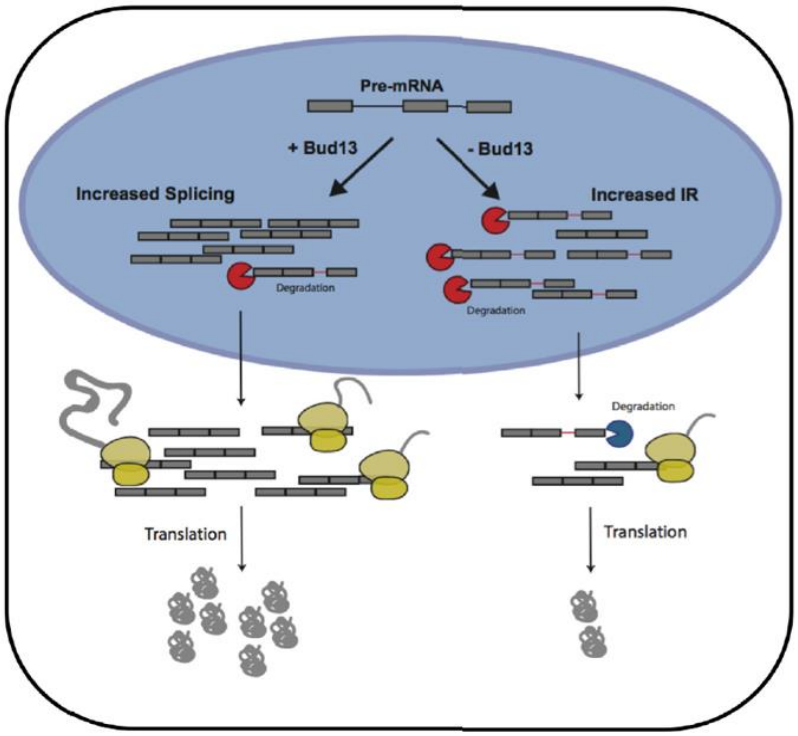

Fig.6. Effect of BUD13 on IRF7 intronic retention (IR) - Knockdown of BUD13 apparently correlates with an increased retention of introns in IRF7 pre-mRNA processing leading to its rapid degradation via nonsense -mediated decay and a decrease in mature IRF7 transcripts, ultimately reducing IRF7 protein and dampening type I interferon response. Adopted from Frankiw et al., 2019.

Furthermore, Nussbacher and Yeo carried out a computational screen of eCLIP data (enhanced version of Crosslinking and Immunoprecipitation) from the publicly available ENCODE project to discover RNA binding proteins that regulate micro-RNA levels (Nussbacher J.K. and Yeo G.W., 2018). BUD13 protein was found to interact and stabilise miR-144 along cooperatively with ILF3 besides suppressing miR-210 processing to subsequent mature species.

1.7.3. BUD13 function from GWAS studies-Population Genetics perspective

Genome-wide association studies (GWASs) are observational studies aimed to investigate associations of genetic variants or SNPs (Single Nucleotide Polymorphisms) and possible associated traits to account for population wide determinants of human

disease. Most of the *BUD13*-associated studies aimed at uncovering heritable variants in metabolic disorders & cardiovascular diseases, and determined not only exonic but also noncoding and intergenic SNPs. Several GWASs have revealed a strong correlation of gene clusters containing *BUD13* with triglyceride metabolism in European and Asian populations (Kim H et al., 2019; Bandesh K et al., 2019, Zhang et al., 2017, Parra EJ et al., 2017, Hebbar P et al., 2017, Teslovich TM et al., 2015). Polymorphisms present in gene clusters including the trio of *BUD13/ ZNF259/ APOA5* have been repeatedly described at the 11q23.3 chromosomal region to influence coronary artery disease and dyslipidemia occurrences.

1.7.4. Complexity owing to overt simplicity: Intrinsic Disorder in BUD13

Intrinsically Disordered Proteins (IDPs) or simply unfolded proteins are polypeptide chains that challenge the key protein structure model in that a well-defined structure is a necessary prerequisite for the correct function of a protein. IDPs contain sites of unstable tertiary structure under physiological conditions in –vitro; such a site adopts a well-defined structure, such as alpha-helices or beta-sheets, only upon the binding of a target molecule (Dyson HJ and Wright PE, 2005; Dunker AK et al., 2008). They constitute a fourth class of proteins in addition to the globular, fibrous and membrane proteins (Andreeva A et al., 2014).

BUD13 protein has been labelled as the most highly disordered protein under the category of non-abundant proteins in the spliceosomal proteome. The Pfam domain at the C-terminal of the protein has been shown to map to disordered regions of spliceosomal proteins (Korneta et al., 2012). Interestingly, this domain is associated with RES complex function and is highly conserved from yeast to man (Korneta et al., 2012; Fernandez et al., 2018; Frankiw et al., 2019); however, mammalian BUD13 consists of a long N –terminal component, absent in yeast, whose properties in terms of intrinsic disorder are still not explicated.

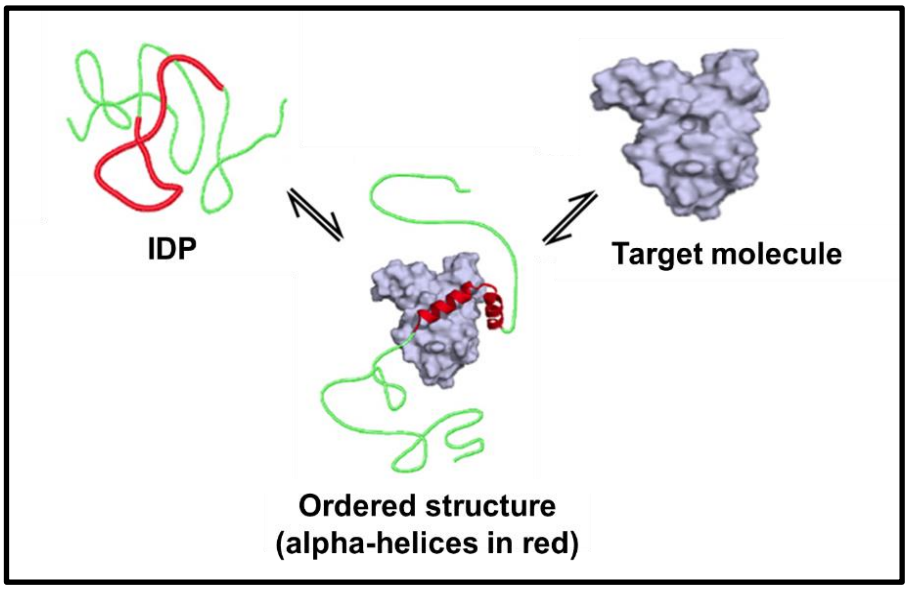

Fig.7. Intrinsically disordered proteins (IDPs) lack well-defined structures, which they attain only upon the binding of specific target molecules.

Chapter 2: Methods

2.1. General Cell culture methods

2.1.1. Maintenance and Expansion of Cultured Cells

Skin fibroblasts from skin biopsies from patients A1-A5 were isolated according to a standard protocol. The cells were maintained in AmniomaxTM C-100 basal medium (Invitrogen) supplemented with AmniomaxTM C-100 supplement (Invitrogen). Immortalised HeLa and U2OS cell lines were maintained in DMEM high-glucose (Lonza) supplemented with 10% fetal calf serum (FCS, Gibco), 1% ultraglutamine (Lonza) and 1% penicillin-streptomycin (PEN-STREP, Lonza). All the cells were maintained in a humidified incubator at 37℃ & 5% CO2 and the medium was changed every 3 or 4 days.

When the cultured cells reached about 80-90% confluency, they were split into new flasks-the adherent cells were washed with Dulbecco's phosphate buffered saline (DPBS, Gibco) and trypsinised with 0.05% trypsin-EDTA (Gibco) for 1-2 minutes at 37℃ until detachment, immediately followed by the resuspension of the cells in fresh medium and redistribution into new flasks in a ratio depending on the cell line and purpose.

2.1.2. Embryonic stem cell (ESC) culture

This work has been supported by Malte Spielmann, PhD and Miguel Rrodriguez, MSc from the Charité Universitäsmedizin Berlin and Max Planck Institute for Molecular Genetics, Berlin.G4-ESCs were cultivated on CD1 feeders and maintained in ES+LIF medium as described by Kraft et al. (2015). All cells were grown at 37°C and 5% CO2.

2.1.3. MEF isolation

Following the sacrifice of pregnant mice at E13.5, embryos were isolated and minced in a 6cm dish. Head, liver and spleen were removed using a sharp forcep and the tissue was minced until homogeneous and collected in 5ml 1X PBS (Phosphate-buffered saline) in a 15ml falcon, followed by addition of 5ml Trypsin/EDTA. The falcon was shook and

incubated at 37°C in a water bath for 10 minutes following which it was shook again and letting the tissue fragments settle for 2 minutes. 5ml of this solution was transferred to 25ml medium in a 50mol falcon followed thrice by 5 ml Trypsin/EDTA digestion. After the last digest, the entire suspension was transferred into 50ml medium in a falcon, shook and centrifuged at 100 rpm for 5 minutes. The pellet was re-suspended in fresh medium and seeded into 75 cm^2 cell culture flasks.

2.1.4. Cryopreservation

Long –term cryopreservation of cells was carried out using a freezing medium composed of 50% DMEM high-glucose, 40% FCS and 10% dimethyl sulfoxide (DMSO) in cryovials (Sarstedt) for long-term storage in liquid nitrogen. Briefly, adherent cells were trypsinised and suspended in growth medium followed by centrifugation at 1000 rpm for 5 minutes. The cell pellet so obtained was dissolved in freezing medium and brought to liquid nitrogen tanks.

2.1.5. Thawing of cells

Cryovials containing cells frozen in DMSO medium were thawed at room temperature followed by suspension in growth medium and centrifugation at 1000 rpm for 5 minutes. The supernatant was discarded and the cell pellet was suspended in growth medium and transferred to an appropriate cell culture flask.

2.1.6. Cell number determination

Cell enumeration for various experiments was carried out using a Neubauer commercial chamber (Blaubrand®).

2.1.7. Cellular transfection

Immortalised HeLa and U2OS cell lines were transfected with 2µg of these plasmids using the JetPei® DNA transfection reagent (PolyPlus transfection®) according to manufacturer's instructions.

2.2. Molecular Biology methods

2.2.1. Patient material and cells

The affected individuals A4 & A5 and the parents of patients A1-A3 provided their written consent for genetic testing and the publication of images. From all patients, peripheral blood samples were taken and DNA from lymphocytes was extracted according to standard protocols.

2.2.2. RNA isolation

Cells were lysed in a defined density three days past confluency and Trizol® (Invitrogen) was used for cell lysis. Total cellular RNA was extracted using the Direct-Zol RNA Miniprep kit (ZymoResearch).

2.2.3. cDNA synthesis, RT-PCR analysis and qPCR

cDNA was transcribed using the RevertAid H Minus First Strand cDNA Synthesis Kit (Fermentas) according to the protocol of the manufacturer.

RT-PCR on human and murine samples was performed using FIREPol® DNA polymerase (Solis BioDyne) and cDNAs synthesised as described above. Primer sequences are included in table 1 while reaction mixture and PCR program for RT-PCR are included in table 2. The PCR was carried out on a Proflex PCR system (Applied Biosystems®).

PCR amplified products were loaded on a 1.5% agarose gel prepared in 1X TAE buffer with Ethidium Bromide (1:20,000). Agarose gel-electrophoresis was performed to separate out PCR amplified products combined with a DNA gel loading dye (ThermoFisher Scientific). Visualisation of the bands was done using the gel documentation system, G:Box (Syngene). Differential bands were cut from the gel and DNA was extracted using the NucleoSpin Gel and PCR Clean-up Kit (Macherey-Nagel) as per the manufacturer's instructions. Purified DNA fractions were subjected to direct Sanger sequencing using the PCR primers.

Quantitative PCR was carried out using Eva Green (Solis BioDyne) on a Quant Studio 03 system (ThermoFisher Scientific). The reaction was carried out in 96 well plates in a total volume of 20 µl. The primer sequences are included in table 3 while the qPCR program is included in table 4.

Primer name	**Primer sequence 5' -> 3'**
Human	
hBUD13_F1	TGACTCCTCAGACACTTCACC
hBUD13_R1	GCCCTGGACTTTGTTTATGC
Mouse	
cmBud13_e3-5F	CTCCAGTGCCAAGTGGAAG
cmBud13_e3-5R	GACTCCTTCGAGGTGGAGAG

Table.1. Primers used for RT-PCR for splicing analysis; PCR carried out using cDNA reverse transcribed from RNA that was isolated from human adult fibroblasts and mouse embryonic stem cells.

Reagent	**Amount**
cDNA	5-10 ng
FIREPol®	5 µl
5'- primer (F) (10 µM)	0.5 µl
3'- primer (R) (10 µM)	0.5 µl
ddH2O	upto 25 µl

Temp (°C)	**Time**	**Cycles**
95	05 min	1
95 56 72	50 sec 50 sec 02 min	35
72	10 min	1
4	∞	

Table.2. (A) Reaction mixture and (B) PCR program for RT-PCR carried out for splicing analysis using cDNA reverse transcribed from RNA that was isolated from human adult fibroblasts and mouse embryonic stem cells.

Primer name	Primer sequence 5’ -> 3’
qhBUD13_e3-4F	AAAGCAGATGGAGGCCTTTC
qhBUD13_e3-4R	ATGAATCCGGGGTATCGTG
qhBUD13_e9-10F	ATATCGCTGGGACGGAGTG
qhBUD13_e9-10R	CTCCACTGCCTTCTTGCTG
qhBUD13-jn-patF	CAAGGAGGCCTCAGCATAATTC
qhBUD13-jn-patR	TGGTTCTAGGAGGAGAGGGATC
qhGAPDHF	CTGCACCACCAACTGCTTAG
qhGAPDHR	ACAGTCTTCTGGGTGGCAGT

Table.3. Primers used for qPCR for gene expression; qPCR carried out using cDNA reverse transcribed from RNA that was isolated from human adult fibroblasts and mouse embryonic stem cells.

Stage	Temp (°C)	Time	Cycles
Hold stage	50 95	02 min 10 min	1
PCR stage	95 60	15 sec 60 sec	40
Melt curve stage	95 60 95	15 sec 60sec 01 sec	1

Table.4. qPCR program for gene expression analysis; PCR carried out using cDNA reverse transcribed from RNA that was isolated from human adult fibroblasts and mouse embryonic stem cells.

2.2.4. Generation and Transient Overexpression of BUD13 and BUD13-S1 proteins

i. Generation of pEF5/FRT/BUD13-V5 and pEF5/FRT/BUD13-S1-V5 plasmid vectors

We purchased a pEF5/FRT/V5 (Invitrogen) expression plasmid vector containing the BUD13 open reading frame (ORF) from DNASU (pENTR-BUD13-open).

We subsequently generated pEF5/FRT/BUD13-S1-V5 containing the splice isoform (*BUD13-S1*) as seen in the patients from pENTR-BUD13-S1, which was generated using the Gibson assembly® strategy- a procedure that efficiently joins overlapping DNA fragments in a single-tube isothermal reaction. Briefly, two separate PCR amplified fragments were generated in such a manner that when put together, they would yield the BUD13-S1 insert and the linear vector was generated using restriction enzyme -mediated digestion, thereby totaling three separate fragments. The PCR primers used for the Gibson assembly were made to have two sequence components, an overlap sequence for the assembly of adjacent fragments (5' –end) and a gene-specific sequence for template priming during PCR amplification (3' –end).

Reagent	**Amount for 2-3 fragment assembly**
Total amount of fragments	0.02-0.5 pmols (X µl)
Gibson Assembly Master Mix (2X)	10 µl
Deionised water	10-X µl
Total volume	20 µl

Table.5. Protocol for Gibson assembly® strategy- Samples were incubated in a thermocycler at 50°C for 15 minutes followed by sample storage at -20°C for subsequent transformation using *E.coli*.

ii. Generation of BUD13 and BUD13-S1 proteins fused with GFP

pENTR-BUD13-open and pENTR-BUD13-S1 were recombined with expression vector constructs carrying GFP (pcDNA5/FRT/TO+AcGFP1+rfb) to yield BUD13 and BUD13-S1 proteins fused with GFP. The GFP constructs were kindly provided by Dr. Leo Nijtmans.

iii. Transient Overexpression and quantification of lobulated cells

Immortalised human cell lines, namely the HeLa and U2OS cell line, were transfected with 2µg of these respective plasmids using the JetPei® (PolyPlus) method according to manufacturer's instructions. The average percentage of lobulated nuclei were calculated

for the V5- tagged wild type and mutant BUD13 protein transfections. All differences were analysed using the student's t- test.

2.2.5. Sanger sequencing

Sanger sequencing was performed on genomic DNA to validate the pathogenic variant c.688C>T in *BUD13* (NM_032725) in all the patients A1-A5 as well as to genotype chimeric mice for *Bud13-113del* mutation using genomic DNA isolated from tail or ear-cuts. Reference sequences were downloaded from Ensembl (Hunt S et al., 2018). Primer sequences are summarised in table 6.

Additionally, human and murine RT-PCR products with cDNA were also sequenced to investigate aberrant splicing gained by this pathogenic variant. The RT-PCR primers used in these investigations were utilised for Sanger sequencing as well.

BigDye Terminator cycle sequencing kit (Thermo Fisher Scientific) was used and products were sequenced on an ABI 3730 DNA Analyzer (Thermo Fisher Scientific). The sequencing reaction used is described in table 7.

Primer name	**Primer sequence 5' -> 3'**
Human	
hBUD13_e4F	AAAACTGTGCAGGCCTTTTG
hBUD13_e4R	ACCCAGCCTCTCACTTTTCA
Mouse	
seqBud13_F1	CCACGGTGAAGATGGACATT
seqBud13_R1	AGGGGAGTGGTTATGGGTCT

Table.6. Primers used for Sanger sequencing- genomic DNA and genotyping experiments.

Temp (°C)	Time	Cycles
96 50 60	30 sec 15 sec 04 min	25
8	∞	

Table.7. BigDye v3.1 sequencing reaction

2.2.6. Whole exome sequencing (WES)

WES for patients A1-A3 had been already carried out prior to the beginning of the PhD project. WES for patient A1 and A2 was carried out at Centre National de Génotypage (Evry, France). The DNA sample from patient A3 was whole exome sequenced after approval was obtained from the ethics board of the Charité Universitäsmedizin Berlin. Blood samples from patients A4 and A5 were sent to Centogene AG for routine genetic diagnostic workup and WES.

2.2.7. Transcriptome sequencing

Total cellular RNA from patients A1-A3 and three matched controls was extracted as described above. Poly-A enrichment was performed according to an in house protocol. Sequencing was performed on an Illumina's Hi-Seq 1500 system. 60-70 million sequence reads were generated and raw data were transferred to the work group of Florian Heyd for further processing. Total RNA from murine embryonic stem cells (mESc) was provided to commercial service (Eurofins MWG GmbH, Ebersberg, Germany). Poly-A enrichment was carried out and sequencing was performed on an Illumina NovaSeq 6000 S2 PE150 XP platform. On average, 70 million sequence reads were generated per sample and raw data were transferred to the work group of Florian Heyd for further processing.

2.2.8. Bacterial transformation and plasmid DNA isolation

Chemocompetent *E.coli* cells were thawed on ice. 3ul of ligation reaction mixture was added to 50ul of chemocompetent cells and mixed by gently pipetting up and down and incubated on ice for 30 minutes. Following this, heat shock at 42°C 30 seconds was

carried out in a heating block. The cells were then incubated on ice for at least 2 minutes followed by the addition of 950ul of SOC medium. The bacteria were then incubated at 37°C at 600rpm (for constant shaking) for one hour in a heating block. 50-100ul of the transformation mixture was then plated on pre-warmed LB agar plates containing the appropriate antibiotic (200ug/ml Ampicillin or 50ug/ml Kanamycin). The plates were incubated at 37°C and 5% CO_2 overnight in a bacterial incubator.

Plasmid DNA isolation was carried out for mini and midi preparation using the Invisorb® spin plasmid mini two kit (Invitek Molecular) and the Nucleobond® PC 100 midi kit (Macherey-Nagel) respectively.

2.3. Biochemical methods

2.3.1. Protein extraction from cultured adherent cells

Adherent cells were washed thrice with ice-cold 1X PBS. The PBS was then completely drained off and followed by the addition of ice-cold RIPA buffer ((150 mM NaCl, 50 mM Tris, 5 mM EDTA, 1% Triton X-100, 0.25% deoxycholate, 0.1% SDS supplemented with complete proteinase inhibitor, Roche) to the adherent cells (100ul/10^6cells in a well). The cells were scraped off the dish using a plastic cell scraper and the lysate was transferred into ice-cold eppendorfs, and finally spun in a pre-cooled centrifuge at 13,500 rpm for 15 minutes. The supernatant was immediately transferred to a fresh, ice-cold eppendorfs and the pellet was discarded. The supernatant was then used for protein concentration determination for further experiments.

2.3.2. Determination of protein concentration

Protein concentrations were analysed using the BCA Protein Assay Reagent Kit (Pierce) according to the supplier's protocol. The protein absorbance was measured at 562 nm for the samples and for a set of BSA standards. Protein concentrations were estimated using the BSA standard curve.

2.3.3. SDS-PAGE (Sodium Dodecyl Sulphate- PolyAcrylamide Gel Electrophoresis)

10 µg protein per lane was separated on 4-12% gradient gel (NuPAGE) using 1X NuPAGE running buffer. The electrophoresis was carried out at 60 V for 30 minutes followed by 100 V for a time duration depending on the size of the protein under investigation.

2.3.4. Western blotting- Protein transfer and detection

Nitrocellulose membranes were activated and equilibrated in methanol containing 1X transfer buffer (25mM Tris, 192 mM Glycine, 20% MeOH). The gel-membrane sandwiches were prepared considering the direction of protein transfer for semi-dry blotting (Peqlab) at 10 V for 1.5 hours for two membranes in a single machine.

After blotting, membranes were blocked using the Odyssey® blocking buffer in 1X PBS and probed with primary antibodies overnight at 4 degrees. Depending on the developing protocol, the membranes were incubated with appropriate secondary antibodies.

For chemiluminiscence based detection, the membranes were washed and incubated for an hour with HRP-conjugated secondary antibodies followed by visualisation of bands with ECL reagent (PerkinElmer). For fluorescence based detection, the membranes were washed and incubated for an hour with fluorophore-conjugated secondary antibodies followed by visualisation of bands with using the LICOR® system. All the blots were carried out at least three times with different cell lysates every time. A list of antibodies used for western blotting experiments is provided in table 8.

2.3.5. Quantification of Immunoblot experiments

Images showing the relative expression of BUD13 and GAPDH in three controls and all affected individuals were analyzed using ImageJ. Densitometry values for BUD13 were corrected against GAPDH signals and the relative expression of BUD13 was calculated using one control as calibrator. The values from three independent experiments were averaged and the standard error of the mean was calculated. All differences were analysed using the student's t- test.

	Antibody	Manufacturer	Dilution
Primary antibodies	Rabbit anti-BUD13	Abcam, ab11783	1:1000
	Goat anti-Lamin A/C	Santa Cruz, sc-6215	1:1000
	Rabbit anti-Cathepsin D	Abcam, ab75852	1:1000
	Rabbit anti-H2AX	Cell signaling, 7631T	1:1000
	Rabbit anti-p-H2AX	Cell signaling, 9718S	1:1000
	Mouse anti-GAPDH	Thermo Fisher, AM4300	1:2000
Secondary antibodies	Anti-Rabbit IgG, HRP-	Cell signaling, 7074S	1:2000
	Anti-Mouse IgG, HRP-	Cell signaling, 7076S	1:2000
	Donkey Anti-Goat HRP	Invitrogen, A15999	1:2000
	IRDye® 680RD Donkey anti-Mouse	*LI-COR*	1:10,000
	IRDye® 800RD Donkey anti-Rabbit	*LI-COR*	1:10,000

Table.8. Antibodies used for Western blotting experiments.

2.3.6. Proteomics analysis

The proteomics analysis was carried out and supported by David Meierhofer, PhD at the Mass Spectromtery Facility, Max Planck Institute for Molecular Genetics.

2.4. Cell biology techniques and Cellular Assays

2.4.1. Immunofluorescence (IF)

A defined number of cells depending on the experimental need were seeded and grown on glass coverslips overnight, following which, the next day, they were fixed in 4% paraformaldehyde for 10 minutes at room temperature. This was followed by simultaneous permeabilisation and blocking using 0.4% Triton X-100 in 3% BSA in 1X PBS for 10 minutes. The cells were than washed twice with 1X PBS and incubated with the primary antibody at 4°C overnight. After that, cells were washed three times with 1X

PBS and then stained with secondary antibody at room temperature for 1 hour. The counterstaining was done using DAPI to stain the DNA and the cells were mounted in Fluoromount G. A list of antibodies used for IF experiments is provided in table 9.

	Antibody	Manufacturer	Dilution
Primary antibodies	Rabbit Anti-Emerin	Santa Cruz, sc-15378	1:1000
	Rabbit Anti -GFP	Abcam, ab556	1:1000
	Mouse Anti-V5	Sigma Aldrich, V8012	1:1000
Secondary antibodies	Alexa Fluor® 555, Donkey anti-Rabbit	Thermo Fisher, A31572	1:1000
	Alexa Fluor® 488, Donkey anti-Mouse	Thermo Fisher, A21202	1:1000
	Alexa Fluor® 488, Donkey anti-Rabbit	Thermo Fisher, A21206	1:1000

Table.9. Antibodies used for Immunofluorescence experiments.

2.4.2. DNA damage repair/ UV-irradiation assay

2 X10^5 cells /ml were seeded and grown overnight on coverslips in the 6-well plate format. The cells were irradiated using UV-Stratalinker at 60,000uj/cm-square for 60 seconds followed by fixation using 4% PFA and immunofluorescence staining using appropriate primary and secondary antibodies. The average percentage of high number of the respective foci (γ-H2AX, 53-BP1) between the mutant and control cell lines were evaluated. All differences were analysed using the student's t- test.

2.4.3. Beta-Galactosidase staining

Senescence associated beta-galactosidase staining was carried out using the Senescence β-Galactosidase Staining Kit (Cell Signaling Technology) as per the manufacturer's protocol. Briefly, 30,000 cells/ well were seeded in the 24-well plate format in triplicates for all the patient and control fibroblasts and grown overnight following which

the cells were fixed and stained using manufacturer supplied solutions for ~8 hours at 37°C in the dark. This was followed by the removal of staining solution and subsequent washing of the cells thrice with 1X PBS. The cells were visualised and counted using a light microscope. In the event of excess salt crystals, the stained cells were briefly incubated with dimethyl sulfoxide for 5 minutes.

2.4.4. ROS (reactive oxygen species) assay

The ROS assay was performed by Claire Schlack-Leigers, BSc, using a ROS sensitive dye CM-H2-DCFDA in 1X DMEM cell culture medium and measuring excitation and emission wavelength at 495nm and 530nm respectively using a plate reader.

2.4.5. Immunohistochemistry

Histology of murine fat depots- The fat depots from the gonadal and scapulae region were fixed using 4% PFA overnight followed by sectioning using microtome and staining using Haemtoxylin and Eosin. The microtome sectioning and staining was performed by Björn Fischer-Zirnsak, PhD.

2.4.6. Transmission Electron microscopy

The transmission electron microscopy experiments were carried out at the microscopy and cryo-electron microscopy service group at the Max Planck Institute for Molecular Genetics, Berlin.

2.5. CRISPR/Cas9 mediated Genome Editing and Animal Experiments

The genome editing experiments have been carried out by Malte Spielmann, PhD (Bud13-113 del mouse) and Miguel Rodriguez, MSc (Bud13-106 del mouse). Briefly, Single guide RNAs (sgRNA) with minimal off-target specificity were designed using the CRISPR design tool from the MIT Zhang lab. Complementary strands were annealed, phosphorylated, and cloned into the CRISPR/Cas vector. G4 ESCs (WT) were used as

the template for the CRISPR experiments. Transfection, further handling of the cells, and morula aggregation were all performed as described by Kraft et al., (2015).

The G4 mouse embryonic stem-cell clones obtained after genome editing were characterised using PCR-based methods to select clones homozygous for the mutation introduced. The selected ES cells were aggregated in the transgenic facility of the Max Planck Institute for Molecular Genetics using diploid aggregation.

The subsequent molecular analyses of the clones and the animal work with the chimeras were undertaken by the author, Namrata Saha supported by Björn Fischer-Zirnsak, PhD.

2.5.1. Growth curve

For all animals, the total body weight has been determined every week. On the 37th week after birth, the mice from the first aggregation died from a so far unknown reason. Following the subsequent aggregation, the animals were sacrificed around the same period for further analysis.

2.5.2. Analysis of fat depots

Mice were sacrificed using cervical dislocation. The total body weight at the 37th week of life was determined. From n=13 control and n=11 Bud13^{113del} animals, the fat depots of gonadal and scapulae fat were dissected and the weight was determined.

2.6. Bioinformatics analysis

2.6.1. Bioinformatics on Transcriptome data

The bioinformatics analysis on transcriptome data was carried out by Alexander Neumann, Heyd group, Free University.

Reads were mapped to reference genomes (hg38 for human, mm10 for mouse) using STAR version 2.5.3a (Dobin et al 2012). rMATS version 4.0.2 (Shen et al 2014) was used

for alternative splicing and DESeq2 version 1.24.0 (Anders et al 2012) for differential gene expression analysis. An alternative splicing event was considered differential with an FDR lower than 0.1 and an inclusion level difference greater 0.1 or smaller -0.1. Genes were considered differentially expressed with an adjusted p value smaller than 0.05 and a minimal expression change of 20%. Genes with low expression in both tested conditions (below 10th percentile) were filtered out. Downstream functional profiling was performed using gProfiler version e97_eg44_p13_d22abce (Raudvere et al 2019). The duplicate-merged eCLIP peak file against BUD13 (identifier ENCSR830BSQ, produced in the Yeo lab) was downloaded from ENCODE (doi: 10.1038/nature11247). BAM files were handled using bedtools version 2.29.0 (doi: 10.1093/bioinformatics/btq033).

2.6.2. Interspecies alignment

The following protein sequences were extracted from the UniProt database (Bateman A, 2019). BUD13 (Human): Q9BRD0; Bud13 (Mouse): Q8R149; Bud13 (Yeast): P46947; Bud13 (Zebrafish): F1QH05. Clustal Omega (Sievers F et al., 2011) was used for sequence comparison.

2.6.3. Splice site prediction

Prediction of a potential impact of splicing due to the pathogenic variant c.688C>T in BUD13 (NM_032725) was carried out using Human Splice Finder version 3.0 (Desmet F et al., 2009), while predictions in mouse were carried out using splice site prediction by a tool base on neural network -Berkeley Drosophila Genome Project *(fruitfly.org*) (Adams M et al., 2000).

Chapter 3: Results

The project has focused on understandings towards a novel progeroid disorder, manifested in mild to severe forms, in five different individuals investigated from four consanguineous families of Algeria and Portugal.

3.1. Clinical Phenotype: Segmental Progeroid Disorder

The project began with the study of three individuals (A1-A3) from two unrelated families (figure 8A) in Algeria who were clinically diagnosed with a complex progeroid phenotype with the closest differential diagnosis as Cockayne syndrome. The affected individuals were all offspring of consanguineous mating and displayed mostly normal birth parameters such as those relating to birth weight (ranging between 2.5-3.6 kg) and occipitofrontal circumference (OFC within 33-39 cm). However, in the very first year of life, they developed a progressive postnatal growth retardation with some of the earliest visible representations as slowing down of height and weight gain. The individuals reportedly developed little muscle tissue and exhibited muscle hypotonia. The most prominent feature was acute lipoatrophy, a progressive loss of subcutaneous fat tissue, which led to a prematurely aged facial appearance. In addition, there were feeding problems and the young individuals suffered from achalasia that made it difficult for food and liquid to pass into their stomach. Plasma cholesterol levels were reported to be normal. However, these feeding problems were seemingly not primarily responsible for the missing weight gain since also feeding through gastric tubes did not improve the situation. Complexities such as dry & wrinkled skin, cataracts or corneal clouding, conductive hearing impairment, and rapid stiffening & swelling of joints, besides impaired cognitive development were encountered. The patients had a life span ranging from six to nine years and died due to unknown reasons.

Interestingly, two more individuals (A4-A5) harbouring precisely the same mutation (figure 8A) were discovered from two independent families in Portugal. Although they carry the exact same mutation as the younger individuals who died young, the older individuals exhibit a milder progeroid phenotype and evidently, a much longer lifespan. The latest

report indicated them as 33 and 55 years of age, respectively. These persons were also reportedly born normal (birth weight 3.2 & 3.3 kg respectively and normocephalic OFC). One of the individuals developed a mild short stature whereas the other reportedly developed a height in the lower normal range. Lipoatrophy, dry & wrinkled skin, conductive hearing impairment in conjunction with a progressive bilateral sensorineural hearing loss, corneal clouding, and facial dysmorphism have also been reported in these individuals. Although no feeding problems have been reported except for one of them (A4) being prone to vomiting during childhood, both of them suffer from achalasia. Cognitive development is above average and there is reportedly no joint swelling/ stiffness in either of them. Strikingly, both of them have shown elevated levels of plasma cholesterol, and also show cardiovascular features of aortic valve thickening (patient A4) and mild heart valve regurgitation (both patients A4 & A5). Figure 8(B) table summarises the clinical data from all the five individuals.

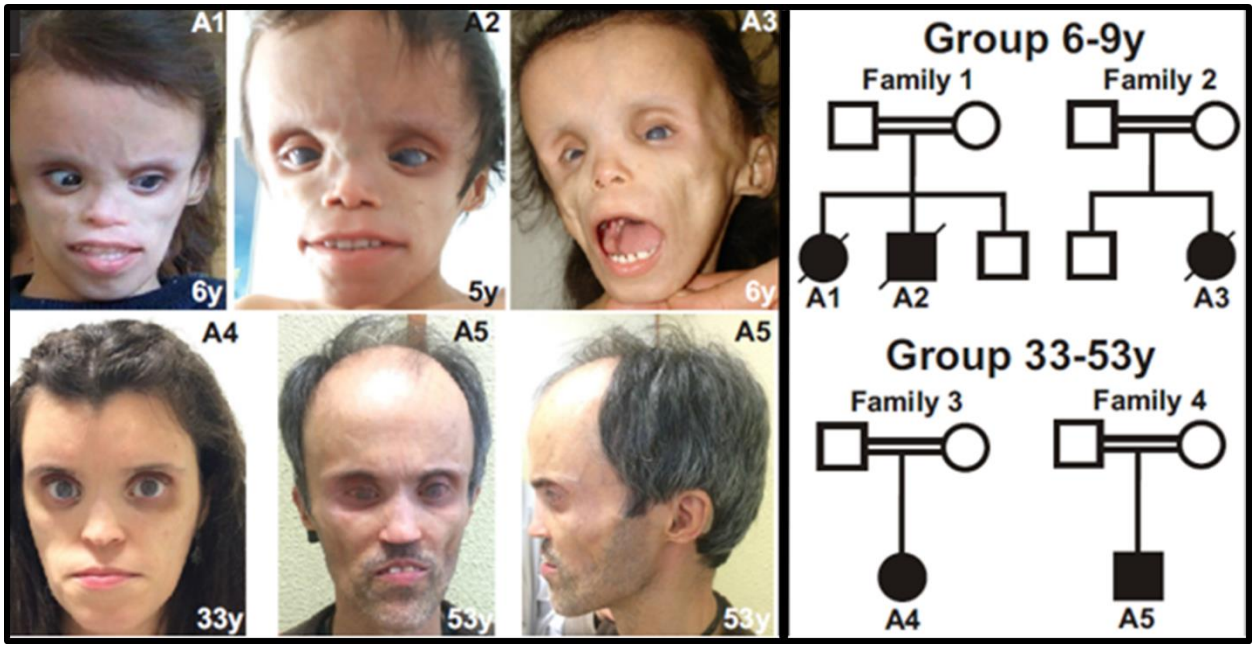

Fig.8. (A) Left to right- Facial appearance of five different individuals (A1, A2, A3, A4, and A5) investigated as a part of the study from four different consanguineous families.

Background	**Patient A1**	**Patient A2**	**Patient A3**	**Patient A4**	**Patient A5**
Sex	female	male	female	female	male
Origin	Algeria	Algeria	Algeria	Portugal	Portugal
Consanguinity	yes	yes	yes	yes	yes
Age at last examination	7 y	9 y	6 y	33 y	50 y
Clinical Data					
Early demise	7 y	9 y	6 y	no	no
Birth weight	2500 g	2770 g	3650 g	3240 g	3300 g
OFC birth	33 cm	39 cm (4 months)	36,5 cm	normocephalic	normocephalic
Weight last examination	13 kg	10.18 Kg	9.05kg (-6SD)	48,5 kg (2nd-9th centile, BMI 19.9)	45 kg (<0.4th centile, BMI 17.9
OFC last examination	47 cm	46.5 cm	48.6 cm (10thcentile)	54,9 cm (25-50th centile)	54 cm (2nd centile)
Height last examination	87 cm	85.7 cm	87cm (-6SD)	156 cm (9th centile)	158,5 cm (4cm < 3rd centile)
Mental retardation	yes	yes	mild delay	no	no
MRI	normal	normal	normal	n.a.	n.a.
EEG	normal	normal	normal	n.a.	n.a.
Demyelinating sensitive neuropathy	yes	yes	n.a.	no	no
Feeding problems	yes	yes	yes	prone to vomiting during childhood	no
Achalasia	yes	yes	yes	yes	yes
Dry, wrinkled skin	yes	yes	yes	yes	yes
Reduced subcutaneous fat tissue	yes	yes	yes	yes	yes
Lipoatrophy	yes	yes	yes	yes	yes
Conductive hearing impairment	yes	yes	yes	yes	yes
Cochlear implants	no	no	no	bilateral	bilateral
facial dysmorphy	yes	yes	yes	yes	yes
progressive joint stiffness /swelling	yes	yes	yes	no	no
retinal dystrophy	yes	yes	n.a.	no	no
Catarct	no	no	yes	yes	yes
Corneal clouding	yes	yes	yes	yes	yes
Plasma Cholesterol	normal	normal	normal	increased	increased
Cardiovascular features	no	no	no	thickening of the aortic valve; mild aortic regurgitation	mild mitral valve regurgitation

Fig.8. (B) Summary of the clinical data from all the five investigated individuals.

3.2. Analysis and Follow-up Investigations from Various Sequencing Approaches

3.2.1. Detection and Validation of Disease-Causing Mutation in *BUD13*

The patients' phenotype was not compatible with any known genetic syndrome. Due to some overlap with Cockayne syndrome, a collaboration partner excluded the known disease genes for this condition. Since obviously a novel disease gene had to be identified, we opted for whole exome sequencing (WES) (figure 8C) in all the affected individuals. The exact same homozygous nucleotide substitution leading to a nonsense (stop) mutation was uncovered in all the five individuals, namely, chr11 (GRCh37):g.116633617G>A, c.688C>T in the *BUD13* gene (NM_032725). The alteration was predicted to lead to a premature termination codon (PTC) p.(Arg230*) in the BUD13 protein known to be involved in post-transcriptional processing or splicing processes. Additionally, we confirmed our findings from exome sequencing using the Sanger sequencing approach using genomic DNA from all the individuals (data excluded).

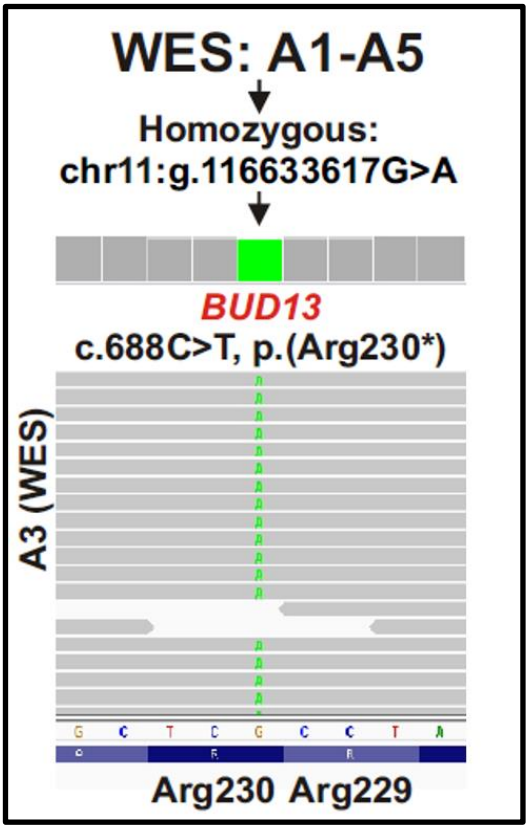

Fig.8. (C) Whole exome sequencing (WES) revealed a homozygous nucleotide substitution leading to a nonsense-mutation in the *BUD13* gene chr11(GRCh37):g.116633617G>A, c.688C>T.

Following the discovery of the mutated gene, literature analysis uncovered BUD13 to play a role in splicing processes as part of a complex called as the pre-mRNA Retention and Splicing (RES) complex. Hence, we followed up our experimental investigations with the molecular genetic analysis of the nonsense mutation (section 2.2) accompanied with transcriptomic analysis (section 2.3) while suspecting a global splicing defect as a probable pathomechanism.

3.2.2. The c.688C>T Mutation in BUD13 creates an abnormal splice site

A splice site analysis for the *BUD13* gene using Human Genome Splice Finder (HGPS, version 3.0) was carried out in order to shed light on any splicing events that may arise within the gene owing to the mutation so observed. The analysis revealed that the nonsense mutation p.(Arg230*) within exon 4 of human *BUD13* activates a cryptic donor splice site (figure 9).

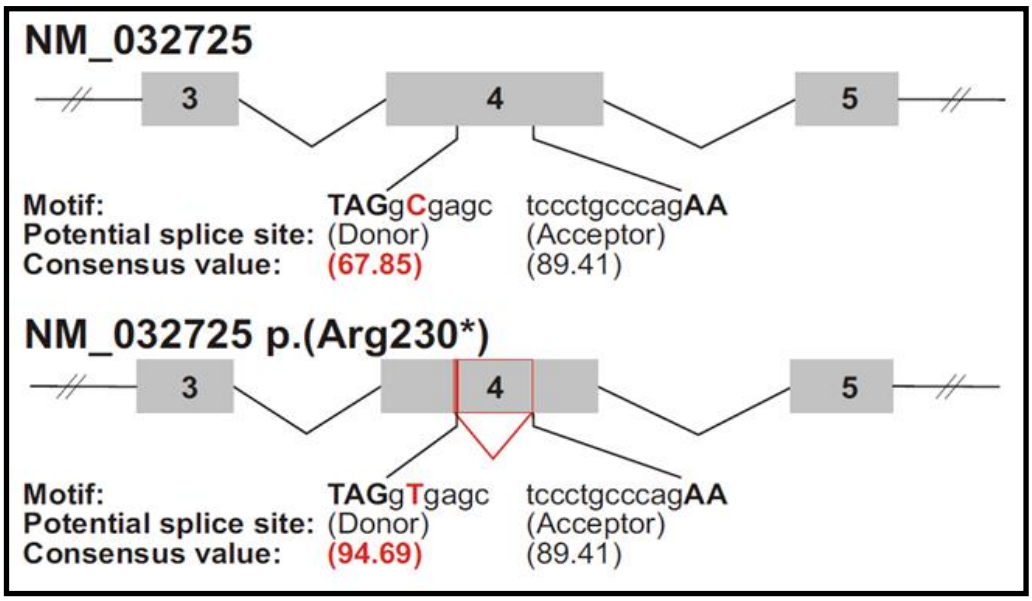

Fig.9. Bioinformatics splice site analysis using Human Genome Splice Finder (HGPS, version 3.0)- splice site anlysis uncovered the activation of a cryptic donor splice site in the presence of nonsense mutation p.(Arg230*) within exon 4 of human BUD13.

To further investigate these findings, we performed a qPCR and a massive reduction of *BUD13* mRNA expression was seen in the young individuals. Approximately, 80% reduction was observed in the relative mRNA expression of the affected gene in the young patient fibroblasts, meaning relative mRNA expression was only 20% of the wild type as seen in control fibroblasts (figure 10A). Interestingly, for the older patients investigated much later, this reduction was observed to be only 50%, as opposed to the 80% in younger patients, resulting in a residual *BUD13* gene expression of about 50% in the older patients. Following this, cDNA amplification (RT-PCR) using primers in exons adjacent to the exon harboring the nonsense mutation showed one additional band in the patient/mutant fibroblasts only, indicative of alternative splicing events (figure 3B). Sanger sequencing performed on cDNA revealed an in-frame deletion of 54 amino acid residues in isoform 1 or S1 (64kD) (figure 10B & 11). The residual 20% and 50%, in the two respective groups of patients, are most likely a consequence of the presence of splice isoform 1, which is not present in healthy individuals (figure 12). Furthermore, in line with the qPCR experiments, a higher expression of splice form 1 is observed in the older patients.

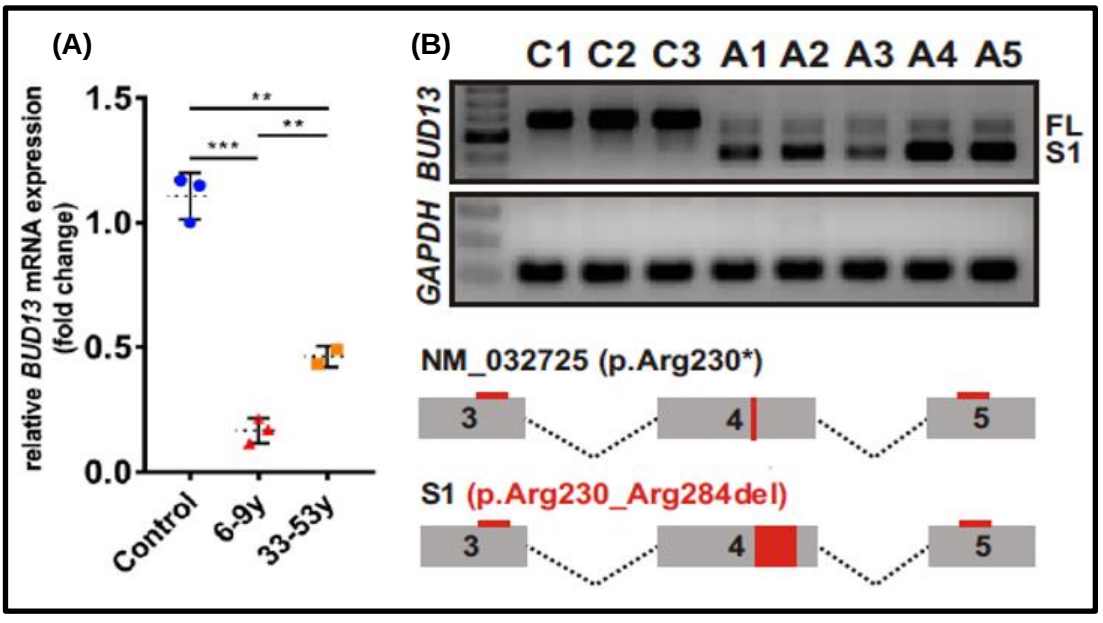

Fig.10. Molecular genetic findings in mutant HAFs from PCR-based approaches- A) qPCR findings- Relative mRNA expression using cDNA from adult human fibroblasts from three control (C1, C2, & C3) and five patient (A1, A2, A3, A4 & A5) cell lines respectively. An 80% reduction was seen in the relative mRNA expression of the affected *BUD13* gene in the younger individuals

(6-9years old) as opposed to the 50% reduction observed in the older ones (33-53 years old). (B) RT-PCR findings- Oligonucleotide primer sequences spanning the nonsense mutation were used to investigate cDNA from the five patient and three control cell lines respectively. One novel isoform (*BUD13-S1 or S1*) was only seen in the affected individuals.

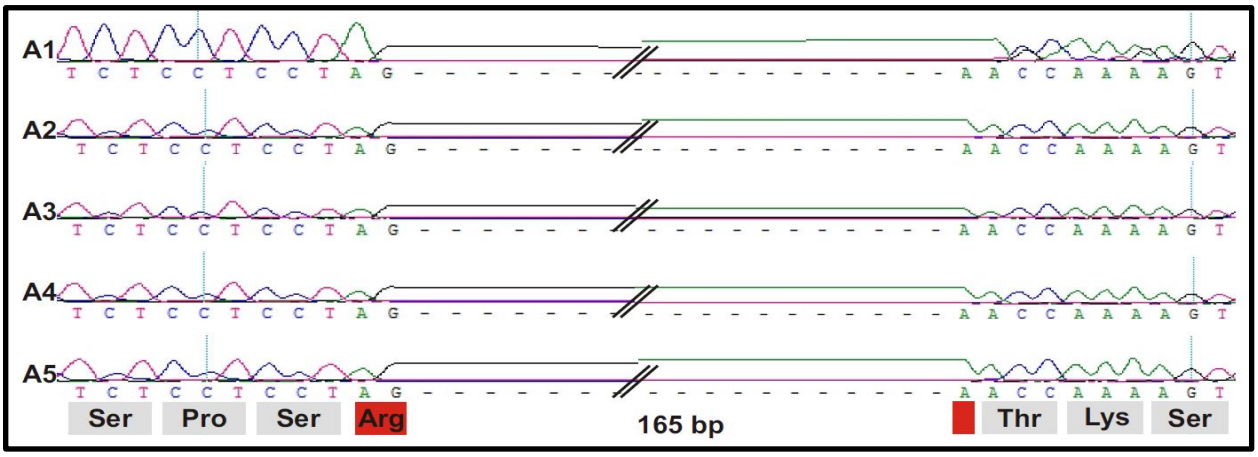

Fig.11. Sanger sequencing findings for all mutant patient HAFs for *BUD13-S1*- All the patients displayed the exact same alternative splicing pattern with an in-frame deletion of 165 base pairs within *BUD13* leading to the generation of *BUD13-S1*.

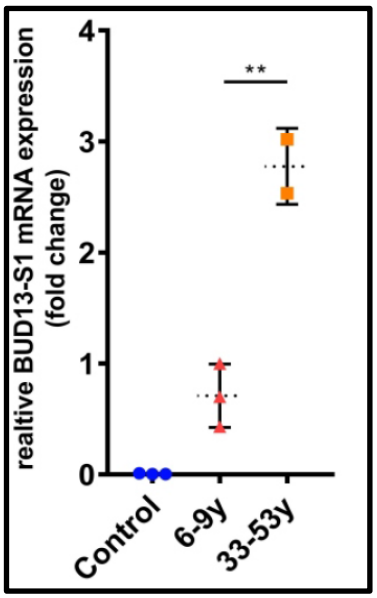

Fig.12. qPCR findings for *BUD13-S1*- Relative mRNA expression of splice form 1 of *BUD13* (*BUD13-S1*) using cDNA from adult human fibroblasts. The relative mRNA expression of *S1* in the older patients (33-53 years old) was almost three times than that observed in the younger patients (6-9years old).

Immunoblotting experiments confirmed the same discrepancy between the two groups of patients, as observed in the PCR based approaches, and in addition revealed the stability of the splice form at the protein level (figure 13).

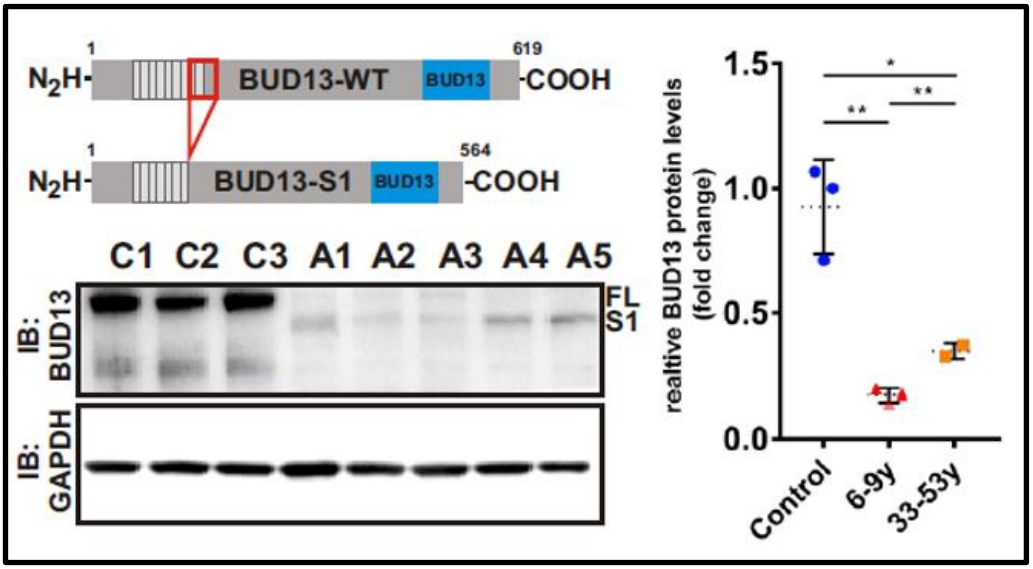

Fig.13. Schematic overviews of splice form 1 (S1) as observed for the affected protein in the patient fibroblasts. Sanger sequencing revealed that Splice form 1 leads to a deletion of 54 amino acids. Immunoblotting (IB) findings- Whole-cell lysates (10ug protein/lane) from control and patient fibroblasts were separated by 4-12% gradient gel SDS-PAGE and immunoblotted with antibodies against BUD13. Equal protein loading was confirmed by re-blotting with anti-GAPDH antibody. S1-BUD13 protein was found to be relatively more abundant in the cells from the older patients.

Both established literature and protein databases (*Ensembl*, *Uniprot*) indicated that in terms of subcellular localisation, the protein normally localises to the nucleus. To assess the impact of the mutation on the normal nuclear localisation of the BUD13 protein, transient heterologous overexpression was carried out using jetPEI® mediated transfection in HeLa and U2OS cell lines followed by visualisation of the cellular localisation of the proteins using immunofluorescence. The results displayed that both

the BUD13-WT and BUD13-S1 green fluorescent fusion proteins (GFP) normally translocate into the nucleus (figure 14).

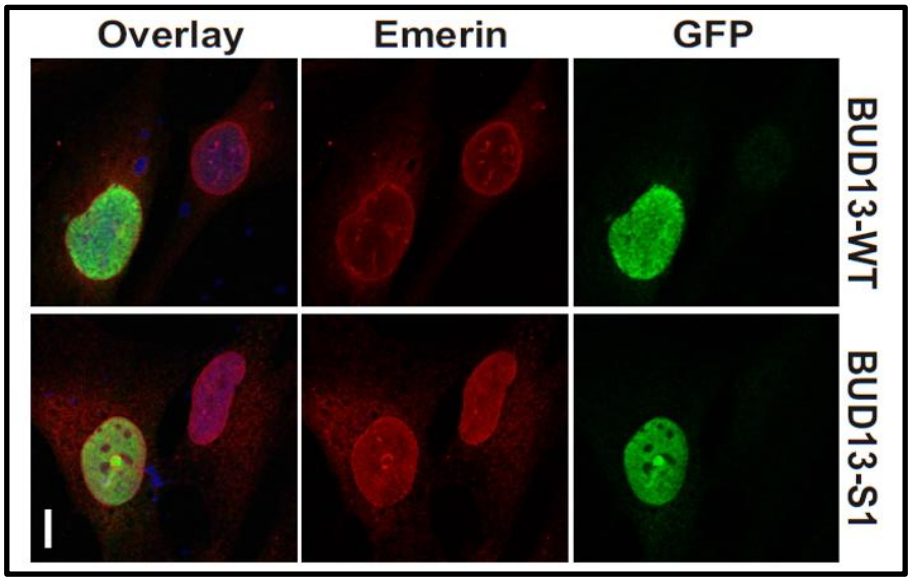

Fig.14. Heterologous overexpression of BUD13-WT and BUD13-S1 GFP fusion proteins in HeLa cells - 250,000 cells/ml were transfected with 2µg plasmid DNA in 1ml of DMEM High glucose medium containing 5% FCS, and 1% Ultra glutamine using jetPEI® transfection (Polyplus) for 8 hours followed by fixation with 4% PFA and staining with anti-Emerin (1:1000) and anti-GFP (1:1000). Cells were visualised under the 40X objective of the confocal microscope.

3.2.3. Transcriptomic Analysis of Patient Fibroblasts

Speculating a splicing defect at the beginning of the project, we sequenced the mRNA isolated from the cultured fibroblasts of only the young individuals in order to analyse global gene expression patterns and uncover novel RNA species and dysregulated pathways. We compared the patient fibroblasts against control cell lines for the given assessment (supported by *Geno Splice* and Alexander Neumann, Heyd group, Free University). The polyadenylation approach was adopted for such an analysis of the transcriptome. It is based on capturing and sequencing most mRNAs carrying a poly(A) tail from total cellular RNA.

Firstly, the RNA-seq identified a striking reduction of the *BUD13* mRNA in all affected individuals (figure 15B). A closer inspection of the transcriptome data revealed altered splice events within the affected *BUD13* exon 4 as was also uncovered in the molecular genetic analysis (figure 15A). However, very few genes with differential alternative splicing patterns and intronic retention were identified. Additionally, the global intron retention rate was not significantly elevated in the young patient fibroblasts (figure 16A). The data were specifically checked for intronic 4 retention in *IRF7* pre-mRNA processing following up from the findings in mouse-bone-marrow-derived macrophages by Frankiw et al., in 2019. However, no anomalies in the patient fibroblasts were observed.

The data upon detailed analysis uncovered 125 genes to be significantly dysregulated (upon considering genes to be differentially expressed when minimal expression change is 20%; Anders S and Huber W, 2012) in cultured fibroblasts from the young individuals (figure 16B). Of particular notice with subsequent qPCR validation was the upregulation of *p21* mRNA expression (discussed further in section 3.5. Cellular Senescence) and the downregulation of the *MAF* gene (encoding a transcription factor) known to play a role in embryonic lens development and chondrocyte terminal differentiation (figure 17). At the later stages of the project upon the discovery of newer patients, we additionally investigated the fibroblasts from the old patients to check for *p21* and *MAF* expression using qPCR. Notably, unlike the young patients, there were no significant changes in gene expression.

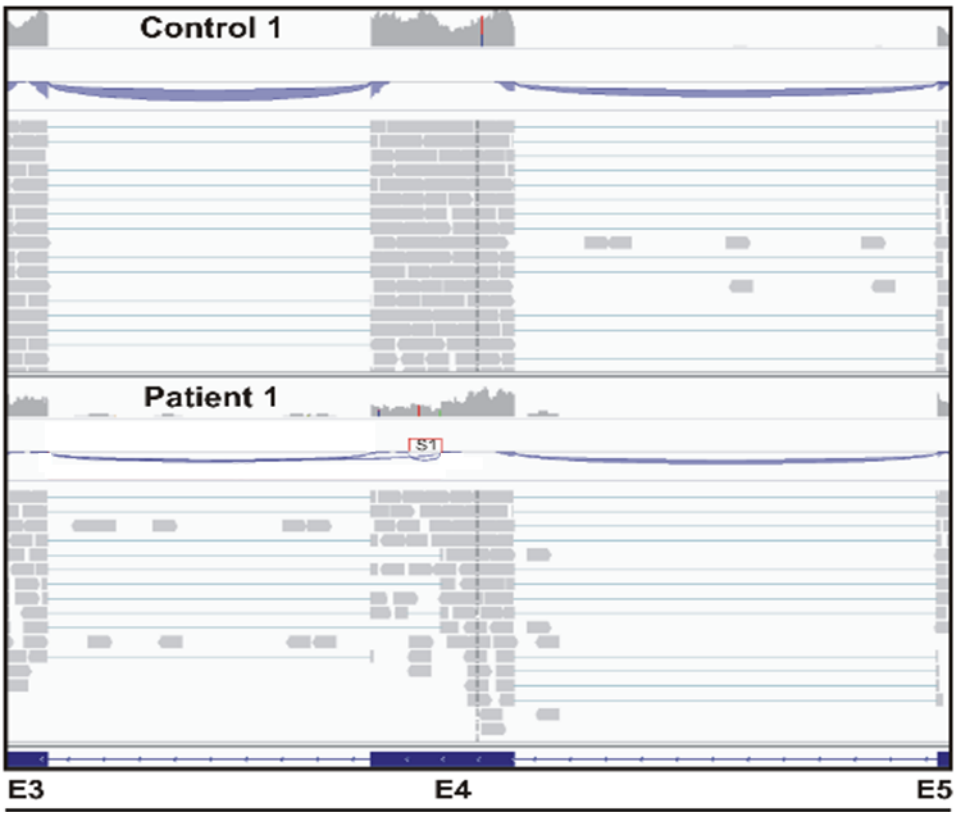

Fig.15. RNA-seq findings for patient fibroblasts (A) Variant Calling Format (Vcf) file screenshot as observed using Integrated Genomics Viewer- Transcriptomic data revealed alternative splicing within the *BUD13* gene to generate a new splice isoform. Fewer reads (in grey blocks) map to exon 4 of *BUD13* in the event of the nonsense mutation as is specifically shown for patient 1 in the lower panel compared to control 1 in the upper panel for comparison.

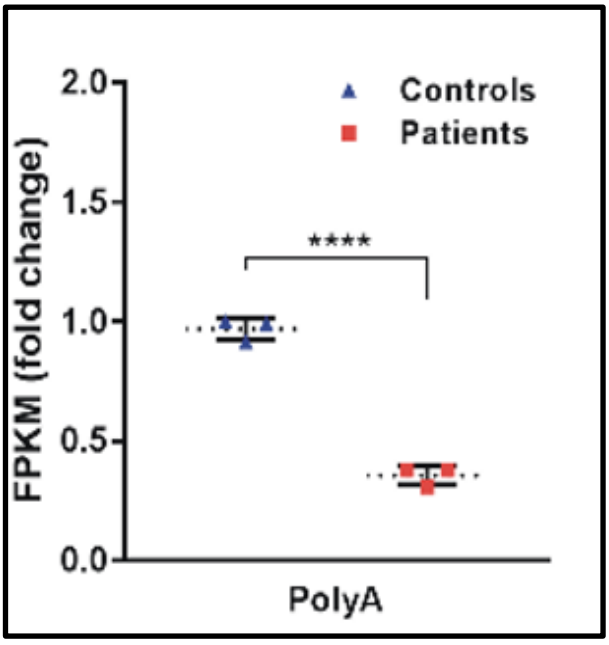

Fig.15. (B) Reduced *BUD13* mRNA in all affected individuals as revealed by the polyadenylation (PolyA) approach.

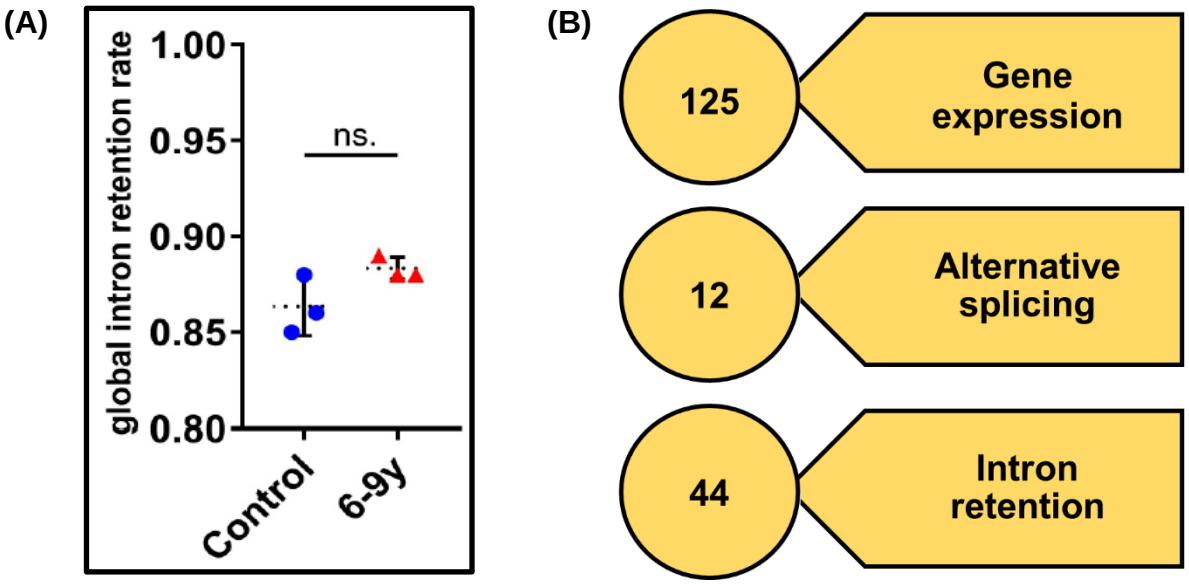

Fig.16. Analysis of ~27,159 genes via the polyadenylation approach for RNA sequencing in cultured fibroblasts from the young individuals as compared to control cell lines.(A) Global intron retention rate was not significantly altered in the young patient fibroblasts compared to control cell lines. (B) Schematic overview of number of events identified for differential gene expression, alternative splicing and intronic retention.

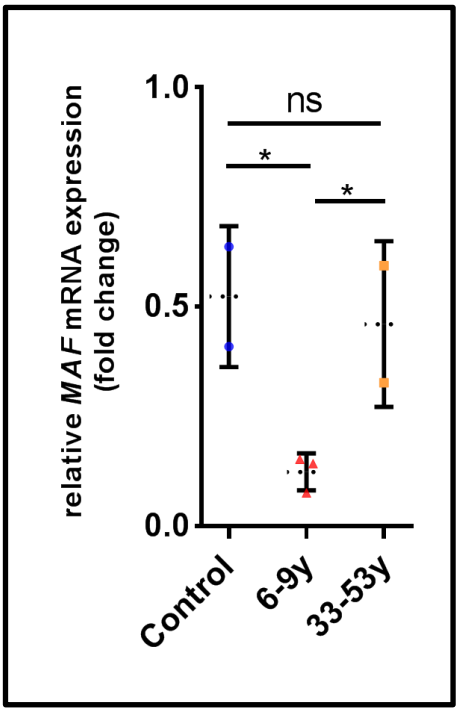

Fig.17. qPCR validation for *MAF* gene expression- *MAF* was found to be downregulated (*<=0.05) in the cultured fibroblasts from the young individuals as opposed to both the controls and the fibroblasts from the old individuals.

Interestingly, combining data from Gene Ontology (GO) analysis and pathway analysis (KEGG and REACTOME) on dysregulated genes revealed the mitotic cell cycle pathway to be the most highly dysregulated pathway, with both the approaches indicating a severe downregulation of several genes involved in mitotic cell cycle division such as *CDC25B* (cell division cycle 25B), *CENPF* (centromere protein F), and *CDKN2B (cyclin-dependent kinase inhibitor 2B/ p15).*

A proteomics analysis was also simultaneously carried out alongside RNA-seq to systematically identify and quantify the proteome of the cultured fibroblasts from the young individuals (supported by David Meierhofer, Mass Spectromtery Facility, Max Planck Institute for Molecular Genetics). The experimental approach involved quantitative mass spectrometry using the metabolic labeling technique of stable isotope labeling with amino acids in cell culture (SILAC) strategy (Meierhofer et al., 2008). The differentially labeled samples are mixed at an early stage of the experimental procedure and analysed together by liquid chromatography with tandem mass spectrometry (LC-MS/MS). The peptide peaks of the differentially labeled samples are then quantified relative to each other, providing the peptide and protein ratios.
The topmost dysregulated pathways as revealed by KEGG analysis were noted. Amongst the downregulated pathways, the lysosomal, the extracellular matrix (ECM) receptor interaction and the cell adhesion molecules (CAMS) were particularly interesting. A large number of amino acid metabolic pathways such as those of arginine, proline, alanine, aspartate, glutamate and tryptophan were found to be significantly upregulated. It was further noteworthy that fatty acid metabolism and peroxisome pathways were also significantly upregulated (figure 18).

A closer look at the cross-section of the two datasets from proteomics and RNA-seq analysis revealed a large number of dysregulated genes encoding proteins for ribosomal subunits or proteins involved in ribosomal biogenesis such as RPS2, RPL13, and RPL18A etc. Strikingly, the intersection between 125 dysregulated genes from our RNA-seq analysis with the eCLIP peak file dataset against BUD13 (Nussbacher J.K. and Yeo G.W., 2018) uncovered 20 genes to have eCLIP peaks with BUD13 of which 7 were ribosomal protein encoding genes (including candidates RPS2, RPL13, and RPL18A). RPL18A, encoding the 60S ribosomal protein L18a, was noted to have the highest number of eCLIP peaks amongst all the 20 genes (figure 19); eCLIP or enhanced UV

Crosslinking Immunoprecipitation is a highly specific method to study RNA-binding proteins (RBPs) in order to capture their endogenous direct RNA targets. It has been demonstrated to show a large-scale robust profiling enabling integrative analysis of diverse RBPs revealing factor-specific profiles, common artefacts of CLIP and RNA-centric perspectives on RNA-binding protein activity (Van Nostrand EL et al., 2016). In their study, Nussbacher J.K. and Yeo G.W utilised two open resources made available via ENCODE- 365 immunoprecipitation-grade RBP antibodies (Sundaraman et al., 2016) and eCLIP dataset for 126 RBPs (Van Nostrand EL et al., 2016) in order to systematically uncover RBPs regulating microRNA levels.

downregulated

1	KEGG_LYSOSOME
2	KEGG_SNARE_INTERACTIONS_IN_VESICULAR_TRANSPORT
3	KEGG_DILATED_CARDIOMYOPATHY
4	KEGG_HYPERTROPHIC_CARDIOMYOPATHY_HCM
5	KEGG_ECM_RECEPTOR_INTERACTION
6	KEGG_CELL_ADHESION_MOLECULES_CAMS
7	KEGG_ARRHYTHMOGENIC_RIGHT_VENTRICULAR_CARDIOMYOPATHY_ARVC
8	KEGG_FOCAL_ADHESION
9	KEGG_PORPHYRIN_AND_CHLOROPHYLL_METABOLISM
10	KEGG_EPITHELIAL_CELL_SIGNALING_IN_HELICOBACTER_PYLORI_INFECTION

upregulated

1	KEGG_PYRIMIDINE_METABOLISM
2	KEGG_ARGININE_AND_PROLINE_METABOLISM
3	KEGG_PURINE_METABOLISM
4	KEGG_ALANINE_ASPARTATE_AND_GLUTAMATE_METABOLISM
5	KEGG_TRYPTOPHAN_METABOLISM
6	KEGG_SYSTEMIC_LUPUS_ERYTHEMATOSUS
7	KEGG_PEROXISOME
8	KEGG_FATTY_ACID_METABOLISM
9	KEGG_LIMONENE_AND_PINENE_DEGRADATION
10	KEGG_GAP_JUNCTION

Fig.18. Proteomics analysis findings- Top 10 significantly dysregulated pathways (*=< 0.05) as revealed by the analysis of the complete proteome of cultured fibroblasts from the young patients.

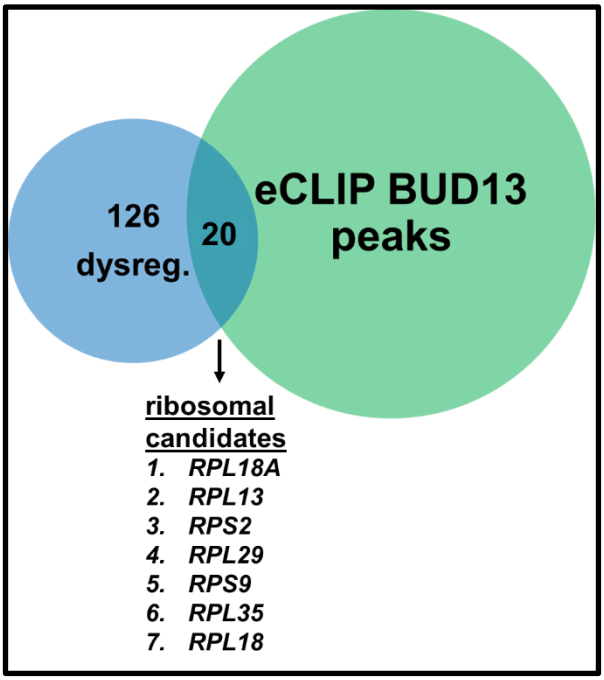

Fig.19. Intersection between dysregulated genes from RNA-seq analysis with eCLIP dataset against BUD13 (Nussbacher J.K. and Yeo G.W., 2018)- 20 dysregulated genes from RNA-seq analysis have eCLIP peaks with BUD13 including ribosomal protein encoding genes.

3.3. Impact of BUD13 deficiency on cellular pathways also involved in ageing

3.3.1. Mitochondrial changes

Given the implication of extensive cellular damage from ROS accumulation (reactive oxygen species) leading to subsequent oxidative damage in both physiological ageing (Green et al., 2011) and human progeroid disorders such as autosomal-recessive cutis laxa type 3, Gorlin-Chaudhry-Moss Syndrome, Cockayne syndrome and Werner syndrome (Ehmke et al., 2017; Fischer, B et al., 2012, Batenburg NL et al., 2015, Werner et al., 2006), we checked for the possibility of an elevated ROS in cultured fibroblasts isolated from the young individuals (6-9 y) and detected an elevated ROS in these fibroblasts (figure 20).

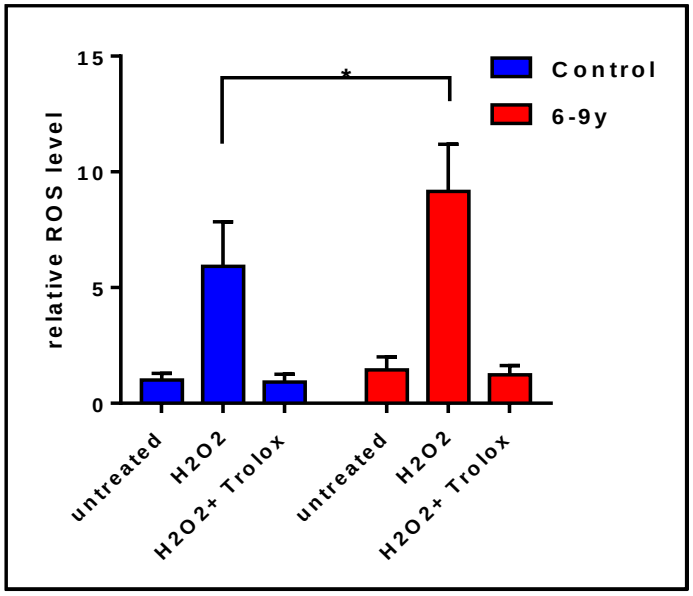

Fig.20. ROS aasay for patient HAFs- Increased production of reactive oxygen species (ROS) indicative of oxidative stress in cultured fibroblasts cultured from the young individuals (*<=0.05).

3.3.2. DNA damage

Since the closest differential diagnosis for patients with mutated *BUD13* is Cockayne syndrome, a progeroid disorder known to have an underlying defective DNA repair

pathway and also linked to a marked increase in ROS production (Rivera-Torres et al., 2013; Scheibye-Knudsen et al., 2013), we investigated DNA damage response in the young patient fibroblasts as the next step.

Preliminary immunofluorescence experiments (figure 21) with the fibroblasts from the young individuals (6-9 years) did not reveal an altered recruitment of proteins involved in early DNA damage (double strand breaks) response following UV- irradiation (60,000 microjoules/cm^2 for 60 seconds). We assessed the DNA damage response using two markers, namely phosphorylation of H2AX (γ-H2AX) and the recruitment of 53-BP1 almost immediately post UV-irradiation (0h/ zero hour) (Mariotti LG et al., 2013).

Strikingly, a closer look revealed a reduction of the core H2AX protein in the high-passaged fibroblasts from young individuals (figure 22 (A)) as compared to passage-matched control fibroblasts. The blot when repeated in order to check for the same in the older individuals did not reveal any changes in core H2AX protein expression. Consequently, upon checking for γ-H2AX in all the individuals, a reduced total γ-H2AX was uncovered in the young patients only (figure 22 (B)).

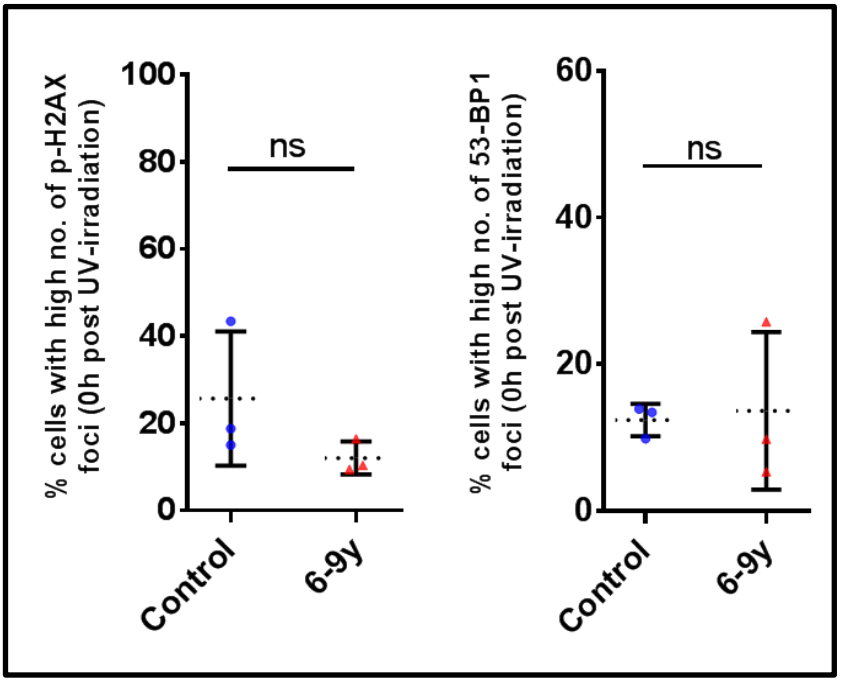

Fig.21. DDR assays in patient HAFs using γ-H2AX and 53-BP1 responses- Two independent experiments to assess γ-H2AX and 53-BP1 responses respectively post UV-irradiation (60,000

microjoules/cm^2) in human adult fibroblasts from the young individuals. Following irradiation for 60 seconds, cells were fixed immediately using 4% PFA followed by staining with anti- Gamma-H2AX (1:500) or 53-BP1 (1:500) and visualized under the 40X objective of the confocal microscope. The average percentage of high number of the respective foci between the patient and control cell lines did not reveal a significant difference (ns>0.05).

(A)

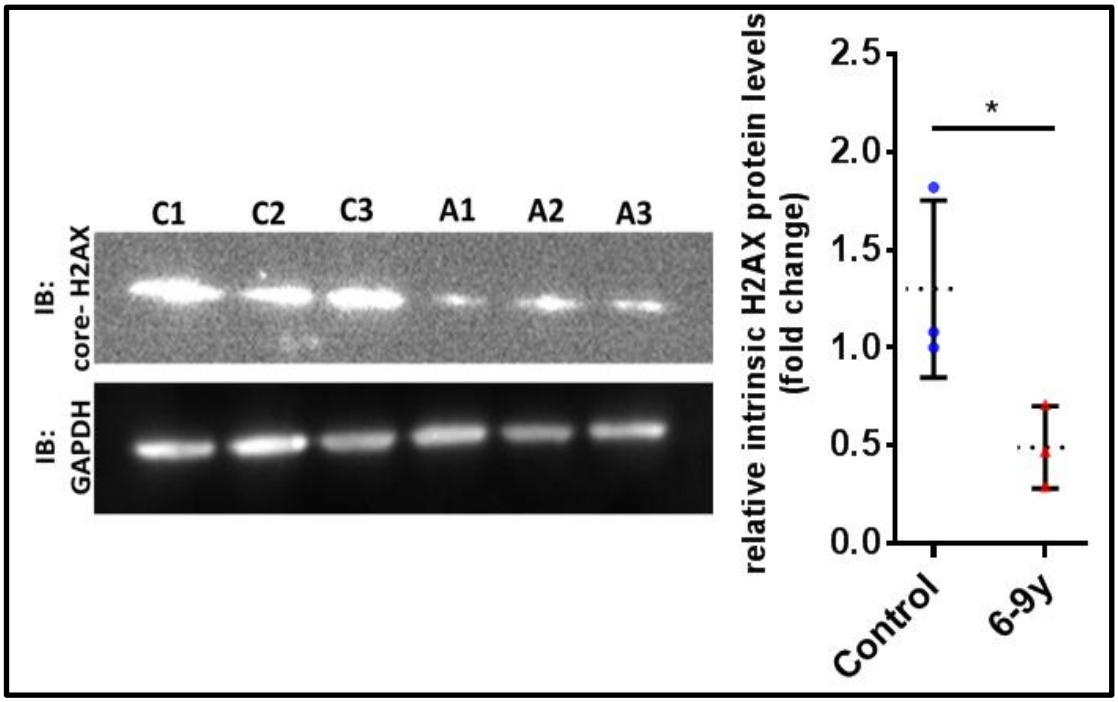

Fig.22. Western blotting results for core H2AX and γ-H2AX protein in patient HAFs- (A) Levels of H2AX (core H2AX) in the high passage (>P10) fibroblasts from the young individuals compared to passage-matched control fibroblasts. The fibroblasts from the young individuals displayed a reduced abundance of H2AX protein level. Whole-cell lysates (10ug protein/lane) from control and patient fibroblasts were separated by 4-12% gradient gel SDS-PAGE and immunoblotted with antibodies against H2AX. Equal protein loading was confirmed by re-blotting with anti-GAPDH antibody.

(B)

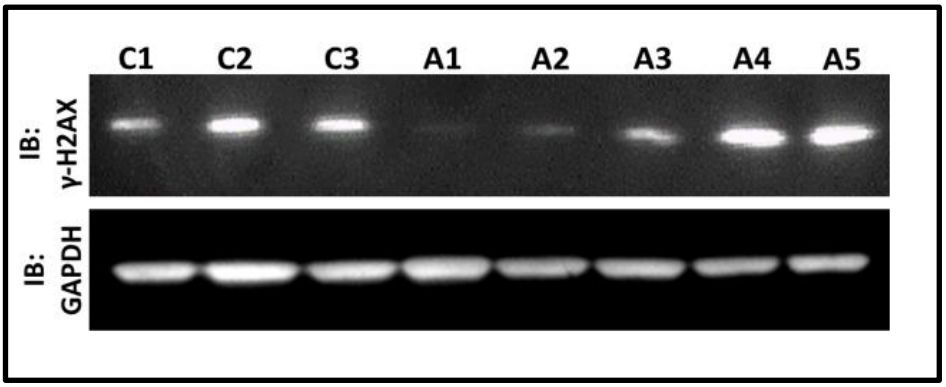

Fig.22. (B) Levels of γ-H2AX protein levels in the high passage matched fibroblasts from the young and the old individuals compared to passage-matched control fibroblasts. The fibroblasts from only the young individuals displayed a reduced abundance γ-H2AX which probably follows from a reduced expression of core protein.

3.3.3. Aberrant Nuclear architecture

Interestingly, further characterisation of the patient fibroblasts using Emerin staining in immunofluorescence revealed altered nuclear morphology in the patient fibroblasts. This finding is similar to the situation as seen in classical Hutchinson Gilford Progeria Syndrome (HGPS). Experiments using cells from HGPS patients have shown that the cell nucleus is highly lobulated owing to mutations in the LaminA/C protein leading to the formation of a toxic protein called as Progerin (Gonzalo et al., 2015). Enumeration showed that the younger patients had almost five times the percentage of invaginated cell nuclei compared to the controls while the older patients had twice as much relative to the control cell lines. There was no real consistency in the invaginations and the subsequent nuclear morphologies so observed (figure 23).

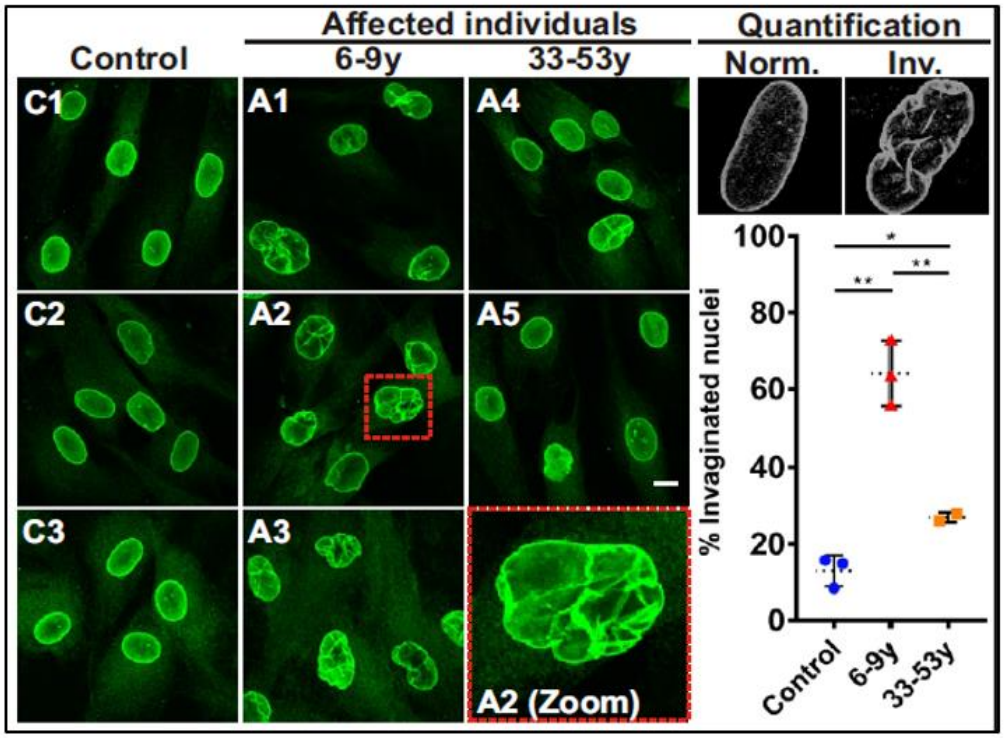

Fig.23. Immunofluorescence findings for aberrant nuclear architecture in patient HAFs - 200,000 cells/ml were seeded in DMEM High glucose medium containing 10% FCS, 1% Pen-Strep and 1% Ultra glutamine following which they were fixed with 4% PFA and stained with anti-Emerin (1:1000). Cells were visualised under the 20X objective of the confocal microscope. Enumeration revealed the highest percentage of invaginated nuclei in the younger patients compared to the control cell lines (*<=0.01; **<=0.05).

We followed this up with a western blot in order to check for the abundance of Lamin A/C protein in all the patient cells. The blot revealed changes neither in Lamin A nor in Lamin C protein abundance and the possibility of progerin expression was also ruled out (figure 24). Chromosomal abnormalities were also not detected upon examination of metaphase chromosomes post cell synchronisation (data excluded).

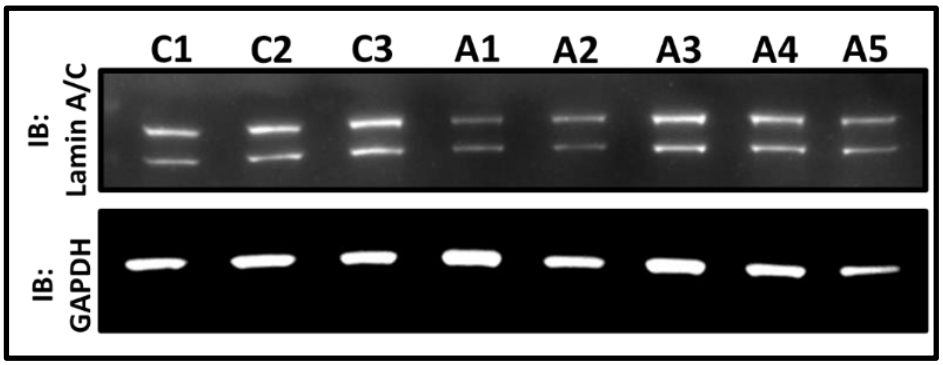

Fig.24. Western blotting findings for Lamin A/C protein- (A) Lamin A/C protein expression using immunoblotting. Whole-cell lysates (10ug protein/lane) from control and patient fibroblasts were separated by 4-12% gradient gel SDS-PAGE and immunoblotted with antibodies against Lamin A/C. Equal protein loading was confirmed by re-blotting with anti-GAPDH antibody.

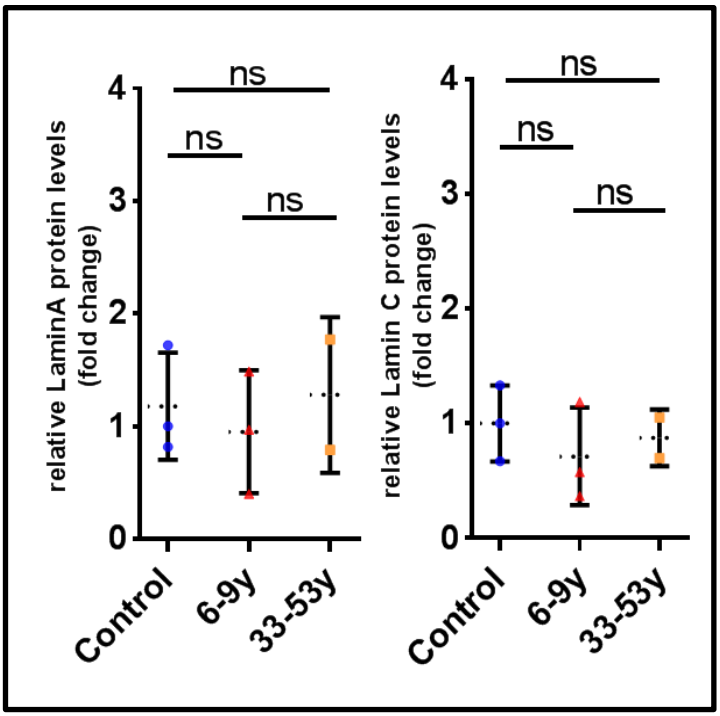

Fig 24. (B) No significant differences in protein abundance were observed between the patient and control cell lines (ns>0.05).

Interestingly, the overexpression of BUD13-S1 apparently led to nuclear invaginations in the cells, a phenotype which is also seen in the patient fibroblasts. Quantification revealed quite a significantly higher percentage of cells with invaginated nuclei transfected with BUD13-S1 as opposed to BUD13-WT protein (figure 25)

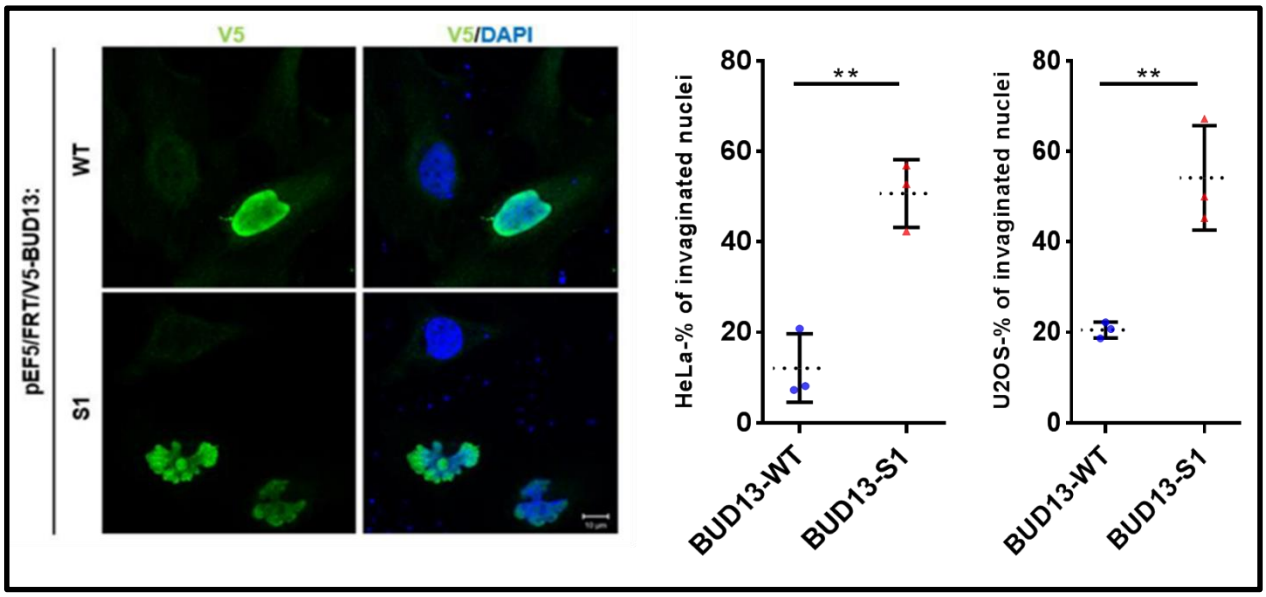

Fig.25. Heterologous overexpression of V5 tagged BUD13-WT & S1 respectively in HeLa and U2OS cell lines- Cells transfected with pEF5/FRT/BUD13-WT-V5 exhibited normal nuclear morphology compared to those transfected with pEF5/FRT/BUD13-S1-V5 exhibiting nuclear invaginations, under the 20X objective of the confocal microscope. Cells were transfected using jetPEI® transfection (Polyplus) for 8 hours followed by fixation with 4% PFA and staining with Anti-V5 (1:1000) and counter staining with DAPI. A significantly higher percentage of both HeLa and U2OS nuclei were invaginated upon BUD13-S1 transfection (**<=0.01)

A closer look the transmission electron microscopy (TEM) images (supported by the Microscopy and Cryo-electron Microscopy service group, Max Planck Institute for Molecular Genetics), for cells from both the younger and the older individuals versus control cell lines, confirmed our findings from IF experiments with regards to abnormal nuclear architecture. In addition, the images revealed numerous electron dense granules in the cell cytoplasm of the younger patients only. The granules, qualitatively, appeared

far more numerous in these fibroblasts compared to the cultures fibroblasts from the older patients (figure 26).

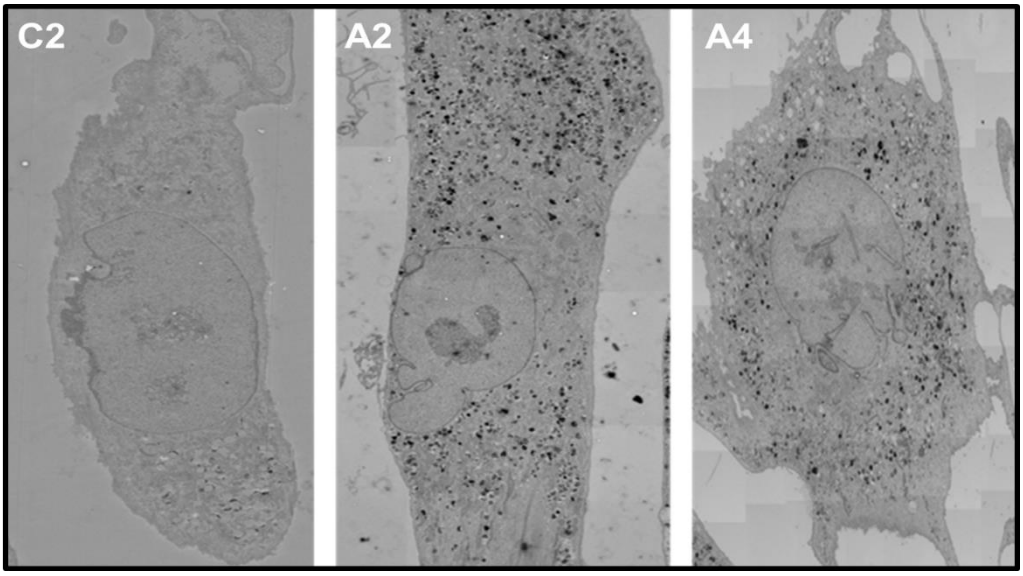

Fig.26. Transmission electron microscopy (TEM) images- HAFs from the young (6-9y, A2) and the old individuals (33-53y, A4) showed abnormal nuclear architecture in comparison to the control cell lines (C2). In addition, the images revealed numerous electron dense granules in the cell cytoplasm of the young patients only. In terms of numerosity of the granules, 6-9y>33-53y>Controls.

3.3.4. Defective Proteostasis

Suspecting an upregulation in lysosomal numbers in the cell cytoplasm from our TEM results, we checked for Cathepsin D protein expression, a proteolytic lysosomal enzyme, using fibroblasts from the patients and healthy control cell lines. A significantly higher relative expression of the heavy chain protein of the fully active mature protease was found in the cells of the younger individuals compared to the healthy controls and the older individuals respectively (figure 27). However, the relative protein abundance in the older patients was similar to that in the control cell lines.

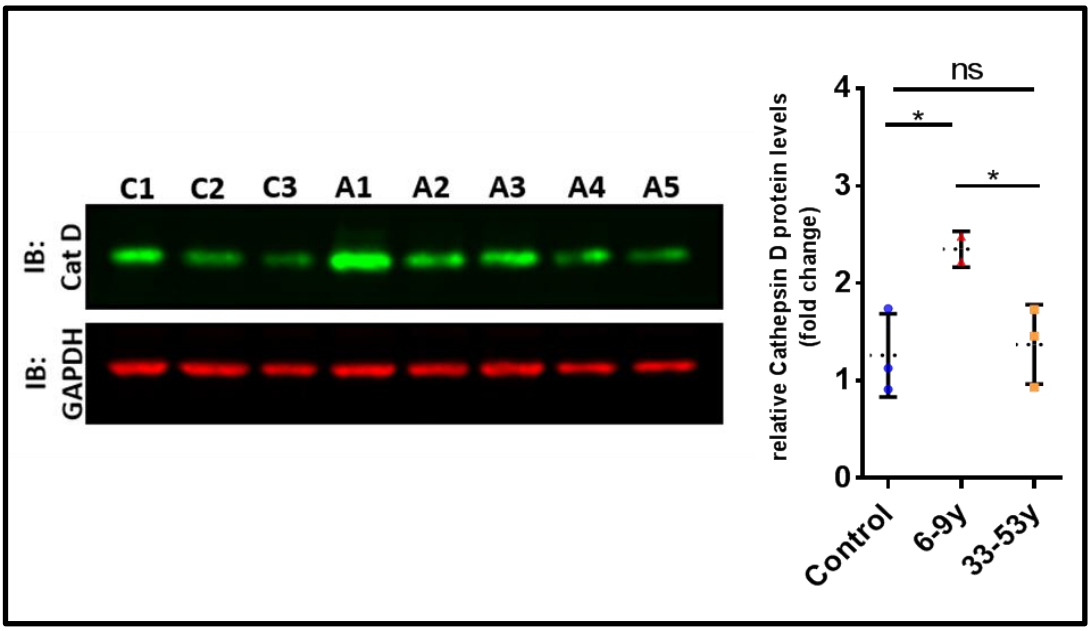

Fig.27. Cathepsin D protein expression using immunoblotting- Whole-cell lysates (10ug protein/lane) from control and patient fibroblasts were separated by 4-12% gradient gel SDS-PAGE and immunoblotted with antibodies against Cathepsin D. Equal protein loading was confirmed by re-blotting with anti-GAPDH antibody. Mature Cathepsin D protein levels were significantly elevated in the younger patients, relative to both the older patients' and control cell lines respectively. * = <0.005.

3.3.5. Cellular Senescence

In addition, upon checking for the presence of senescence-associated beta-galactosidase enzyme, a high percentage of patient fibroblasts displayed the typical blue colour of the enzyme-substrate reaction based assay (figure 28). This was indicative of a positive senescence associated beta-galactosidase staining. This observation is in line with the observation of a marked premature ageing phenotype. In tandem with our previous results, the older patients showed a lower percentage of cells exhibiting the blue colour associated with the senescent phenotype in comparison to the younger patients.

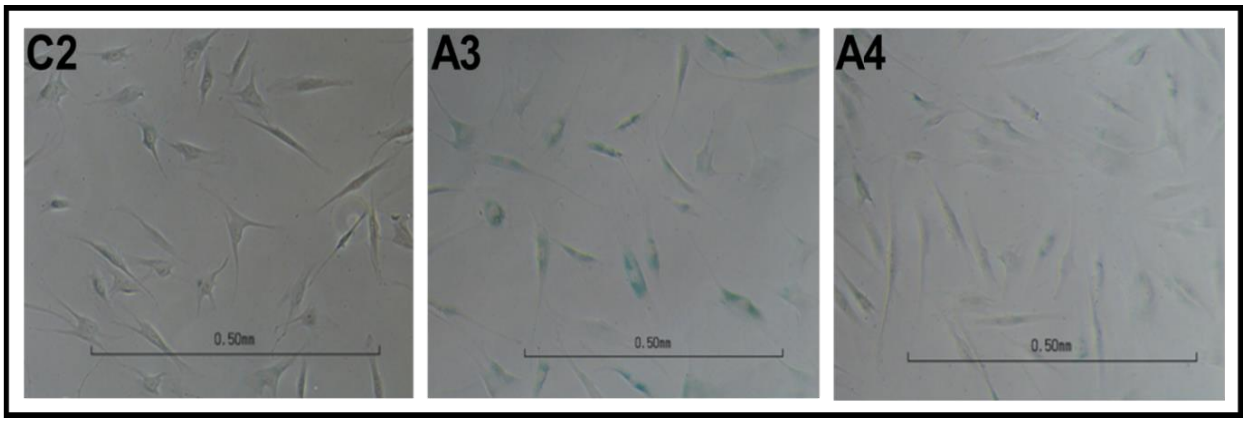

Fig.28. (A) Senescence-associated-beta-Galactosidase staining in patient HAFs- Senescence associated beta-galactosidase staining of control and patient (6-9years and 33-53years respectively) fibroblasts. Positive senescence-related beta-galactosidase stainings shown by the blue granules within cytoplasm were seen most patient cells compared to the control cell lines.

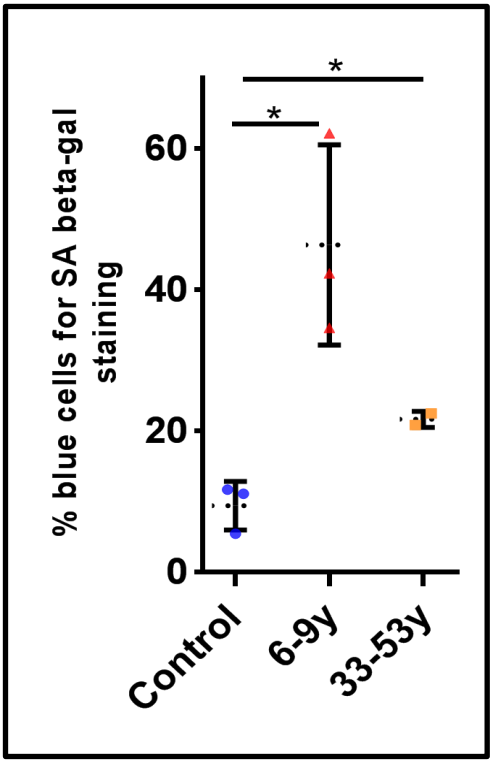

(B) Enumeration revealed the following order, when percentage of cells showing the typical blue colour indicative of positive senescence associated beta-galactosidase staining was calculated :

6-9y> 33-53y>Control (*<=0.05)

Also, in reference to our transcriptomic analysis findings, *p21* mRNA expression was found to be upregulated in the cultured fibroblasts from the young individuals (figure 29), which is interesting in the light of the fact that it encodes a cyclin-dependent kinase inhibitor (CKI) promoting cell cycle arrest in response to various stimuli. Additionally, we checked for p16 expression, another CKI known to regulate cellular senescence (Campisi et al., 2007), in cultured fibroblasts from all individuals. The results, however, despite repeated experiments were inconclusive for p16 expression.

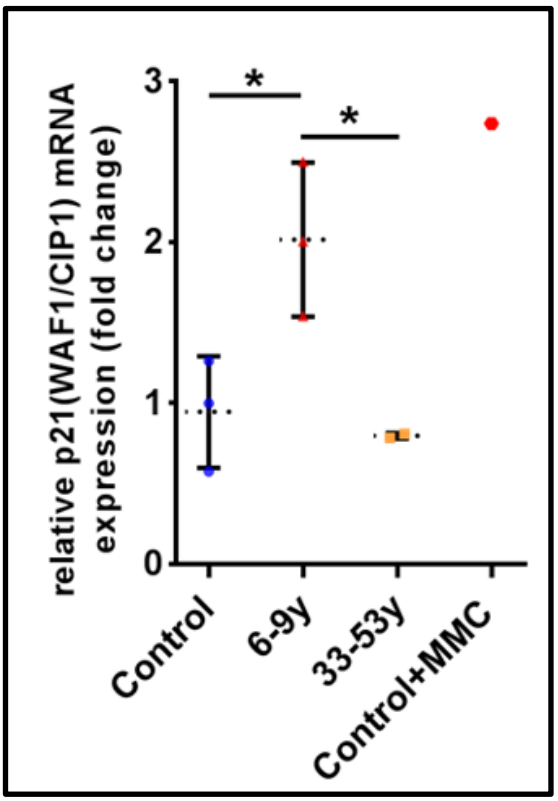

Fig.29. qPCR validation for *p21* gene expression- *p21* was found to be highly upregulated ($p<0.05$) in the cultured fibroblasts from the young individuals as opposed to both the controls and the fibroblasts from the old individuals.

The insertion of the exact human mutation in mice is possible using the CRISPR/Cas9 genome editing system. The recurrent nonsense human mutation in the *BUD13* gene, in spite of being exactly the same in all the patients, presented us with two contrasting phenotypes with features not simply limited to two sets of drastically varying life expectancies. It was hence vital to understand the downstream effects of the precise human mutation in the *Bud13* gene in a mouse model. In addition, it was also of interest to check for the effects, especially if any on global splicing, from the complete knockout of Bud13 protein. Reflecting on a ubiquitous expression of the Bud13 protein in mice as reflected by our qPCR results, we anticipated a multisystem disease manifestation upon genetic modification of the protein using CRISPR/Cas9.

3.4. Findings from Mouse model Investigations

The assessment of *Bud13* relative expression in various tissues and organs of healthy C57BL/6 or ‘’black 6 mice’’ revealed that the gene is highly expressed in the mouse long bone tissue and skin, and in the liver and kidney (figure 30).

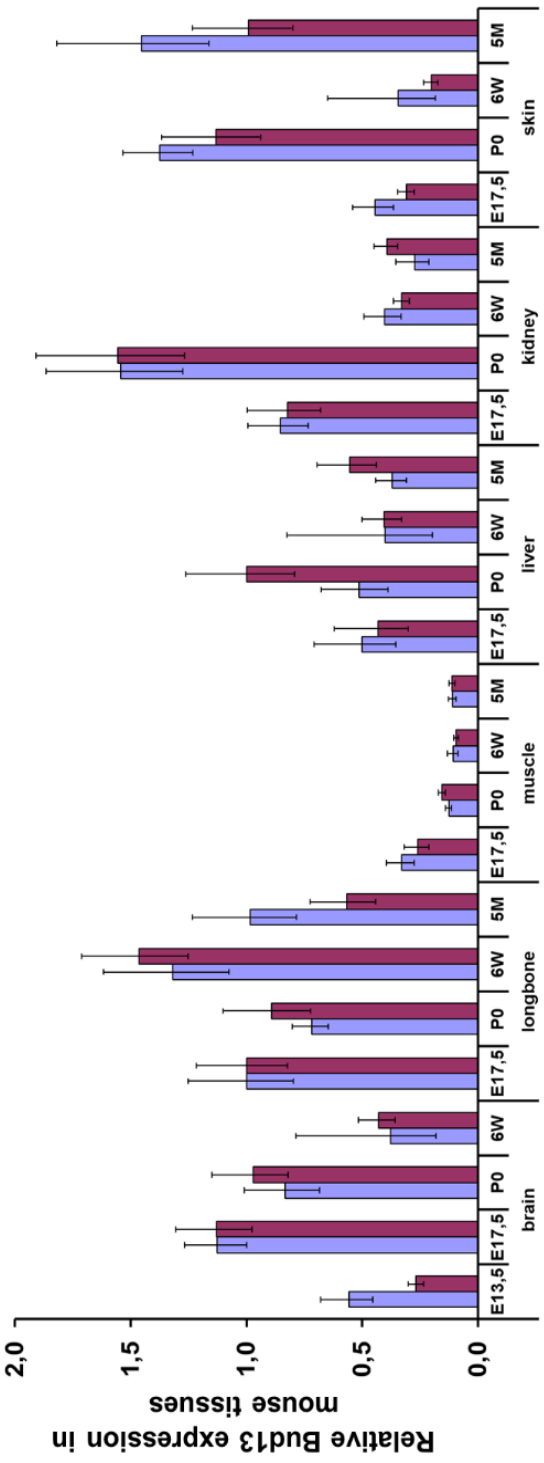

Fig.30. *Bud13* relative gene expression as assessed in different tissues/ organs of healthy black 6 mice using qPCR to check for mRNA expression.

CRISPR/ Cas9 Mediated Genome Editing in *Bud13*

The transversions, as seen in humans, were established using single strand oligonucleotides (ssODN) as templates containing the mutation and single guide RNAs (sgRNA) directing Cas9 activity. The ssODN serves as donor sequence during the repair of the double-strand break via non-homologous end joining (NHEJ) or homology-directed repair (HDR) in murine embryonic stem cells resulting respectively in a deletion or the knock-in of the desired mutation (figure 31).

Fig.31. Brief overview of CRISPR/Cas9 genome editing of mouse embryonic stem cells or mESCs (CRISPR scheme adopted from addgene.org)- repair of site directed double strand breaks (DSBs) via homology-directed repair (HDR) or non-homologues end joining (NHEJ) induced by Cas9 endonculease guided by one or more synthetic guide RNAs (sgRNAs). PAM or protospacer adjacent motifs follow the DNA cleavage site and are directly recognised and cut by Cas9.

Applying CRISVar (Kraft et al., 2015) for the generation of Bud13 mutant mice (supported by Malte Spielmann, Mundlos group, Max Planck Institute for Molecular Genetics and Miguel Rodriguez, Krawitz group, Charité Universitätsmedizin Berlin), mouse embryonic stem cells (ESCs) harbouring two kinds of *Bud13* exonic mutations were generated. The introduction of the exact human mutation p.(Arg230*) in mouse *Bud13* gene exon 4 (Bud13-106del) resulted in early embryonic lethality in the homozygous state. Additionally, since the guide selected for knocking in the human mutation p.(Arg230*) was predicted to have an off-target binding sequence located upstream of the nonsense

mutation, silent mutations were incorporated in the region to avoid a second cut by Cas9 enzyme following HDR. We hence ensured that any effect at the molecular and subsequently at the organismal level is due to only the knock-in so inserted at the genomic level. Furthermore, the examination of a second mouse embryonic stem cell clone (Bud13-113del) carrying a genomic frameshift mutation (p.Leu199Ilefs*11) led to the generation of viable chimeric animals reflecting some features of the human progeroid phenotype.

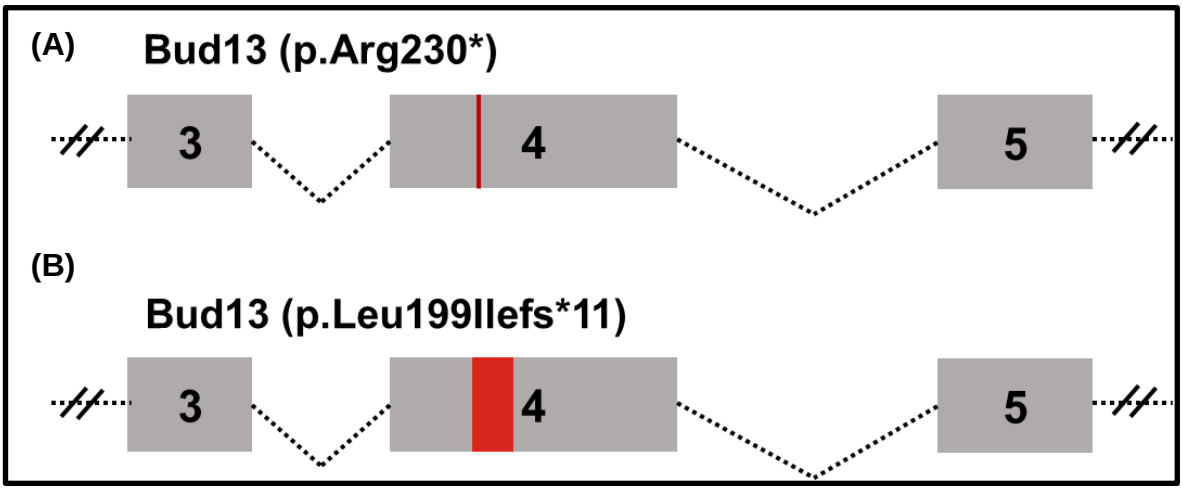

Fig.32. Scheme of the predicted consequences of different exonic *Bud13* mouse mutations at the genomic level- (A) insertion of the exact human mutation p.(Arg230*) and (B) frameshift mutation (p.Leu199Ilefs*11) in exon 4 of *Bud13*.

3.4.1. Molecular Genetic Analysis of *Bud13* Mutations in Mice

Bioinformatic in-silico splice predictions (*Fruitfly*) for the exact human mutation p.(Arg230*) in the mouse *Bud13* gene revealed a splicing event following the activation of a cryptic donor splice site, similar to that seen in humans. It was hypothesised that the human mutation in the murine system might lead to a viable germline knockout, which can serve to further investigate the pathomechanism of this novel progeroid syndrome. However, the aggregation of ESC clone did not even result in viable first generation chimeric animals. Molecular investigations in the mouse embryonic stem cells using RT-PCR (figure 33) revealed that the knock-in emulating the human mutation resulted in two alternatively spliced out products: first, a lowly expressed, larger isoform containing a

much larger deletion of 318 base pairs or in other words, a 106 amino acid in-frame deletion (compared to the much smaller, in-frame deletion of 55 amino acids generated by the human mutation) and a second, smaller isoform containing a premature termination codon.

We also simultaneously generated a second mouse model targeting a 75 base pair frameshift mutation (p.Leu199Ilefs*11) in the same exon carrying the human mutation p.(Arg230*), that is, exon 4 of the *Bud13* gene with the objective of studying the downstream effects of the knockout of the Bud13 protein. Molecular investigations presented that the genomic deletion leads to an alternative splicing event creating a product with an in-frame deletion of 339 base pairs or 113 amino acids. Interestingly, the splice site used in this case was not predicted via bioinformatics splice site analysis.

Immunoblotting results (figure 34) revealed a scenario, which was in tandem with our RT-PCR results. The larger splice isoform generated as a result of alternative splicing in *Bud13* in 106-del showed a very low protein level expression, somewhat reflecting a situation similar to that observed in our young patients (6-9 years) who had a less abundant splice form 1 (20%) of human BUD13. The smaller isoform arising from alternative splicing in the same model evidently underwent nonsense mediated decay owing to the premature termination codon and hence, was undetectable at protein level expression. On the other hand, the 113-del mice displayed an evidently higher Bud13 protein expression, representing a situation similar to that observed in the older patients (33-53 years) who had a higher abundance (50%) of splice form1 of BUD13 protein.

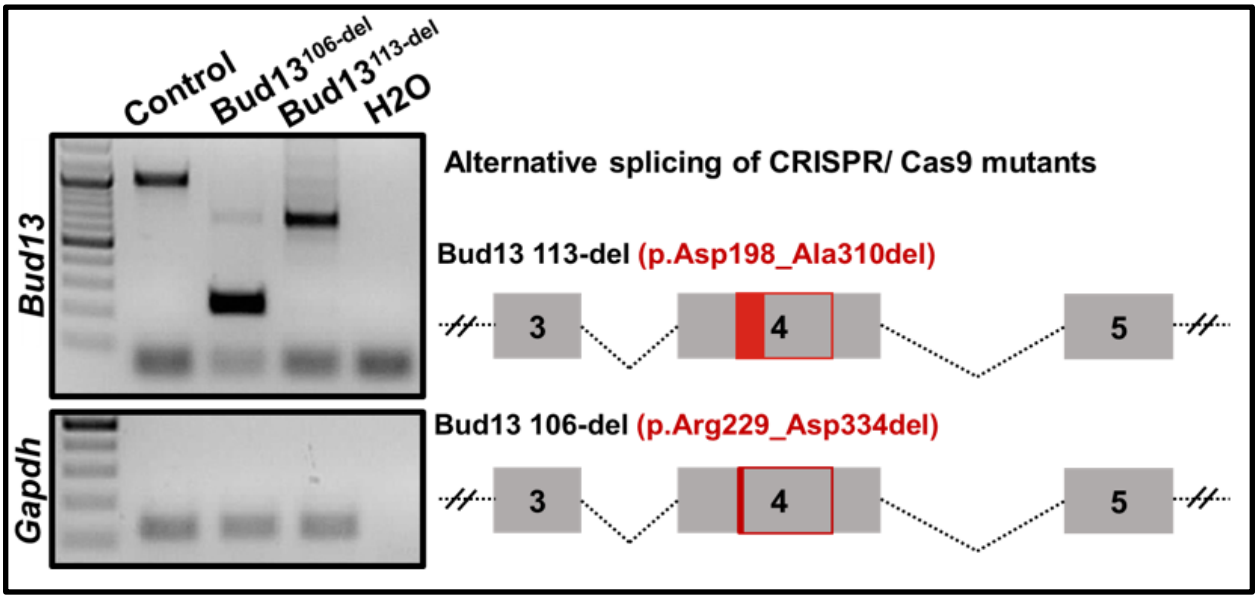

Fig.33. RT-PCR findings from mouse embryonic stem cells (Bud13-113del and Bud13-106del) - Oligonucleotide primer sequences spanning exon 4 of the mouse *Bud13* gene were used to investigate cDNA isolated from the mouse ESCs.

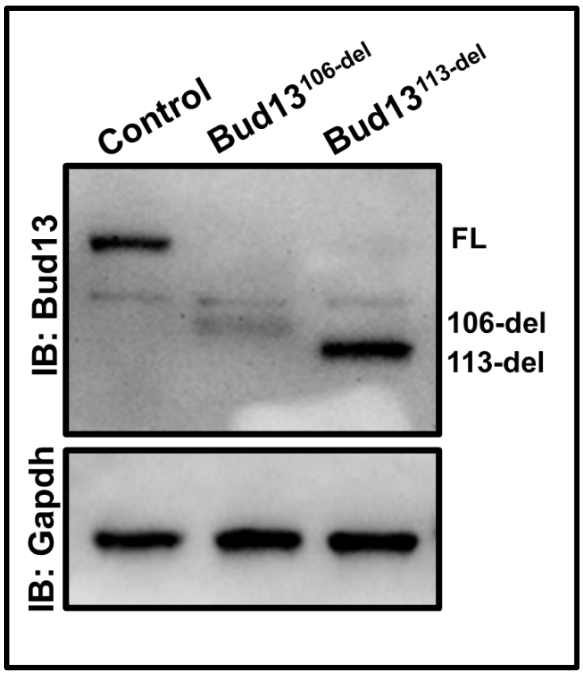

Fig.34. Immunoblot analysis of CRISPR/ Cas9 genome edited mouse embryonic stem cells (Bud13-106del and Bud13-113del) - alternative splicing events yielded a truncated Bud13 protein generated by a 106amino acid and 113 amino acid deletion respectively. The protein generated in the 106-del mouse model was evidently much less abundantly expressed than that generated in the 113-del mouse.

3.4.2. Findings from Aggregation of Mouse Embryonic Stem Cells (mESCs)

The aggregation of the mESCs for Bud13$^{106\text{-del}}$ did not lead to the generation of even chimeric animals, indicating that the residual expression of the Bud13 protein caused due to the knock-in of the exact human mutation and subsequent alternative splicing was apparently incompatible with life.

However, the aggregation of mESCs for Bud13$^{113\text{-del}}$ resulted in first generation (P_0) highly chimeric mice (*Bud13*$^{113\text{delCh}}$) that were generated using diploid aggregation. The animals were viable and were born without any sign of a disease phenotype.

The chimeras seemingly continued to grow normally. We crossed the chimeras, first with wild-type (WT) animals with an aim to obtain the F_1 generation of heterozygous (50% knockout) animals followed by inbreeding within F_1 to obtain the F_2 generation of homozygous (100% knockout) animals (scheme outlined in figure 28 pedigree). Genotyping experiments carried out to genetically stratify the offspring from the final crossing revealed only heterozygotes and wild type animals that is in strong contrast to the Mendelian ratio. We concluded that crossing of the germline heterozygotes did not give homozygotes. Additionally, investigation of embryos up to embryonic stage E8.5 animals also did not reveal any homozygotes. A homozygous knockout of the germline mutation for the Bud13 frameshift mutation was concluded to be embryonic lethal. The table in figure 28 summarises the various mouse *Bud13* mutations and the consequences so observed.

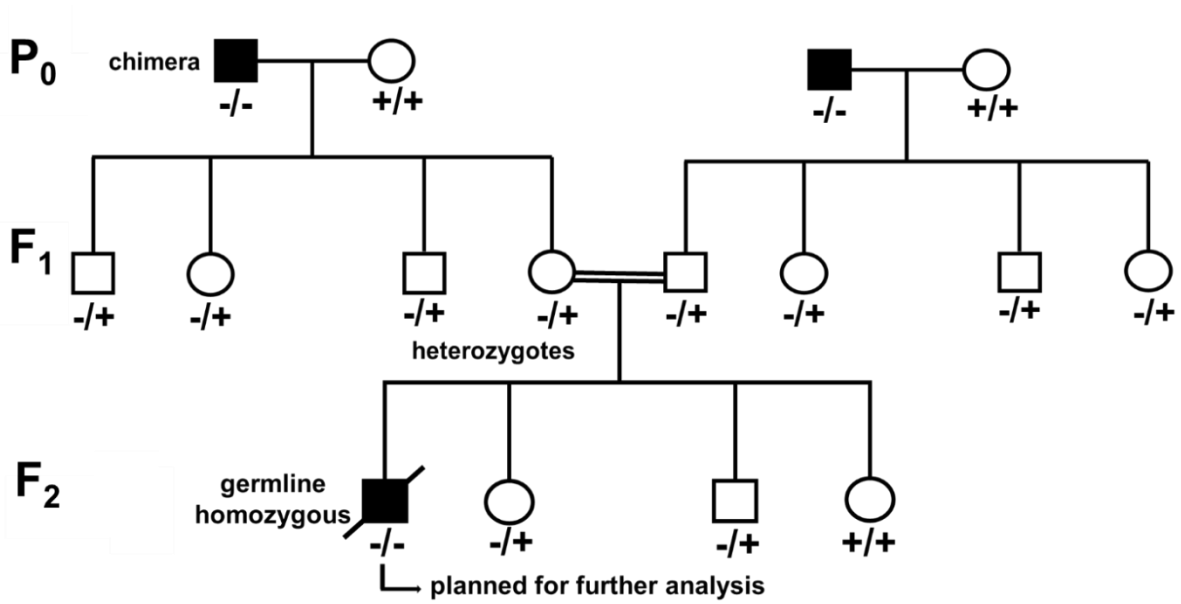

Fig.35. Pedigree chart representing the scheme for generation of various mouse lines aimed at ultimately generating mice carrying homozygous germline mutation for the *Bud13- 113-del* for further analysis. However, inter-litter mating between the germline heterozygotes from the same parent mice did not result in any germline homozygotes.

Predicted (genomic)	Alternative splicing of CRISPR/ Cas9 mutants	Protein expression	Chimera viability	Germline hetero	Germline homo
p.Leu199Ilefs*11	Bud13 113-del (p.Asp198_Ala310del) 	high	viable	possible	impossible
p.(Arg230*) knock-in	Bud13 106-del (p.Arg229_Asp334del) 	low	unviable	impossible	impossible

Fig.36. Consequences of mouse *Bud13* mutations- The modification of mouse embryonic stem cells using CRISPR/Cas9 yielded different outcomes at genomic-, RNA-, protein-, and organismal level.

Interestingly, the chimeric animal after approximately 20 weeks of life displayed a marked kyphosis. In comparison to the control animals, the *Bud13*^{113delCh} mice progressively lost body weight and exhibited variable lens clouding (figure 37). Fat pad analysis from the

two fat depots, namely scapulae fat and gonadal fat of these animals uncovered a reduced subcutaneous fat content compared to the control animals (figure 38). In addition, histological staining using eosin and hematoxylin revealed a much smaller diameter of the fat cells/ adipocytes in the experimental animals compared to the controls (figure 39). *Bud13*^{113delCh} mice ultimately died around the 38th week of life reproducing several aspects of the human progeroid condition.

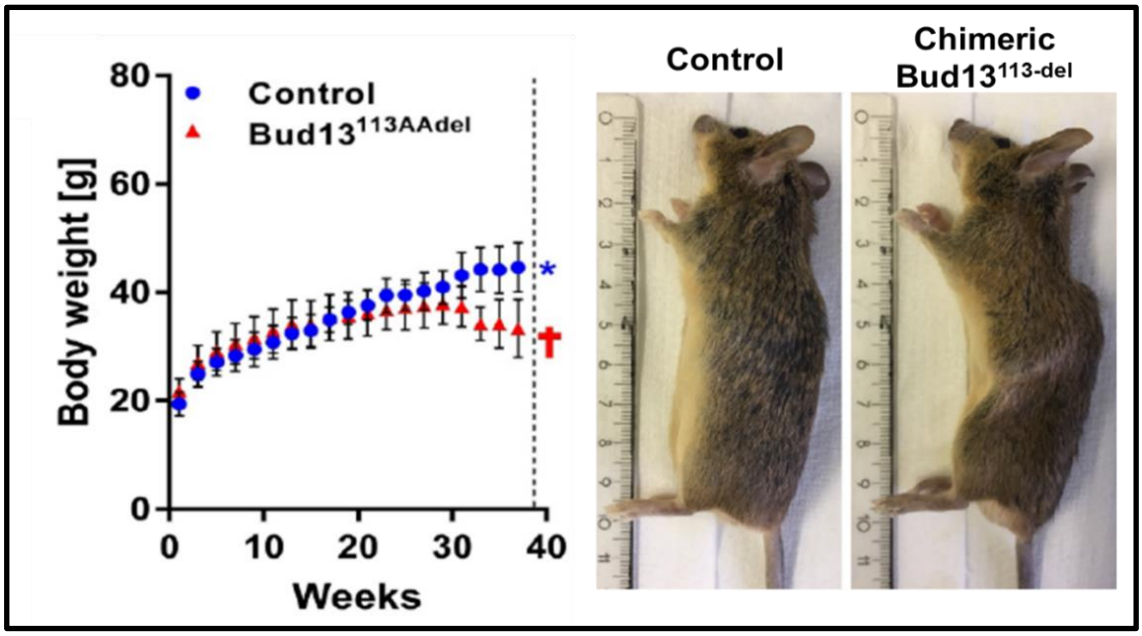

Fig.37. Growth curve for Bud13^{113delCh} mice- These mice exhibited a growth phenotype similar to that seen in the patients, especially the younger individuals. The mice, although born normal, begun to show complications such as progressive severe lipoatrophy, a kyphosis, and some of them cataracts after approximately 30 weeks of life. The mice ultimately died around the 37th week of life.

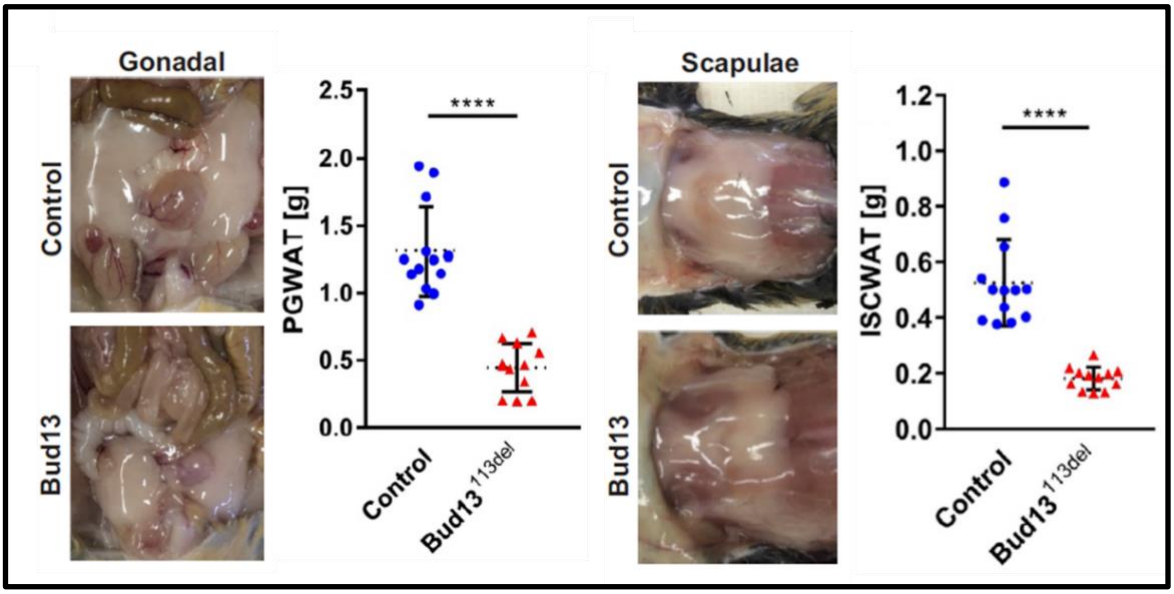

Fig.38. Fat pad analysis for Bud13^{113delCh} mice- Images and corresponding graphs quantifying the analysis of fat depots from Bud13^{113delCh} mice- The amount of both scapulae and gonadal fat (grams (g)) of these animals indicated an extremely reduced subcutaneous fat content compared to the control animals. Graph exhibiting a reduced mass of gonadal fat tissue in these animals.

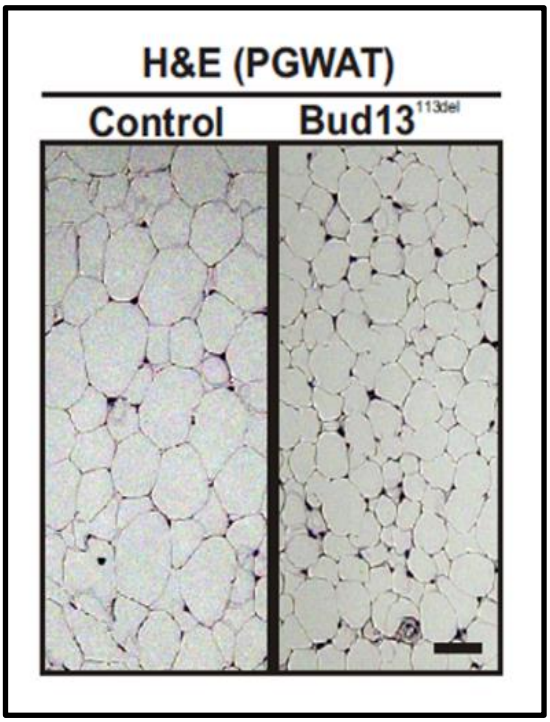

Fig.39. Histological staining of the gonadal fat tissue from Bud13^{113delCh} mice - Smaller fat cells/adipocytes as revealed by hematoxylin & eosin staining of gonadal fat depot of Bud13^{113delCh} mice.

However, a closer look at the nuclear structure and cytoplasm of the *Bud13*^{113delCh} mouse embryonic stem cells as did not reveal anomalies similar to those seen in the human adult fibroblasts (data excluded). Hence, we additionally generated mouse embryonic fibroblasts (MEFs) from the *Bud13*^{113delCh} chimeric embryos to cross check our findings from the human cells. The possibility of ROS-associated oxidative damage was ruled out since, unlike the HAFs, no change in the core H2ax protein was observed and furthermore, abnormal nuclear architecture and an unusual accumulation of electron dense granules in the cell cytoplasm were also not observed (data excluded). The mutant MEFs reflected a growth behaviour similar to the wild type mouse embryonic fibroblast cell lines, clearly negating onset of early cellular senescence. Additionally the prospect of a DNA damage repair defect was eliminated as well due to a normal γ-H2ax response post UV-irradiation (60,000 microjoules/cm^2) (figure 40).

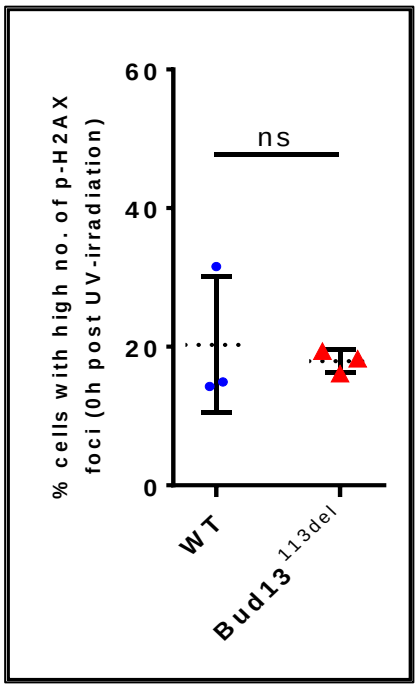

Fig.40. γ-H2ax response post UV-irradiation (60,000 microjoules/cm^2) in mouse embryonic fibroblasts generated from Bud13^{113delCh} mice embryos. Following irradiation for 60 seconds, cells were fixed immediately using 4% PFA followed by staining with anti- Gamma-H2AX (1:500) or 53-BP1 (1:500) and visualized under the 40X objective of the confocal microscope. The average percentage of high number of the respective foci between the mutant and control mouse cell lines did not reveal any change.

Interestingly, the MEFs displayed a downregulation of *Maf* gene expression similar to that observed in the human adult fibroblasts (figure 41).

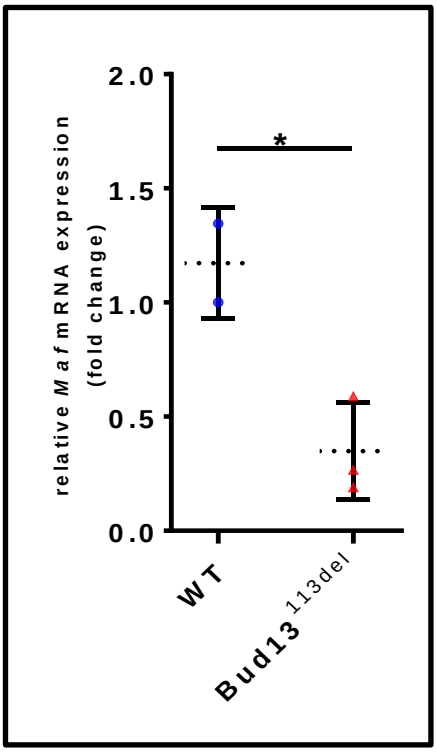

Fig.41. qPCR validation for *Maf* gene expression- *Maf* was found to be downregulated (*<=0.05) in the cultured mouse embryonic fibroblasts from the *Bud13*^{113delCh} chimeric embryos as opposed to the wild type mouse embryonic fibroblasts.

3.4.3. Transcriptomic analysis of mESCs

RNA-seq analysis of the mouse ES cells (mESCs), similar to our results from the human adult fibroblasts of the young patients, did not hint towards any splicing abnormalities- the global intron retention rate for pre-mRNA processing revealed no significant changes in either of the mouse models compared to the control mouse cell lines (figure 42).

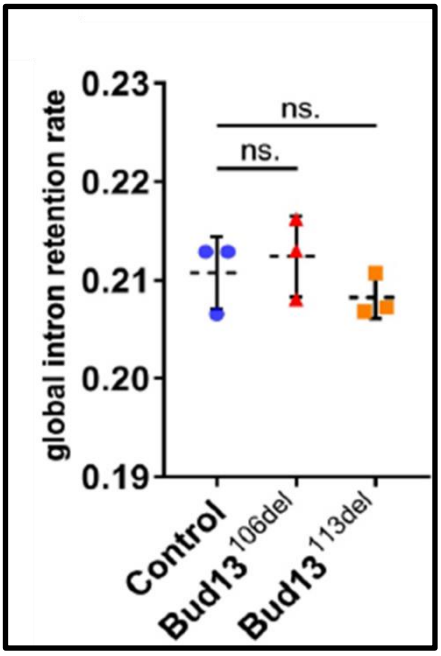

Fig.42. RNA-seq results for mouse embryonic stem cells- The global intron retention in the two mouse models, Bud13-106del and Bud13-113del, was not found to be differentially regulated.

Chapter 4: Discussion

The investigation of five individuals diagnosed with a complex progeroid phenotype, affecting multiple tissues, led us to the discovery of a single disease-causing mutation in the *BUD13* gene. The gene is known to encode a subunit of the RES complex, which plays a role in splicing (Dziembowski A et al., 2004, Brooks MA et al., 2009, Fernandez et al., 2018, Frankiw et al., 2019). However, the only significant splicing anomaly induced by the mutation as detected in patient-derived skin fibroblasts, was an abnormal, alternatively spliced variant in *BUD13,* as indicated by our molecular genetic findings and confirmed by Sanger sequencing and RNA sequencing analysis. Associated with this abnormal splice variant or hypomorphic *BUD13* allele are a spectrum of clinical manifestations, cellular phenotypes and molecular consequences that are discussed in this section.

4.1. Development of a Novel Progeroid Disorder

In our results section, we had tabulated and put across the different phenotypic features as observed in each of these patients. In this section, we try to understand as to what extent our own molecular findings and other well-understood mechanisms can explain the observed phenotype, and additionally draw a comparison to diseases where similar phenotypic features are observed.

4.1.1. Variable disease severity and life expectancy

The major anomaly that this study presented us with, was that the five individuals investigated displayed the exact same mutation, chr11 (GRCh37): g.116633617G>A, c.688C>T leading to a premature termination codon (PTC) in the *BUD13* gene but a highly varying disease expressivity. This variability, at the very outset, is reflected by the differences in life expectancy between the young and the old individuals harbouring the mutation. At the molecular level, following whole exome sequencing analysis, the Sanger

sequencing results confirmed the presence of a homozygous nucleotide substitution that leads to an alternative splicing event causing a truncated protein. The expression levels of this truncated version or the mutant protein, referred to by us as BUD13-S1, is co-relatable with not only the life expectancy of the patients, but also influencing the severity of the associated clinical presentations. Our western blot results quantifying BUD13-S1 protein expression showed that the demised young individuals within 6-9 years of age expressed only about 20% of the normal protein while, on the other hand, the older individuals between 33-55 years of age who continue with life, express almost about 50%. In agreement with these findings, a higher proportion of mutated *BUD13* transcripts seem to undergo nonsense-mediated decay (NMD) in the dermal fibroblasts isolated from the young individuals as compared to our adult patients. As a result, fewer transcripts seem to undergo the alternative splicing event to render *BUD13-S1* in young individuals, that eventually correlates to their residual 20% expression. Thus, NMD and alternative splicing, together are the crucial underlying molecular mechanisms determining the residual expression of the mutant protein, the expressivity and the variability of the disease.

The explanations to why alternative splicing and NMD operate variably could be, in part, attributed to the differing genetic backgrounds and environmental influences on the two groups. The younger individuals hailed from North Africa (Algeria) while the older individuals were traced to be inhabitants of Southern Europe (Portugal). Additionally, one may speculate that the Algerian patients may harbour critical locus/loci outside *BUD13*, which modify the phenotype to more deleterious as opposed to that observed in the Portuguese patients. However, our study is restricted to only five individuals that have been reported for the given mutation and disease. Therefore, an increasing number of patients with different ethnic background may shed light on this question.

A variable expressivity of a mutant protein is likely expected in the event of varying mutations contained within a gene. However, variable expressivity for exact same mutations, although rare, has previously been reported mostly for mutations contained in factors involved in pre-mRNA splicing. For instance, variable expressivity was observed for the same specific splicing machinery/ trans mutation in the *PRPF3* gene causing autosomal dominant retinitis pigmentosa (ADRP) in 22 individuals of a Swiss family (Vaclavik V et al., 2010). The same mutation led to variable expressivity in the age of

onset of night blindness and the severity of the disease progression. The gene codes for a ribonucleoprotein playing a role in in pre-mRNA splicing as a component of the U4/U6-U5 tri-snRNP complex involved in spliceosome assembly and as a component of the precatalytic spliceosome (spliceosome B complex). Additionally, the clinical phenotype associated with hypoplastic amelogenesis imperfecta was shown to vary in expressivity in a family carrying a heterozygous splicing donor site mutation in an intron of the ENAM protein (Koryucu et al., 2018). Interestingly, Carlston CM et al. In 2017 reported variable expressivity in a large family with non-classical Diamond-Blackfan anemia (DBA) related to a specific splice variant of ribosomal protein L11 (RPL11). Therefore, these studies, including our findings in *BUD13*, suggest that mutations affecting splicing lead to a variable expressivity of the disease even though patients harbor the same mutation.

4.1.2. Physiological manifestations

Postnatal growth retardation was observed in at least four individuals in terms of height & weight parameters (while the fifth individual, one of the older individuals presented values in the lower normal range), reflecting a downstream problem of generalised nutrient absorption. The lack of nutrient absorption and a general failure to thrive despite tube feeding in one of the younger individuals additionally reflected a much more severe systemic problem. This manifestation was presumably present in all the younger individuals who died at an early stage of life. The severity is further reflected with sensory neuropathy, little muscle tissue and muscular hypotonia or weak muscle tone in these young individuals. In addition, from our proteomics data for the fibroblasts isolated from the young patients, many amino acid metabolic pathways are upregulated as revealed by KEGG analysis. The upregulation of the general amino acid metabolism hints towards a counteractive measure against severe deprivation of amino acids in the young individuals. Our observations from proteome analysis are interesting in the light of previous literature showing downregulation of mTOR complex 1 (mTORC1) activity by amino acid deprivation (Li M et al., 2013), which contributes to various disease states due to its involvement in diverse processes. These include glucose homeostasis, adipocyte metabolism, body mass & energy balance, learning and ageing amongst others (Magnuson B et al., 2012).

The common phenotype of achalasia observed in all the five individuals may have well compounded the weight loss. Achalasia is described as an oesophageal motility disorder marked by an impairment of the lower oesophageal sphincter relaxation and loss of oesophageal peristalsis; consequentially, people with achalasia experience difficulties in swallowing food, one of whose presenting symptoms is weight loss (Arora Z et al., 2017). Although limited, studies aimed at evaluating findings from oesophageal manometry, a test to assess the function of the lower oesophageal sphincter and the muscles of the oesophagus, between older adults with an esophageal disorder and non-older adults have indicated that ageing is an important influential factor in increasing oesophageal motor abnormalities (Kunen et al., 2020, Andrews et al., 2008). However, there are very few human syndromes involving achalasia and the symptoms are reportedly caused by damage to the nerves of the oesophagus (Stuart et al., 2016). The most enigmatic one is probably the triple A syndrome caused by mutations in ALADIN, also a nuclear protein like BUD13. The BUD13 protein has been described to be present in the nucleus where it reportedly ensures correct splicing and release of mature mRNA through the RES complex, at least for a specific subset of introns (Fernandez et al., 2018, Sundararaman et al., 2016). In contrast, ALADIN is a protein present specifically in the nuclear pore and its loss from the nuclear pore complex (NPC) hinders nuclear transport of several proteins. The mutant protein in case of triple A syndrome selectively impairs transport of discrete import complexes through the NPC causing the decreased nuclear accumulation of proteins such as aprataxin, a repair protein for DNA single strand breaks, and DNA ligase I, which leads to disease development (Hirano et al. 2006). It is interesting to note that both BUD13 and ALADIN have nuclear transport functions and that their impairment is associated with clinical representation of neuropathy including damage to the oesophageal nerves, leading to achalasia. Hirano et al. additionally proposed that oxidative stress and consequent DNA damage, beyond the restricted capacity of the repair proteins possibly contribute to eventual cell death in case of triple A. We have also uncovered evidence for oxidative stress, DNA damage, and cellular senescence in the backdrop of mutant *BUD13,* which we have detailed in section 4.4 focused on cellular alterations.

Moreover, although variable in degree, all individuals display lipoatrophy or a subcutaneous loss of adipose/fat tissue. In our proteomics analysis of cultured fibroblasts from the young individuals, we observed that the fatty acid metabolism and peroxisomal

pathways are upregulated. Perhaps, the breakdown of fat as a source of energy hints towards a compensatory mechanism to balance the energy requirements, which are otherwise unmet due to a lack of nutrient absorption. This is further substantiated by the observation of a rapid loss of fat in these individuals. It is noteworthy that lipoatrophy is a common phenotype in several accelerated ageing or human progeroid disorders such as Hutchinson-Gilford Progeria syndrome, Werner syndrome, Néstor-Guillermo progeria syndrome, and several forms of Cutis laxa (Carrero et al., 2016). Additionally, the older individuals with a longer life span exhibit an increased level of plasma cholesterol in addition to cardiovascular features such as aortic valve thickening and mild heart valve regurgitation, that probably accompany cholesterol accumulation. The feature is striking in the light of the fact that several GWAS studies have implicated a strong association between gene clusters containing *BUD13* single-nucleotide polymorphisms (SNPs) with triglyceride metabolism and cardiovascular diseases (Han et al., 2019, Parra et al., 2017, Fu et al., 2015). Our clinical data is in line with these studies in pointing towards a possible function of BUD13 protein in lipid metabolism. Thus, *BUD13* mutation causing reduced abundance of the protein possibly leads to a variable degree of alteration in lipid metabolism depending on the residual protein expression.

In the light of potential alterations in the lipid metabolism in patients harbouring *BUD13* nonsense mutation, studies focused on the differentiation of bone marrow multipotent mesenchymal stem cells into osteoblasts or adipocytes have shown the process to be governed under an ageing associated switch mechanism. It has been demonstrated that the switch, progressively with age, is directed towards adipogenesis and is accompanied by decreased bone density (Ucelli et al., 2008). Interestingly, the basic leucine-zipper transcription factor, *Maf* was shown central to the osteoblast lineage commitment in mice, and with increased oxidative stress, a reduced *Maf* expression was associated with an increased expression of peroxisome proliferator-activated gamma (*PPARG*), leading to increased adipogenesis (Nishikawa et al.,2010, McCauley L. K.,2010). Moreover, *Maf* is known to play a role in chondrocyte terminal differentiation or the end state of chondrocyte differentiation pathway, which is known to make chondrocytes hypertrophic and is essential for bone growth and development (Goldring M, 2012). This is interesting to note especially because in addition to a generalised nutrient absorption issue combined with achalasia, all the individuals in this study have undergone growth retardation with the younger individuals having additionally exhibited progressive joint stiffening.

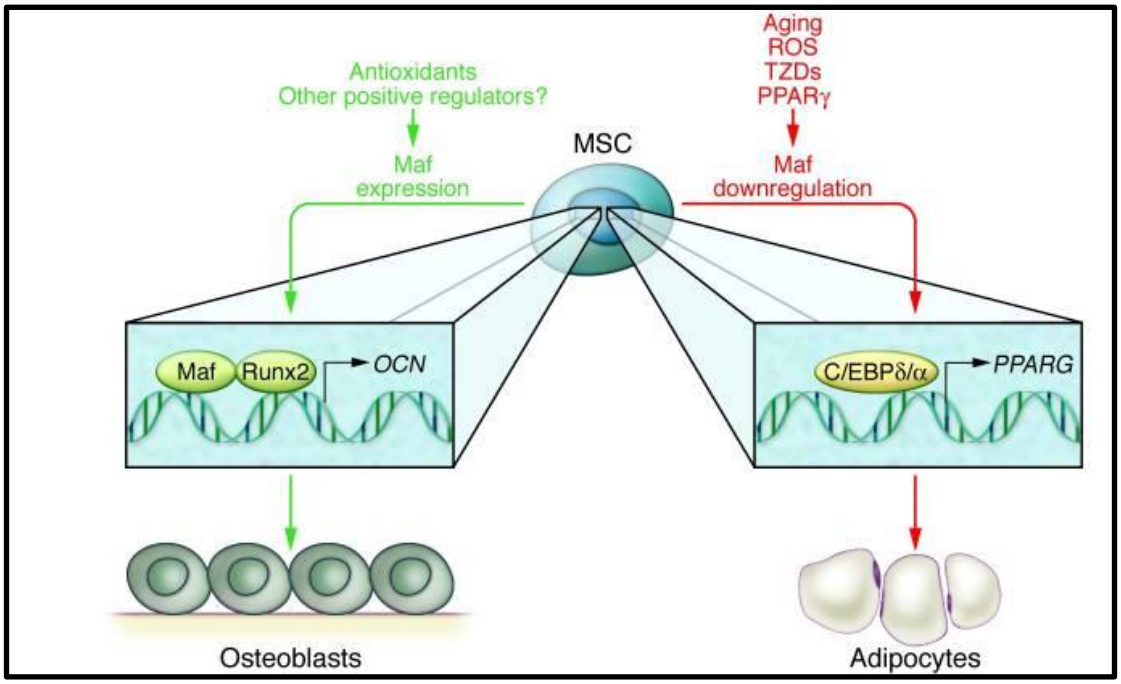

Fig.43. Expression of *Maf* is determinant in whether mesenchymal stem cells differentiate into osteoblasts or adipocytes-*Maf* is downregulated in ageing as well under elevated levels of reactive oxygen species (ROS). Downregulated Maf leads to increased PPARG expression and thereby increased adipogenesis (adopted from McCauley L. K.,2010).

While an increased adipogenesis could be speculated as part of the compensatory mechanism in the light of lipoatrophy, we have observed both a reduced *MAF* expression and an increased level of ROS in the young individuals under study. Strikingly is the protein not only critical in view of its role in bone development and growth, but it is also known to control the expression of multiple crystallin genes and embryonic lens development. Specifically, *c-MAF*, which is amongst the large *Maf* subfamily members containing a putative activation domain at the N terminus, can transactivate the γF-crystallin promoter and is thereby required for vertebrate lens differentiation through its action on crystallin gene expression, thus, unsurprisingly, mutations in *MAF* gene have been reported with several ocular defects including congenital cataract (Reza et al., 2020, Anand et al., 2018, Kim et al., 1999). In line with these studies, we also observed cataracts and corneal clouding in the young and older individuals with *BUD13* deficiency. In conclusion, the downregulation of the *MAF* gene in the young individuals may offer an explanation to why they underwent growth retardation and cataracts or corneal clouding at a very early stage of life as part of the severe progeroid phenotype. The older

individuals, on the other hand, had a significantly higher relative *MAF* expression that was comparable to the controls. This fits to the observation of a slower and progressive progeroid phenotype development than younger individuals. However, since we also observed cataract in the older individuals, we hypothesise that the cells contained in the eye lens are more sensitive to hypomorphic *BUD13* mutation even though *MAF* is normally expressed.

4.1.3. Neurological presentations

Although no structural brain defects were reported, the young individuals exhibited mild mental retardation. Coupled to the fact that they also suffered from conductive hearing impairment, it does not come as a surprise that a normal cognitive development was hampered in contrast to older individuals who underwent bilateral cochlear implants. Notably, Fernandez et al., showed that a loss of function mutation in *Bud13* led to strong structural brain defects and widespread cell death in the central nervous system (CNS) with a particular reduction in the number of differentiated neurons, including both excitatory and inhibitory neuronal populations (Fernandez et al., 2018). This *BUD13*-dependent CNS function is probably directly proportional to *BUD13* expression levels and that perhaps an expression level even lower than 20% (as is true for the *S1* splice isoform in the young patients) may lead to more severe brain defects. Interestingly, a higher expression of the same mutant splice isoform *S1* apparently overcomes neurological defects as is seen in the older individuals. These patients, aided with bilateral cochlear implants to overcome hearing problems, show a near perfect cognitive development in addition to normal brain structure. Furthermore, the older individuals additionally displaying a progressive bilateral sensorineural hearing loss hinting towards BUD13 protein functions also in the direction of structure & metabolism of the inner ear.

In summary, referencing back to the classical definition from literature, ageing is a complex set of changes that gradually occur over a period, resulting in progressive weakening of physiological being. Of the classic macroscopic features, it is recognisable that many of these are presented in all or most of the individuals in our study and include loss of fat tissue and muscle mass, poor vision and hearing ability, and arthritic inflammation accompanied with a higher risk of developing heart diseases in the surviving

individuals. **The severity of these presentations is associated with the residual expression of the alternatively spliced *BUD13-S1* arising from the hypomorphic *BUD13* allele.**

4.2. Molecular consequences of a homozygous hypomorphic *BUD13* allele

4.2.1. Structure of the BUD13 protein and its evolution

A close inspection of the *BUD13* locus reveals specific structural features, including a compositional bias, and include: several repeats of the specific amino acid combinations, Proline-Arginine-Arginine (PRR) and Proline-Arginine-Lysine (PRK), an arginine-rich domain at the N-terminal and a coiled coil domain overlapping the RES at the C-terminal. The coiled coils are versatile motifs that can potentially function as molecular spacers separating different functional domains within a polypeptide or can communicate conformational modifications along their length (Truebestein and Leonard, 2016). Additionally, BUD13 is an intrinsically disordered protein (IDP), a property typical of proteins with multiple functions that lack specific tertiary structures. Notably, RES complex was described to be enriched in regions of long, compositionally biased disorder that were proposed to function as sensors for the spliceosome (Korneta and Bujnicki, 2012). BUD13 protein, that participates in the splicing activities of RES, was described as the most highly disordered protein in the spliceosomal proteome with no Pfam domain corresponding to ordered structural domains; (Korneta and Bujnicki, 2012). A prediction tool called DISPROT to visualise the disordered regions in BUD13 (figure 45) revealed that most of the protein is composed of intrinsically disordered residues. Furthermore, splice form 1 of the protein (BUD13-S1) including the RES domain showed similar to BUD13 an intrinsic disorder (Figure 45).

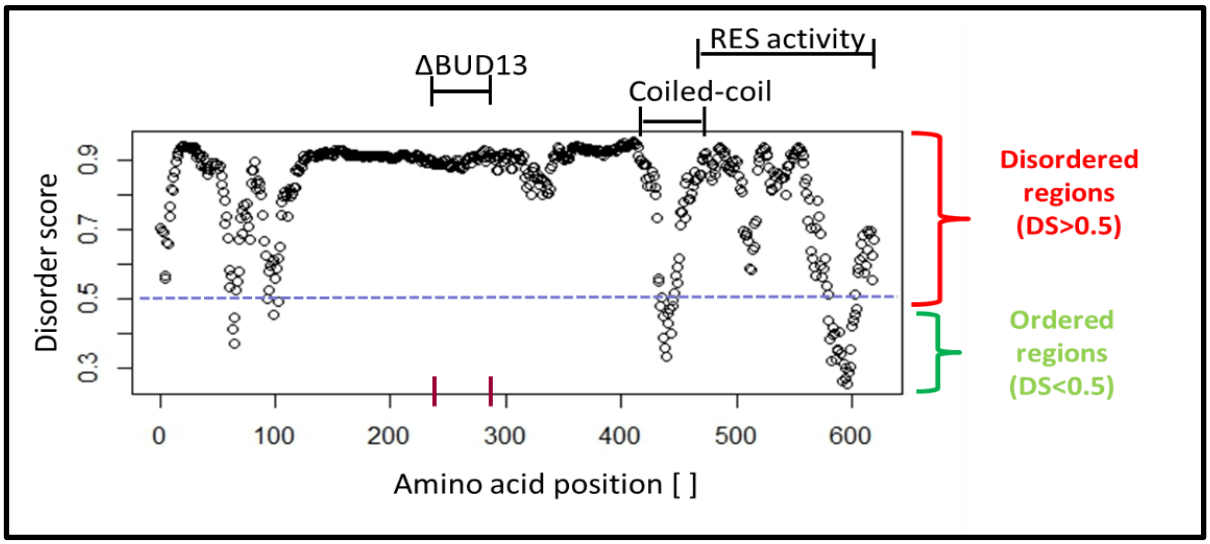

Fig.44. Prediction of intrinsically disordered regions in BUD13 using VL3H analysis (neural network based) of DISPROT-Predictor of Protein Disorder.

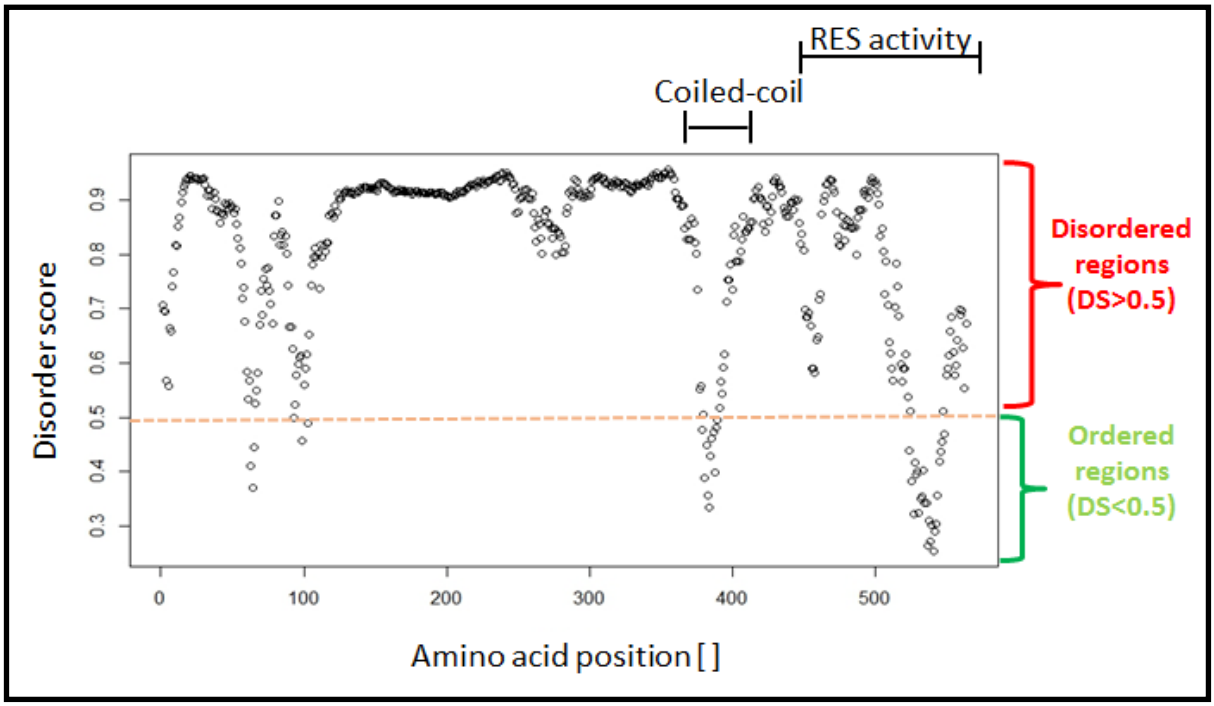

Fig.45. Prediction of intrinsically disordered regions in BUD13-S1 using VL3H analysis (neural network based) of DISPROT-Predictor of Protein Disorder.

The lack of specific tertiary structures (or presence of intrinsic disorder) is perhaps, essential for the protein to acquire different specific functions upon its interaction with other target proteins. While the RES-associated, C-terminus of BUD13 is aimed towards pre-mRNA retention and splicing, it is interesting to reflect on additional functions for the remainder of the protein considering that the 55 amino acid deleted N-terminus leads to a rather complex progeroid disease. Interestingly, BUD13 protein evolution from yeast to human has incorporated a longer N-terminal sequence that is completely absent in the yeast (figure 46). This hints towards additional functions of the protein in higher and more complex organisms while the RES-associated C-terminal remains highly conserved.

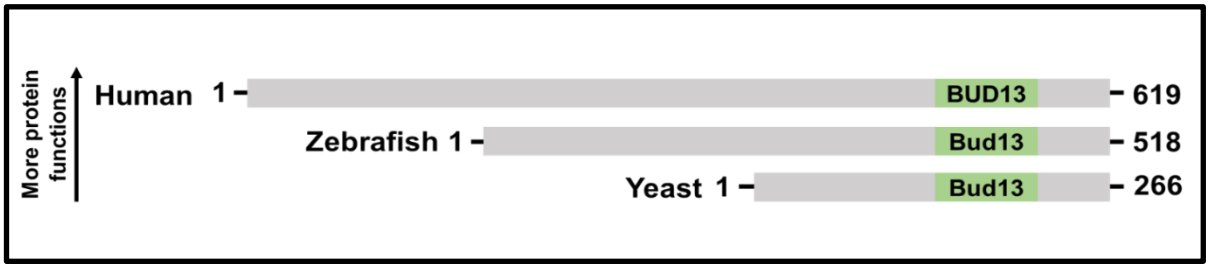

Fig.46. Protein alignment of a longer human BUD13 vs a shorter Zebrafish Bud13 and the shortest Yeast Bud13 as estimated using Uniprot database (Bateman A, 2019) and Clustal Omega alignment tool (Sievers F. et al., 2011) for sequence comparison.

Structural and functional evidence for RES complex members in humans, described as a heterotrimer of three proteins-BUD13, RBMX2 & SNIP1, is also inadequate. So far, established literature mentions the disease phenotype brought about by only one of the components of the RES, namely *SNIP1* wherein, a homozygous mutation was in three Amish patients led to psychomotor retardation, epilepsy and craniofacial dysmorphism (Puffenberger et al., in 2012). The RES components are often not detectable in approaches using cross-linking and mass spectrometry to prepare stalled spliceosome preparations (Frankiw et al., 2019, Brooks M et al., 2009, Bertram et al., 2017). However, given the protein-protein interactions between the components, as reiterated in various databases such as STRING (Szklarczyk D et al., 2019) and InTACT (Orchard S et al., 2013), we attempted to detect the intact complex in the event of *BUD13* nonsense

mutation using functional approaches such as non-denaturing, native gel electrophoresis and co-immunoprecipitation (co-IP) experiments. However, owing to the structural complexities of protein-protein interactions within the complex and other technical limitations, we were unable to detect the whole complex. Therefore, we speculate whether the protein complex, besides its organisational complexity, is also characterised by a rather transient interaction for its splicing-associated role.

4.2.2. Impact of the hypomorphic *BUD13* mutation

4.2.2.1. Differential Splicing within *BUD13* pre-mRNA

The further investigation of the nonsense mutation uncovered by whole- exome sequencing revealed a noteworthy splicing event within *BUD13*. Using PCR- based approaches and Sanger sequencing, we confirmed that the mutation activates a cryptic splice site for alternative splicing, which leads to the shortening of its N-terminus, thereby generating a truncated *BUD13-S1*. Our qPCR, RT-PCR and western blot results, taken together, show that the stop mutation containing transcripts most likely undergo nonsense-mediated decay (NMD) as is typical for transcripts harbouring pre-mature termination codons (PTCs). The shorter alternatively spliced form or splice isoform 1, also referred to as *BUD13-S1* by us, is a stable protein product of about ~64kD. However, the expression of the *S1* form is varying between the two groups of individuals investigated as a part of this study- **A variable expression of *BUD13-S1* (20-50%) was found associated with differing severity of the complex progeroid phenotype.** The mutation may lead to a rather deleterious phenotype depending on the abundance of S1, wherein an expression level of about 50% of the normal protein level is compatible with an obviously higher life expectancy compared to a marginal 20% abundance; but both the scenarios are accompanied by complications reducing the quality of life. Our study and its findings are the first functional evidence showing a human *BUD13* nonsense mutation, which gives rise to the N-terminal truncated form called *S1*. Moreover, upon checking exclusively for *BUD13-S1* relative mRNA expression in fibroblasts isolated from healthy individuals, our qPCR results confirmed that his truncated version of the protein is not normally produced in healthy control fibroblasts.

A deeper look using Sanger sequencing combined with bioinformatics splice site prediction using Human Genome Splice Finder (version 3.0) revealed that the *BUD13* stop mutation in exon 4 leads to a massive leap in the consensus value (defined as the probability of a splice site used for alternative splicing) of an alternative cryptic donor splice site from 68% to almost 95%. The activated cryptic site eliminates the mutation starting from exactly one nucleotide before the mutant nucleotide until the next acceptor splice site whose high consensus value of nearly 90% remains unchanged in the event of the mutation, thereby generating an in-frame 165 base pair deletion (55 amino acids ~6.18kD). This comes across as a remarkable mechanism of the cell to eliminate the defect contained within its arginine-rich domain at the N-terminal and preserve the overlapping coiled-coil and RES domains at the C-terminal.

It is noteworthy that the human disease arising from the *BUD13* mutation in our case study may not be the first instance of a scenario where splice anomalies associated with a splicing factor correlate to the severity/expressivity of a human disease. The upregulation of novel isoforms, additionally, has also been observed before in several human disease. This part of the discussion is taken up in greater detail in the section entitled 3. Alternative splicing in human disease.

4.2.2.2. Lack of global splicing defect- Inferences from Transcriptomic analysis

Literature evidence for RES-associated protein function in yeast and zebrafish splicing processes indicate, that in the whole picture of splicing and associated proteins, RES can be characterised as a *trans*-acting, enhancer spliceosome element recruited after the recognition of *cis* splicing elements (Dziembowski A et al., 2004, Brooks MA et al., 2009, Fernandez et al., 2018). Additionally, we know that the mammalian RES complex has been described as a heterotrimer of three proteins-BUD13, RBMX2 & SNIP1 (Frankiw et al., 2019, Betram et al., 2017). Thus, in the backdrop of a hypomorphic *BUD13* allele and a splicing-associated role for RES, we initially hypothesised a global splicing defect arising due to the *BUD13* variant.

We performed RNA sequencing to assess for a generalised splicing defect as a possible disease mechanism underlying the novel progeroid phenotype. However, the revelation

of only a very few genes undergoing differential alternative splicing and intronic retention gives rise to the following school of thought: Despite an in-frame deletion at the N-terminus of the protein leaving the C-terminus associated RES domain intact, *BUD13-S1* continues to preserve the highly evolutionarily conserved C-terminal RES domain that is apparently sufficient for

a) cooperative binding and assembly of complex components,
b) interactions of the complex specifically those within the components, and
c) execution of normal RES-associated splicing activities.

This ruled out the possibility of an effect on the global splicing machinery through RES (spliceosomopathy), in that the spliceosomal components by themselves can probably carry out their intended function. This, in turn, indicates that the nonsense mutation activating a cryptic splice site, which regulates alternative splicing, is operative in disease development. **Taken together, our results overall indicate that the development of the progeroid phenotype is attributable to either the overall reduced expression of the BUD13 protein, or specifically, to the shortened N-terminus, or perhaps, even a combination of both.**

These observations are also interesting in the light of the findings from the other model organisms evaluated for the importance of RES function, particularly the zebrafish and the yeast. Notably the RES domain associated with *Bud13* was disrupted and was accompanied with general splicing changes. Fernandez et al., 2018 generated *Bud13* zebrafish mutants using CRISPR/Cas9 to introduce a seven- nucleotide deletion that generated a premature termination codon and disrupted protein function including the RES domain. The transcriptomic analysis of the *Bud13* mutants uncovered a global defect in intron splicing, with strong mis-splicing of a subset of introns that were short, rich in GC content and flanked by GC depleted exons, features that are associated with intron definition (Fernandez et al., 2018). Moreover, the *Bud13* zebrafish mutants were embryonically lethal. Additionally, in the yeast model, deletion of *Bud13* also including the RES domain correlated with a greater accumulation of unspliced, intron containing pre-mRNAs (Dziembowski A et al., 2004, Zhou Y et al. 2017). However, inactivation of *Bud13* was shown to alter yeast budding pattern and cause slow growth and thermosensitivity (Dziembowski A et al., 2004, Ni and Snyder, 2001), but not affect overall organism

viability. These studies confirmed our observations, that intact RES domain of mutant BUD13 maintain normal splicing properties of the RES complex in our patients. In addition, it is worth reiterating the evolution of the Bud13 protein and its accompanying role in more complex organisms: The loss of the protein is associated with lethality of more complex organisms, as in the case of vertebrates (Fernandez et al., 2018) as well as in humans and mice (section 4.5 of discussion), whereas in yeast not.

To understand the downstream effects of the *BUD13* hypomorphic allele, in addition to the analysis of polyA+ RNA from the cultured fibroblasts of the young individuals (6-9years), we simultaneously investigated the proteome, comparing the two findings against respective datasets from control cell lines cultivated under similar cell culture conditions. We drew a cross-section of the two datasets. The cross-section of the proteomics and RNA-seq datasets as well as that of dysregulated genes from RNA-seq analysis with the eCLIP peak file against BUD13 (Nussbacher J.K. and Yeo G.W., 2018) revealed several dysregulated ribosomal proteins leading us to speculate whether BUD13 may potentially regulate ribosomal biogenesis and influence global cellular translational processes. Typically, ribosomopathies are the diseases arising from defects in ribosomal components, ribosomal RNA processing or in ribosomal assembly factors (Narla A. and Ebert B.L., 2010). Rewired cellular protein & energy metabolism and extensive oxidative damage stress causing DNA damage are some hallmarks of well understood ribosomopathies such as Diamond-Blackfan anemia (DBA), Treacher Collins syndrome (TCS), cartilage hair hypoplasia (CHH) and other skeletal dysplasias (Kampen et al., 2019). These are cellular and molecular phenotypes also observed in our case study. Diamond-Blackfan anemia (DBA) is a constitutional erythroblastopenia marked by either absence or decrease of erythroid precursors (Draptchinskaia et al., 1999). Notably, mutations in *RPL18A* and *RPL35,* which are genes that have been uncovered as dysregulated ribosomal candidates in our transcriptomics/targeted proteomics cross-section, have been found associated with DBA (Wang et al., 2014). In another instance, *RPL13* variants, also uncovered in our cross-sectional dataset, were recently found associated with varying expressivity of SEMD, a heterogenous group of disorders that are accompanied with variable growth failure and skeletal impairments, reminiscent of clinical presentations also seen with the *BUD13* nonsense mutation (Constantini et al., 2021). TCS, a condition that primarily affects the bones and other tissues of the face and is almost always accompanied with hearing loss but normal intelligence, as is also

observed in most of our patients, arises from a lack of polymerase I/III activity owing to mutations in *TCOF1, POLR1C and POLR1D,* leading to a reduction of mature ribosomes and lowering overall translation, which weakens cells and promotes quiescence (Plomp RG et al., 2015, Trainor and Merrill, 2014).

In the light of a moonlight function for *BUD13* in mammals, it is worth considering if the BUD13 protein has additional roles in ribosomal function besides its splicing-associated activities via RES, and perhaps if the N-terminal is maybe dedicated to such an additional function. This marks a path for future experiments to further investigate the ribosomal candidates uncovered in the study and assess for a potential ribosomopathy.

4.3. Alternative splicing in human disease

Splicing factor mutations can either affect constitutive or alternative splice sites resulting in cis effects, or affect one or more components of the splicing machinery, thereby causing trans effects (Faustino and Cooper, 2003). The stop mutation contained in *BUD13* disrupted a constitutive splice site resulting in the generation of a truncated, yet stable mRNA splice isoform.

Such splicing pattern modifications resulting in distinct mRNA splice isoforms have also been observed previously in other human progeroid diseases such as Marfan syndrome (Takahara et al., 2002, Jacquinet A et al., 2014) and Hutchinson-Gilford Progeria syndrome (Goldman R.D. et al., 2004). A *de novo* donor splice site mutation in the *FBN1* gene causing a neonatal progeroid variant of Marfan syndrome with congenital lipodystrophy reportedly led to the skipping of one entire exon and the subsequent production of a truncated yet stable protein with an altered C-terminal (Jacquinet A et al., 2014). The *BUD13* splicing anomaly and the subsequent *BUD13-S1* associated nuclear aberration closely resembles to what is seen in Classical Progeria, also called as Hutchinson-Gilford Progeria Syndrome. The disease results from the mis-splicing of the *LMNA* gene encoding the lamin A and lamin C proteins. About 80% of the HGPS cases arise from a *de novo* point mutation causing a heterozygous base substitution (C->T) that result in the activation of a cryptic splice site within exon 11 of the gene affecting mature lamin A production. The use of the cryptic splice for alternative splicing site results in a

truncation of 50 amino acids at the carboxy terminus of prelamin A protein that is permanently farnesylated (LA∆50) and cannot undergo further processing to render mature lamin A (Eriksson et al., 2003, Young, S et al., 2006). LA∆50 is associated with the aberrant nuclear changes as seen in cultured patient derived HGPS fibroblasts (Goldman R.D. et al., 2004). Amongst splice site mutations in other diseases, upregulated novel isoforms have been reported for diseases like Ehlers-Danlos syndrome and X-linked retinitis pigmentosa. For instance, a splice-acceptor variant in the *COL5A1* gene causing Ehlers-Danlos syndrome leads to the production of several transcripts (Takahara et al., 2002). X-linked retinitis pigmentosa can be caused due to mutations in the retinitis pigmentosa GTPase regulator (*RPGR)* gene. Both misspliced and novel splice variants have been reported in cases of *RPGR* mutations that have been found to be differentially regulated in several human tissues indicating that the gene splicing is a part of the pathogenic mechanism underlying the severity of the disease (Schmid F et al., 2010).

Interestingly, BUD13 posed an additional complexity: -we initially suspected an effect through the spliceosome machinery, or in other words, a spliceosomopathy since the protein is a component of the splicing machinery by virtue of its activity in RES complex (Dziembowski A et al., 2004, Wysoczanski P et al., in 2014, Fernandez et al., 2018, Frankiw et al., 2019). Nevertheless, our findings from RNA-seq carried out in both the patient fibroblasts as well as in our mouse models hinted at the absence an effect on the global splicing machinery. This indicated the combined effects of alternative splicing and nonsense-mediated decay owing to the exonic *BUD13* mutation being operative in disease development. However, it must be stated that disease mutations contained in the core elements of the splicing machinery are rare. Some examples of such diseases include retinitis pigmentosa (RP) and spinal muscular atrophy (SMA). Amongst these, cases that additionally show splice anomalies present within the factors are even rarer. RP is characterised by progressive retinal degeneration and associated complexities eventually causing complete blindness. It has been associated with mutations in splicing factor *PRPF31,* which prevents the association of U4/U6 snRNP with the U5 snRNP, and the subsequent assembly of the active spliceosome (Makarov et al., 2002). SMA is diagnosed with a progressive loss of motor neurons of the spinal cord and most cases arise due to mutations in the SMN complex components (SMN1 and SMN2) that are

involved in the assembly of the snRNPs- U1, U2, U4 and U5, which are spliceosome components (Sossi et al., 2001).

4.4. Cellular alterations caused by BUD13 deficiency

4.4.1. Genomic Instability

As one of the starting points of investigation, the human progeroid phenotype caused by the *BUD13* point mutation in the young individuals was diagnosed to closely resemble the Cockayne syndrome phenotype by the administering physicians. Individuals with Cockayne syndrome are characterised by short stature, a characteristic facial appearance, sensorineural hearing loss, cataract, progressive neurological dysfunction, and intellectual deficit. Subcutaneous lipoatrophy is additionally present that can lead to signs of premature ageing of the skin. In classical type I form of the disease, the first symptoms generally appear during the first year of life (Batenburg et al., 2015, Scheibye-Knudsen et al., 2014).

The underlying pathomechanism involves accumulation of excessive lesions owing to defects in the DNA repair mechanism. Mutant cells tend to show a defective or inefficient DNA damage repair (DDR) signaling cascade upon UV exposure, with persistent DNA damages leading to cell death, cancer, and ageing (Batenburg et al., 2015). We checked for any potential signals for DDR in the dermal fibroblasts isolated from the young individuals, using a controlled dose of UV-irradiation.

In the case of exposure to DNA-damaging agents such as UV-radiation, phosphorylated or γ-H2AX is well known to represent repair foci for double strand breaks (DSB) (Löbrich M et al., 2010). On the other hand, 53BP1 is an important mediator of the DSB repair that recruits the downstream responsive proteins of the signaling cascade and promotes non-homologous end joining-mediated DSB-repair; the 53BP1 foci tend to co-localise with those of γ-H2AX (Campisi et al., 2007, Fradet-Turcotte A et al., 2013, Panier & Boulton, 2014). Interestingly, we observed the unaltered recruitment of γ-H2AX and 53BP1 upon UV-C irradiation of the fibroblasts. UV-C is known to have the highest energy and shortest

wavelength in the UV-spectrum (UV-A, UV-B, and UV-C). Notably, a controlled dose of such an irradiation on cultured fibroblasts from the young individuals did not affect the double-strand break repair signaling cascade. Next, we checked for H2AX and γ-H2AX protein levels without any UV-irradiation and uncovered a reduced abundance of basal levels of H2AX and γ-H2AX proteins in the young individuals. This perhaps could be attributable to chronic oxidative stress that can lead to progressive accumulation of reactive oxygen species (ROS), which can promote H2AX degradation by the proteasome. This may prevent normal accumulation of γ-H2AX at the end and has indeed previously been reported in triple-negative breast cancers (Gruosso et al., 2016). Therefore, it may not be prudent to assume from our findings that an impaired DNA damage repair response is not the underlying pathomechanism here, as is for Cockayne syndrome, but is rather a downstream effect of the cellular stress brought about by *BUD13* nonsense mutation.

Strikingly, on the other hand, a relatively high abundance of γ-H2AX is seen in passage-matched fibroblasts from the older patients compared to the control fibroblasts. This observation is like what is seen in some human progeroid disorders such as Werner syndrome and Hutchinson-Gilford Progeria syndrome. An increased level of γ-H2AX is additionally accompanied by increased substrates of other DNA damage markers like 53BP1, and phosphorylated ATM/ATR. Furthermore, patient cells have a reduced proliferative potential, increased senescence associated-β-gal markers, upregulated expression of senescent marker genes $p16^{Ink4a}$ and $p21^{Waf1}$, and activation of senescence associated secretory phenotype. Noteworthy is that, compared to young healthy donors, an elevated histone H2AX phosphorylation is also observed in elderly individuals as a part of a cellular phenotype observed in physiological ageing (Ashapkin et al., 2019, Carrero et al., 2016). In patients with BUD13 deficiency, a 50% residual BUD13-S1 protein expression is associated with a relatively mild progeroid phenotype and is marked by a slower progression towards cellular senescence, which has been further discussed in section 4.4.4.

4.4.2. Irregular Nuclear Architecture

The nuclear architecture in cultured patient fibroblasts is distorted as shown in our results of the transmission electron microscopy and additionally confirmed via immunofluorescence staining of nuclear protein emerin in patient HAFs. In terms of quantification, unsurprisingly, the younger individuals had a way higher percentage (five times) of invaginated nuclei than the older individuals that carried a lower proportion of invaginated nuclei comparable to those in the control cells. This is in line with a classical marker/feature of several progeroid disorders having inconsistencies in nuclear organisation and an unstable nuclear envelope (Dechat et al., 2008). Particularly, the nuclear phenotype in fibroblasts from our patients closely resembled to that seen in the Classical HGPS arising from progerin production and it is especially interesting as the BUD13 protein is localised to the nucleus (Na, I et al., 2016, Goldman R et al., 2004). In the Nestor-Guillermo progeria syndrome (NGPS) (Loi et al., 2016) and restrictive dermopathy (RD) (Columbaro et al., 2010) as well, the mutations are not necessarily contained within LMNA in case of a nuclear aberration, however, the respective mutations can affect prelamin A mediated interactions in the chromatin (NGPS, Loi et al., 2016) or the overall processing of prelamin A (RD, (Moulson et al., 2005; Navarro et al., 2005). Therefore, we checked for production of the toxic protein, permanently farnesylated lamin A (also called as progerin) as is seen in HGPS. However, in western blot we did not observe any progerin expression in the patient fibroblasts.

Interestingly, a lower expression of BUD13 protein in-vivo (as BUD13-S1) correlates with a higher degree of nuclear aberration and a more severe disease phenotype. It is worth reflecting on whether the toxicity exerted by S1 is dosage dependent. We conclude that normal BUD13 expression is critical to maintain a proper nuclear architecture and function and perhaps, a truncated BUD13 may be variably toxic dependent on its expression levels.

Furthermore, the heterologous overexpression of BUD13-S1, in vitro, mimics the nuclear phenotype in immortalised cells such as HeLa and U2OS. Taken together, it would be interesting to uncover in future experiments if the invagination replicated in vitro is also dependent on expression levels of S1 (as is observed in vivo in terms of the degree of nuclear invagination differences within the patients) to understand whether BUD13

operates within a myriad of nuclear proteins involved in a feedback loop crucial for maintenance of nuclear architecture and proper mitotic cell division.

A classical parallel of the distorted nuclear structure with progeroid disorders such as HGPS and NGPS, the nuclear function of BUD13 is enlightening. Given the rather significant effect exerted by a truncated BUD13, it is possible to assume that the protein may play an influential role in nuclear assembly and mitotic cell division. This is further supported by our findings of -

(i) a highly dysregulated mitotic cell division pathway from both gene ontology (GO) and pathway analysis from our RNA-seq findings from the young patients, and

(ii) although an unspecific marker, an elevated mRNA expression of *p21* is indicative of cellular stress in the background of *BUD13* mutation, which is well documented to inhibit the cell cycle and promote cyclin-dependent kinase inhibition and cell cycle arrest in the G1/ S phase of the mitotic cell division.

Also, the absence of chromosomal aberrations upon investigation of metaphase chromosomes using cytogenetics approaches ruled out chromosomal anomalies

4.4.3. Accumulation of cytosolic aggregates

A clear qualitative difference in the numerosity of the cytosolic, electron dense granules (as seen in transmission electron microscopy results) was observed between the young and the old individuals. Th dermal fibroblasts from the young individuals displayed a much denser accumulation of such granules. Experiments focused on plasmid- mediated heterologous overexpression of the BUD13-S1 protein in HeLa and U2OS cells showed that BUD13-S1 is still able to localise within the nucleus. The possibility thus, of mislocalisation for splice form 1 or BUD13-S1 in the cytoplasm was ruled out.

Although we were unable to uncover the exact nature of the granules, the finding in combination with some of our other observations, hint at a few possible directions that need to be further investigated in future experiments. Firstly, we have additionally

detected an upregulation of the lysosomal enzyme, Cathepsin D (the fully active mature form of the aspartic endopeptidase) in only the young individuals. As one of the most abundant proteases, enzymatically active Cathepsin D has the primary biological function of protein degradation in an acidic environment of lysosomes (Benes et al., 2009; Tatti et al., 2012). The investigation of the lysosomal pathway might be interesting for future studies to determine if altered lysosomal activity perhaps plays a part in such an accumulation of cytosolic granules, especially since progeroid diseases, such as those caused by nuclear mutations or genomic instability, were shown to exhibit a marked activation of autophagic proteolysis in progeroid mice. The accumulation of damaged proteins was seen as accumulated cytosolic granules and was proposed as a general measure of accelerated catabolism as a pro-survival strategy (Marino et al., 2010). The investigation of the lysosomal-autophagy pathway thus, might be interesting to unravel if there is also a similar pro-survival strategy to which the pathway contributes to in the case of our progeroid disorder under study.

Secondly, some splice factor proteins were shown to contribute to cell survival in the event of oxidative stress by associating with stalled ribosomes localised to stress granules, a feature not observed under steady state; for instance, frontotemporal lobar dementias and amyotrophic lateral sclerosis caused by the loss of a splicing factor called TDP43. While short term stress led to a transient association, long term/ lethal stress caused the protein to completely dissociate from the stress granules (Tollervey J.R. et al., 2011, Higashi S. et al., 2013). Remarkably, in our case study, elevated levels of reactive-oxygen species were detected in the dermal fibroblasts of the young patients, indicating oxidative stress. The fibroblasts are under long-term stress, reaching cellular senescence early as compared to healthy control fibroblasts. Also, there were no signs of mutated BUD13 protein in the cytoplasm. It is interesting to speculate if the cytosolic granules in the event of *BUD13* mutation are also representative of stress granules associated with impaired ribosomal activity. As we have observed several dysregulated ribosomal proteins from the intersection of the transcriptomics and proteomics data, it would be interesting to perform follow- up experiments investigating a potential pathomechanism involving altered translation or in other words, a ribosomopathy indication.

Thus, experiments focused on investigating the lysosomal-autophagy pathway and/or ribosomal candidates may help in shedding light on the precise nature of these electron dense granules in the cell cytoplasm, observed in the backdrop of a highly reduced expression of BUD13 protein.

4.4.4. BUD13-S1 Production Accompanied by Cellular Senescence

Cellular senescence can be induced by several stress factors or stressors associated with a myriad of cellular and molecular functions. One of the better understood pathways is the regulation of senescence by the p53 (tumor suppressor regulating cell cycle) and p16 -pRB (retinoblastoma protein) tumor suppressor pathways (figure 48). Upon activation by a signal such as DNA damage response, p53 is known to induce senescence growth arrest by inducing p21 expression, which in turn suppresses the phosphorylation of pRB protein by cyclin-dependent kinases (CDKs). This eventually inhibits the proliferation inducing activity of the E2F protein (a transcription factor) that controls the expression of genes for cell-cycle progression. In contrast, signals for senescence involving the p16-pRB pathway ply by inducing p16 expression. This prevents phosphorylation and causes subsequent inactivation of pRB via CDKs, thereby suppressing E2F activity (Campisi et al., 2007). Interestingly, especially in the light of splicing-associated changes with *BUD13*, the mechanism that has only recently begun to be better understood due to alternative splicing, which is emerging as an important contributor to both senescence and ageing.

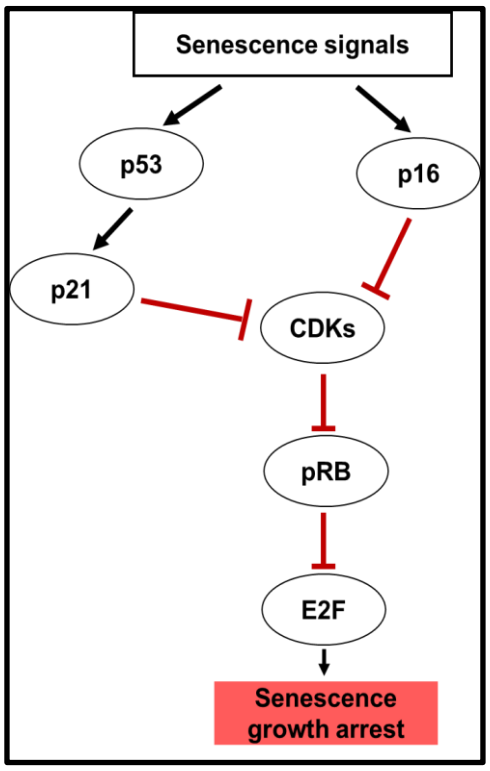

Fig.47. Schematic representation of induction of cellular senescence by p53 or p16 - Active p53 induces senescence growth arrest by inducing p21 expression while p16-pRB suppress E2F expression that controls the expression of genes for cell-cycle progression.

The synergism between alternative splicing of *BUD13* and cellular senescence in *BUD13-S1* containing fibroblasts is thought provoking. The alternative splicing event leading to the production of *S1* leads to cellular senescence in cultured fibroblasts in both sets of individuals expressing different levels of BUD13-S1 protein. However, the rate at which senescence approaches the two sets of cultured fibroblasts is apparently different- while a residual 20% S1 expression causes an elevated p21 expression and a highly positive signal for senescence-associated beta-galactosidase, a 50% residual S1 expression is associated with a relatively mild disease phenotype and marked by a slower progression towards cellular senescence. A p21 expression comparable to control cell lines in the fibroblasts from the older individuals (further supported by a normal growth behaviour in cell culture) is probably indicative of a lower impact of progressive stress-induced senescence. Furthermore, the p16 expression results were inconclusive. However, it must be noted that p16 and p21 are not equivalent, and that although the regulation between p53 and p16-pRB pathways may be reciprocal, there may be differences in how cells in culture behave when one or the other pathways regulate the senescence response (Campisi et al., 2007, Sherr, C.J. & Roberts, J.M., 1999). This might offer an explanation to our inconclusive p16 expression results.

Our findings are also interesting in the light of a recent study evaluating spliceosomal genes influencing both replicative senescence (RS) and oxidative stress- induced senescence (OSIS). The study in primary human fibroblasts uncovered 58 significantly and commonly associated spliceosomal genes in both RS and OSIS transcriptomes. The genes, including *BUD13*, exhibited a common shift in expression at the pre-senescent stage and their perturbation was concluded to trigger cells to enter senescence, suggesting their role as a gatekeeper (Kwon et al., 2020). As *BUD13* splicing- associated changes in this study not only include a definitive evidence of cellular senescence but also the development of a premature ageing disease phenotype, this study provides functional evidence to propose alternative splicing in *BUD13* or the generation of *BUD13-S1* as a crucial regulator of cellular senescence and additionally, physiological ageing. A remarkable example in this light is progerin, that is reportedly generated in diseases such as Hutchinson-Gilford Progeria syndrome. The protein, as seen in disease condition owing to aberrant *LMNA* splicing, has also been detected in primary fibroblast cultures obtained from the skin of normal donors at old ages owing to the sporadic occurrence of the same splicing event as seen in HGPS and therefore, has been of immense interest to ageing researchers (Righolt et al., 2011; Scaffidi and Misteli, 2006).

An in-depth, cellular characterisation of the mutant fibroblasts thus, revealed changes in the nuclear lamina, elevated ROS levels, accumulation of electron dense, cytosolic aggregates and poor proliferation accompanied by signs of cellular senescence. As is the case for variable clinical severity, the extent of these cellular changes or the damage also correlate to the residual *BUD13-S1* expression. The cellular phenotypes are, moreover, reminiscent of classical hallmarks observed in physiological ageing as well as several human progeroid disorders. The findings hint *BUD13* as perhaps a crucial candidate regulating physiological ageing and cellular senescence, perhaps through alternative splicing.

4.5. Comparison of *BUD13* human mutation with *Bud13* mutations in mice

Mouse models have gained a lot of momentum in being excellent mammalian systems to study ageing. Firstly, they have a relatively short lifespan, which makes it feasible to monitor the ageing process in a reasonable window frame. Secondly, the mouse gestation period can be more frequent and quicker compared to other higher mammalian systems, lasting on an average of about three weeks. This makes it relatively faster to obtain more progeny in a given frame of time to obtain a high *n* number for experiments. However, despite a popular model choice for disease modeling, the relevance of mice in disease studies has been questioned due to obvious species differences and various false positives that have been reported previously for mouse data. Also, the reliance of most mouse studies on a single genetic background may delimit the expanse of inferences that may be drawn (Gasch et al., 2016).

4.5.1. Consequences of the insertion of exact human mutation: mouse *Bud13*^{106del}

The knock-in of the precise human mutation in the mouse *Bud13* gene led to two alternative splicing events resulting in the production of two transcripts at the mRNA level:

(i) One large isoform of Bud13 (p. Arg229_Asp334del), “106-del”, which is almost the same size as the splice isoform generated in the 113-del mouse model, and

(ii) A more abundant shorter isoform carrying a premature termination codon (PTC)

Since the large isoform was not as abundantly expressed and the shorter isoform underwent nonsense-mediated decay due to the PTC, the overall protein-level residual expression of the Bud13 protein in the 106-del mouse was probably deleteriously low and may explain the unviability of even the first-generation chimeric animals. Interestingly, although the knock-in of the precise human mutation does lead to an alternative splicing event, the size of the deletion brought about as a result is much larger in the mouse as compared to the human situation (55 amino acid deletion).

4.5.2. Consequences of a large N-terminal deletion: mouse *Bud13*^{113del}

On the other hand, a targeted frame-shift mutation in *Bud13* N-terminal region resulted in an alternative splicing event creating a Bud13 product, deleted in-frame for 113 amino acids (p. Asp198_Ala310del) and expression levels similar to the wild type protein. Evidently, *Bud13* from our observations, besides its greatly discussed RES associated activity in the spliceosome, has come across as a highly alternative splicing prone pre-mRNA with both the activation of cryptic splice sites and the generation of new splice sites upon exonic mutations.

However, the diploid aggregation of mouse embryonic stem cell clones carrying a 113-amino acid deletion in the Bud13 protein led to the generation of only viable chimeras and germline heterozygotes but not germline homozygotes. This observation re-iterates the observation as seen in vertebrates (Fernandez et al., 2018), that a fully functional Bud13 protein is very crucial for the overall organismal viability and functionality in mice and that truncations present in the germline homozygous state may lead to early embryonic lethality.

Predicted (genomic)	Alternative splicing of CRISPR/ Cas9 mutants	Protein expression	Chimera viability	Germline hetero	Germline homo
p.Leu199Ilefs*11	Bud13 113-del (p.Asp198_Ala310del) 	high	viable	possible	impossible
p.(Arg230*) knock-in	Bud13 106-del (p.Arg229_Asp334del) 	low	unviable	impossible	impossible

Summary of the outcomes of different mouse *Bud13* mutations- The modification of mouse embryonic stem cells using CRISPR/Cas9 yielded different outcomes at genomic-, RNA-, protein- and organismal level.

4.5.3. *Bud13* deletions versus *BUD13* human mutation

In comparison to the 55-amino acid deletion in the BUD13 protein arising from the human mutation, the deletions owing to the CRISPR/Cas9 mediated genetic engineering in mouse Bud13 are more than double the size of the human mutation. This may potentially explain why the mouse mutations are so deleterious- the 106 amino acid deletion (106-del) in murine ESCs did not even give rise to chimeras while the 113-del was not compatible with life in germline homozygotes. However, there is one interesting similarity to the human condition in terms of a correlation between protein expression levels and life expectancy.

The splice isoform generated because of alternative splicing in *Bud13* in 106-del with a very low expression level of the protein reflected a situation similar to that observed in our young patients (6-9 years) who harboured a less abundant splice form 1 (20%) of human BUD13. They underwent a more severe phenotype and early demise like that observed in 106-del mice.

On the other hand, the 113-del mice with an evidently higher Bud13 protein expression and still a lot more compatibility with life as seen with the viability of chimeric animals and germline heterozygotes, represented a situation similar to that observed in the older patients (33-53 years) who, with a higher abundance (50%) of splice form1 of BUD13, are undergoing a much slower and progressive phenotype. The absence of a disease phenotype at birth and a rather late onset of disease in the chimeras may be considered a similarity to the human phenotype in the late onset. The approach used for the generation of chimeric animals was the diploid aggregation method. It involves aggregation between wild type embryo from the foster mother and the mutant diploid embryo where mutant cells should ideally contribute to all cell lineages, unless they are restricted by the CRISPR/Cas9 mediated genetic modification (Artus and Hadjantonakis, 2011). Hence, the presence of wild type cells in the chimeras may have been responsible for delaying the onset of the mutant phenotype to help us uncover a later effect of the *Bud13* mutation as is also seen in the human phenotype.

The histological finding of smaller fat cells in $Bud13^{113delCh}$ along with the observation of reduced fat pad are an indication of a progressive lipoatrophy phenotype similar to that

seen in humans. The absence of a DNA damage repair defect in the presence of UV-radiation was also similar to that seen in humans.

Overall, given the observation that the insertion of the exact human mutation in *Bud13* leads to an alternative splicing event causing a large in-frame deletion of 106 amino acids, an ideal mouse model to mimic the human mutation would be a CRISPR/Cas9 mediated, 55 amino acid in-frame deletion at the N-terminus, which is of the exact size as the human mutation. Following the deletion, downstream investigations would be instrumental in conclusively indicating if the Bud13-protein expression in mice and the resulting organismal (un)viability is really corelateable to the size of the deletion contained in the N-terminus.

Interestingly, the RNA-seq analysis of the mouse embryonic stem cells also did not indicate any signs of dysfunctional splicing processes. Our observation is in line with the findings from Buskin et al., 2018 showing that CRISPR/Cas9 edited iPSCs for the most severe clinical phenotype of retinitis pigmentosa brought about clear abnormalities in the differentiated retinal pigment epithelium despite very little splicing deficiency reflected by very few differential splicing events. The absence of a high rate of global intron retention rate is a clear evidence of unaffected global pre-mRNA processing, indicative of an unaffected RES complex function as is also seen in humans. A protein alignment of mutated BUD13 (human) versus mutant Bud13 (mouse) reinstates that the C-terminus might be sufficient for splicing associated activities of the protein (figure 49).

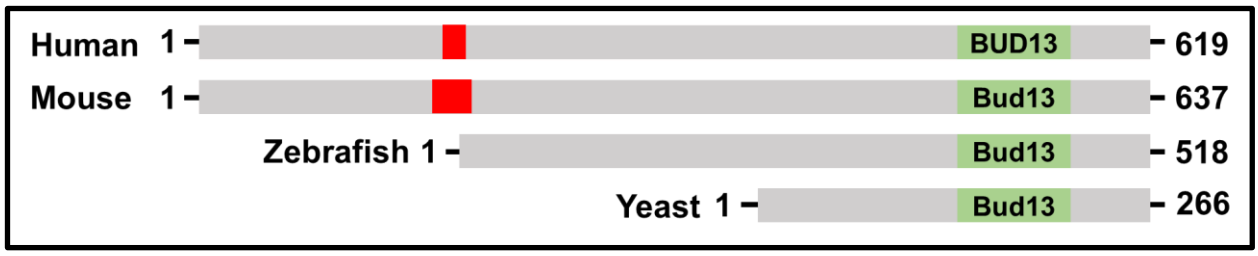

Fig.48. Protein alignment of a mutant human BUD13 p.(Arg230*) versus mouse Bud13 (Bud13-106del/ Bud13-113del) versus a shorter Zebrafish Bud13 and the shortest, Yeast Bud13 as estimated using Uniprot sequence database (Bateman A, 2019) and Clustal Omega alignment tool (Sievers F. et al., 2011) for sequence comparison.

5. Summary and Outlook

5.1. Findings from *BUD13* Human Mutation

In summary, at the time of submission of this report, our results are the very first evidence to the scientific community about the effects of *BUD13* mutation pathogenicity in humans and the downstream effects of the possible variations, therein, as observed in nature. Our findings intersect with several molecular/cellular hallmarks of ageing and human progeroid disorders including classical, Hutchinson Gilford Progeria Syndrome, corroborating our statement that the disease is a progeroid phenotype.

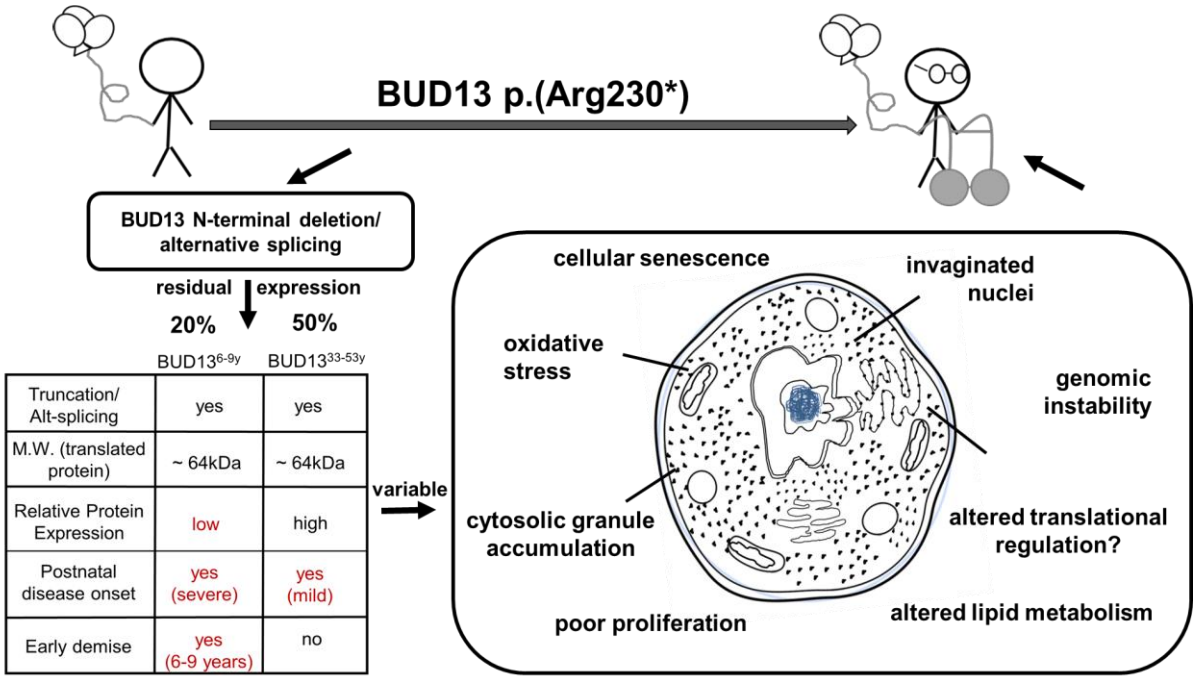

Fig.49. Summary of the effects of BUD13 p.(Arg230*) nonsense mutation at organismal, molecular and cellular level, leading to a progeroid phenotype in humans.

Although at the molecular level, the *BUD13* -associated splicing activity of RES complex apparently remains unaffected, the pre-mRNA itself undergoes an incredible splicing event yielding an isoform that we refer to as *BUD13-S1* or simply *S1*: the expression levels of *S1* are decisive of both the lifespan and the severity of the disease phenotype. An extensively reduced expression of S1 protein leads to a rapidly accelerated ageing or

progeroid phenotype that is accompanied at the cellular level, at least in dermal fibroblasts, by rapidly accumulating oxidative stress, invaginated cellular nuclei, genomic instability, and cellular senescence. A variable degree of lipoatrophy in all the individuals hints towards an altered lipid metabolism. Additionally, the fibroblasts isolated from the patients exhibit numerous aggregates in the cytoplasm. It remains to be understood with future experiments as to what is the exact nature of the rapidly assimilating electron dense granules, especially in the cell cytoplasm of the young individuals. Could this observation have a link to the suspected additional role of the N-terminus of BUD13? A detailed investigation of potential pathomechanisms involving the lysosomal-autophagy pathway and altered ribosomal biogenesis & translational regulation were proposed to shed light on this question.

Furthermore, what causes the strange invaginations in *BUD13* mutated nuclei? Unlike progeroid laminopathies, the nuclear envelope for *BUD13* mutant cells is seemingly intact. S1 protein is not toxic to cellular nuclei as seen in the case of the older patients. There are some hints of hindrances in mitotic cell division, but it is unclear at what stage and which proteins are affected in the process. Future experiments must be focused on understanding the downstream effects of *BUD13* nonsense mutation on the progression of cell cycle checkpoints.

5.2. Findings from *Bud13* Mouse mutations

In support of our observations in humans, we have corresponding mouse models mimicking the disease statuses to some extent. Although, at the genomic level, we were able to insert the exact human mutation in *Bud13*, it led to an alternative splicing event (106-del) different to that observed in case of the human mutation. This event in addition to the embryonic lethality of the exact homozygous nonsense mutation in *Bud13* in mouse is most likely due to the vast inter-species differences. Our work provides functional evidence to speculations from previous RES- associated investigations in showing how the protein has evolved over the course of evolution with increasing complexity of higher organisms, from yeast to zebrafish to mammals such as mice and the more complex, human beings. The protein, understandably so far, represents an under-investigated candidate that maybe extremely influential in physiological ageing processes.

	Bud13$^{106\text{-del}}$	Bud13$^{113\text{-del}}$
Truncation/ Alt-splicing	yes	yes
M.W. (translated protein)	~ 59kDa	~ 58kDa
Relative Protein Expression	low	high
Chimera viability	unviable	viable
Germline (homozygous)	impossible	unviable

Fig.50. Summary of the effects of Bud13 protein mutations on mice at a molecular level and organismal, leading to a potentially deleterious phenotype in mice.

As a future experiment, it would be interesting to circumvent the rather interesting nature of the mouse *Bud13* to eliminate genomic mutations via pre-mRNA alternative splicing and bring about a CRISPR/Cas9 mediated deletion in only the RES activity associated, C-terminal domain (keeping the N-terminal intact) to check

(i) first, the extent to which splicing processes are affected using RNA-seq and compare them against the changes observed in the backdrop of N-terminal variations, or in other words, differentiate between N and C-terminal functions, and

(ii) if there are changes in splicing (which are expected in the light of RES-associated activities), what are the consequential proteome or metabolome level disparities? Do such changes affect organismal viability or in other words, is RES complex crucial to mammalian organismal viability?

Bibliography

1. Adams MD, Celniker SE, Holt RA, Evans CA, Gocayne JD, Amanatides PG, Scherer SE, Li PW, Hoskins RA, Galle RF, George RA, Lewis SE, Richards S, Ashburner M, Henderson SN, Sutton GG, Wortman JR, Yandell MD, Zhang Q, Chen LX, Brandon RC, Rogers YH, Blazej RG, Champe M, Pfeiffer BD, Wan KH, Doyle C, Baxter EG, Helt G, Nelson CR, Gabor GL, Abril JF, Agbayani A, An HJ, Andrews-Pfannkoch C, Baldwin D, Ballew RM, Basu A, Baxendale J, Bayraktaroglu L, Beasley EM, Beeson KY, Benos PV, Berman BP, Bhandari D, Bolshakov S, Borkova D, Botchan MR, Bouck J, Brokstein P, Brottier P, Burtis KC, Busam DA, Butler H, Cadieu E, Center A, Chandra I, Cherry JM, Cawley S, Dahlke C, Davenport LB, Davies P, de Pablos B, Delcher A, Deng Z, Mays AD, Dew I, Dietz SM, Dodson K, Doup LE, Downes M, Dugan-Rocha S, Dunkov BC, Dunn P, Durbin KJ, Evangelista CC, Ferraz C, Ferriera S, Fleischmann W, Fosler C, Gabrielian AE, Garg NS, Gelbart WM, Glasser K, Glodek A, Gong F, Gorrell JH, Gu Z, Guan P, Harris M, Harris NL, Harvey D, Heiman TJ, Hernandez JR, Houck J, Hostin D, Houston KA, Howland TJ, Wei MH, Ibegwam C, Jalali M, Kalush F, Karpen GH, Ke Z, Kennison JA, Ketchum KA, Kimmel BE, Kodira CD, Kraft C, Kravitz S, Kulp D, Lai Z, Lasko P, Lei Y, Levitsky AA, Li J, Li Z, Liang Y, Lin X, Liu X, Mattei B, McIntosh TC, McLeod MP, McPherson D, Merkulov G, Milshina NV, Mobarry C, Morris J, Moshrefi A, Mount SM, Moy M, Murphy B, Murphy L, Muzny DM, Nelson DL, Nelson DR, Nelson KA, Nixon K, Nusskern DR, Pacleb JM, Palazzolo M, Pittman GS, Pan S, Pollard J, Puri V, Reese MG, Reinert K, Remington K, Saunders RD, Scheeler F, Shen H, Shue BC, Sidén-Kiamos I, Simpson M, Skupski MP, Smith T, Spier E, Spradling AC, Stapleton M, Strong R, Sun E, Svirskas R, Tector C, Turner R, Venter E, Wang AH, Wang X, Wang ZY, Wassarman DA, Weinstock GM, Weissenbach J, Williams SM, WoodageT, Worley KC, Wu D, Yang S, Yao QA, Ye J, Yeh RF, Zaveri JS, Zhan M, Zhang G, Zhao Q, Zheng L, Zheng XH, Zhong FN, Zhong W, Zhou X, Zhu S, Zhu X, Smith HO, Gibbs RA, Myers EW, Rubin GM, Venter JC. The genome sequence of Drosophila melanogaster. Vol. 287, Science. American Association for the Advancement of Science; 2000. p. 2185–95.

2. Afzal M, Zaman Q, Kornak U, Mundlos S, Malik S, Flöttmann R. Novel splice mutation in LRP4 causes severe type of Cenani-Lenz syndactyly syndrome with oro-facial and skeletal symptoms. Eur J Med Genet. 2017 Aug 1;60(8):421–5.

3. Allison DF, Wang GG. R-loops: formation, function, and relevance to cell stress. Cell Stress. 2019 Feb 11;3(2):38–46.

4. Anand D, Agrawal SA, Slavotinek A, Lachke SA. Mutation update of transcription factor genes FOXE3, HSF4, MAF, and PITX3 causing cataracts and other developmental ocular defects. Hum Mutat. 2018 Apr 1;39(4):471–94.

5. Anders S, Huber W. Differential expression analysis for sequence count data. Genome Biol. 2010 Oct 27;11(10).

6. Andreeva A, Howorth D, Chothia C, Kulesha E, Murzin AG. SCOP2 prototype: A new approach to protein structure mining. Nucleic Acids Res. 2014 Jan 1;42(D1).

7. Andrews JM, Heddle R, Hebbard GS, Checklin H, Besanko L, Fraser RJ. Age and gender affect likely manometric diagnosis: Audit of a tertiary referral hospital clinical esophageal manometry service. J Gastroenterol Hepatol. 2009 Jan;24(1):125-8

8. Anna A, Monika G. Splicing mutations in human genetic disorders: examples, detection, and confirmation. Vol. 59, Journal of Applied Genetics. Springer Verlag; 2018. p. 253–68.

9. Arora Z, Thota PN, Sanaka MR. Achalasia: current therapeutic options. Vol. 8, Therapeutic Advances in Chronic Disease. SAGE Publications Ltd; 2017. p. 101–8.

10. Ashapkin V V., Kutueva LI, Kurchashova SY, Kireev II. Are there common mechanisms between the Hutchinson-Gilford progeria syndrome and natural aging? Vol. 10, Frontiers in Genetics. Frontiers Media S.A.; 2019.

11. Bachir S, Aouar A. Study of the impact of consanguinity on abortion and mortality in the population of Beni Abbes (southwestern Algeria). Vol. 20, Egyptian Journal of Medical Human Genetics. Springer; 2019.

Baker KE, Parker R. Nonsense-mediated mRNA decay: terminating erroneous gene expression. Curr Opin Cell Biol. 2004 Jun;16(3):293-9

12. Bandesh K, Prasad G, Giri AK, Kauser Y, Upadhyay M, Basu A, Tandon N, Bharadwaj D. Genome-wide association study of blood lipids in Indians confirms universality of established variants. J Hum Genet. 2019 Jun 1;64(6):573–87.

13. Bao P, Will CL, Urlaub H, Boon KL, Lührmann R. The RES complex is required for efficient transformation of the precatalytic B spliceosome into an activated Bact complex. Genes Dev. 2017 Dec 1;31(23–24):2416–29.

14. Barzilai N, Huffman DM, Muzumdar RH, Bartke A. The critical role of metabolic pathways in aging. Vol. 61, Diabetes. 2012. p. 1315–22.

15. Bateman A. UniProt: A worldwide hub of protein knowledge. Nucleic Acids Res. 2019 Jan 8;47(D1):D506–15.

16. Batenburg NL, Thompson EL, Hendrickson EA, Zhu X. Cockayne syndrome group B protein regulates DNA double-strand break repair and checkpoint activation. EMBO J. 2015 May 12;34(10):1399–416.

17. Ben-Dov C, Hartmann B, Lundgren J, Valcárcel J. Genome-wide analysis of alternative pre-mRNA splicing. Vol. 283, Journal of Biological Chemistry. 2008. p. 1229–33.

18. Bener A, Mohammad RR. Global distribution of consanguinity and their impact on complex diseases: Genetic disorders from an endogamous population. Egypt J Med Hum Genet. 2017 Oct 1;18(4):315–20.

19. Bikkul MU, Clements CS, Godwin LS, Goldberg MW, Kill IR, Bridger JM. Farnesyltransferase inhibitor and rapamycin correct aberrant genome organisation and decrease DNA damage respectively, in hutchinson-gilford progeria syndrome fibroblasts. Biogerontology. 2018;19(6):579–602.

20. Blanco FJ, Bernabeu C. Alternative splicing factor or splicing factor-2 plays a key role in intron retention of the endoglin gene during endothelial senescence. Aging Cell. 2011 Oct;10(5):896–907.

21. Blanco FJ, Grande MT, Langa C, Oujo B, Velasco S, Rodriguez-Barbero A, Perez-Gomez E, Quintanilla M, López-Novoa JM, Bernabeu C. S-endoglin expression is induced in senescent endothelial cells and contributes to vascular pathology. Circ Res. 2008 Dec 5;103(12):1383–92.

22. Blanco MR, Martin JS, Kahlscheuer ML, Krishnan R, Abelson J, Laederach A, Walter NG. Single Molecule Cluster Analysis dissects splicing pathway conformational dynamics. Nat Methods. 2015 Nov 1;12(11):1077–84.

23. Blasco MA. Telomere length, stem cells and aging. Vol. 3, Nature Chemical Biology. Nature Publishing Group; 2007. p. 640–9.

24. Borroni AP, Emanuelli A, Shah PA, Ilić N, Apel-Sarid L, Paolini B, Manikoth Ayyathan D, Koganti P, Levy-Cohen G, Blank M Smurf2 regulates stability and the autophagic–lysosomal turnover of lamin A and its disease-associated form progerin. Aging Cell. 2018 Apr 1;17(2).

25. Brooks MA, Dziembowski A, Quevillon-Cheruel S, Henriot V, Faux C, van Tilbeurgh H, Séraphin B. Structure of the yeast Pml1 splicing factor and its integration into the RES complex. Nucleic Acids Res. 2009;37(1):129–43.

26. Brooks MA, Dziembowski A, Quevillon-Cheruel S, Henriot V, Faux C, van Tilbeurgh H, Séraphin B. Structure of the yeast Pml1 splicing factor and its integration into the RES complex. Nucleic Acids Res. 2009;37(1):129–43.

27. Buchwalter A, Hetzer MW. Nucleolar expansion and elevated protein translation in premature aging. Nat Commun. 2017 Dec 1;8(1).

28. Budak G, Srivastava R, Janga SC. Seten: A tool for systematic identification and comparison of processes, phenotypes, and diseases associated with RNA-binding proteins from condition-specific CLIP-seq profiles. RNA. 2017 Jun 1;23(6):836–46.

29. Buskin A, Zhu L, Chichagova V, Basu B, Mozaffari-Jovin S, Dolan D, Droop A, CollinJ, Bronstein R, Mehrotra S, Farkas M, Hilgen G, White K, Pan KT, Treumann A, Hallam D, Bialas K, Chung G, Mellough C, Ding Y, Krasnogor N, Przyborski S, Zwolinski S, Al-Aama J, Alharthi S, Xu Y, Wheway G, Szymanska K, McKibbin M,

Inglehearn CF, Elliott DJ, Lindsay S, Ali RR, Steel DH, Armstrong L, Sernagor E, Urlaub H, Pierce E, Lührmann R, Grellscheid SN, Johnson CA, Lako M. Disrupted alternative splicing for genes implicated in splicing and ciliogenesis causes PRPF31 retinitis pigmentosa. Nat Commun. 2018;

30. Cabanillas R, Cadiñanos J, Villameytide JA, Pérez M, Longo J, Richard JM, Alvarez R, Durán NS, Illán R, González DJ, López-Otín C. Néstor-Guillermo progeria syndrome: A novel premature aging condition with early onset and chronic development caused by BANF1 mutations. Am J Med Genet Part A. 2011 Nov;155(11):2617–25.

31. Campisi J, D'Adda Di Fagagna F. Cellular senescence: When bad things happen to good cells. Vol. 8, Nature Reviews Molecular Cell Biology. 2007. p. 729–40.

32. Carlston CM, Afify ZA, Palumbos JC, Bagley H, Barbagelata C, Wooderchak-Donahue WL, Mao R, Carey JC. Variable expressivity and incomplete penetrance in a large family with non-classical Diamond-Blackfan anemia associated with ribosomal protein L11 splicing variant. Am J Med Genet Part A. 2017 Oct 1;173(10):2622–7.

33. Carrero D, Soria-Valles C, López-Otín C. Hallmarks of progeroid syndromes: Lessons from mice and reprogrammed cells. Vol. 9, DMM Disease Models and Mechanisms. Company of Biologists Ltd; 2016. p. 719–35.

34. Chan WL, Steiner M, Witkos T, Egerer J, Busse B, Mizumoto S, Pestka JM, Zhang H, Hausser I, Khayal LA, Ott CE, Kolanczyk M, Willie B, Schinke T, Paganini C, Rossi A, Sugahara K, Amling M, Knaus P, Chan D, Lowe M, Mundlos S, Kornak U. Impaired proteoglycan glycosylation, elevated TGF-β signaling, and abnormal osteoblast differentiation as the basis for bone fragility in a mouse model for gerodermia osteodysplastica. PLoS Genet. 2018 Mar 1;14(3).

35. Colombo EA, Fontana L, Roversi G, Negri G, Castiglia D, Paradisi M, Zambruno G, Larizza L. Novel physiological RECQL4 alternative transcript disclosed by molecular characterisation of Rothmund-Thomson Syndrome sibs with mild phenotype. Eur J Hum Genet. 2014 Nov 5;22(11):1298–304.

36. Columbaro M, Mattioli E, Schena E, Capanni C, Cenni V, Levy N, Navarro CL, Del Coco R, Squarzoni S, Camozzi D, Hutchison CJ, Wehnert M, Lattanzi G. Prelamin

A processing and functional effects in restrictive dermopathy. Vol. 9, Cell Cycle. Taylor and Francis Inc.; 2010. p. 4766–8.

37. Costantini A, Alm JJ, Tonelli F, Valta H, Huber C, Tran AN, Daponte V, Kirova N, Kwon YU, Bae JY, Chung WY, Tan S, Sznajer Y, Nishimura G, Näreoja T, Warren AJ, Cormier-Daire V, Kim OH, Forlino A, Cho TJ, Mäkitie O. Novel RPL13 Variants and Variable Clinical Expressivity in a Human Ribosomopathy With Spondyloepimetaphyseal Dysplasia. J Bone Miner Res. 2021 Feb;36(2):283-297.

38. Coppé J-P, Desprez P-Y, Krtolica A, Campisi J. The Senescence-Associated Secretory Phenotype: The Dark Side of Tumor Suppression. Annu Rev Pathol Mech Dis. 2010 Jan;5(1):99–118.

39. Dechat T, Pfleghaar K, Sengupta K, Shimi T, Shumaker DK, Solimando L, Goldman RD. Nuclear lamins: Major factors in the structural organization and function of the nucleus and chromatin. Vol. 22, Genes and Development. 2008. p. 832–53.

40. Demir E, Sabatelli P, Allamand V, Ferreiro A, Moghadaszadeh B, Makrelouf M, Topaloglu H, Echenne B, Merlini L, Guicheney P. Mutations in COL6A3 cause severe and mild phenotypes of Ullrich congenital muscular dystrophy. Am J Hum Genet. 2002;70(6):1446–58.

41. Deschênes M, Chabot B. The emerging role of alternative splicing in senescence and aging. Vol. 16, Aging Cell. Blackwell Publishing Ltd; 2017. p. 918–33.

42. Desmet FO, Hamroun D, Lalande M, Collod-Bëroud G, Claustres M, Béroud C. Human Splicing Finder: An online bioinformatics tool to predict splicing signals. Nucleic Acids Res. 2009;37(9).

43. Dimopoulou A, Fischer B, Gardeitchik T, Schröter P, Kayserili H, Schlack C, Li Y, Brum JM, Barisic I, Castori M, Spaich C, Fletcher E, Mahayri Z, Bhat M, Girisha KM, Lachlan K, Johnson D, Phadke S, Gupta N, Simandlova M, Kabra M, David A, Nijtmans L, Chitayat D, Tuysuz B, Brancati F, Mundlos S, Van Maldergem L, Morava E, Wollnik B, Kornak U. Genotype-phenotype spectrum of PYCR1-related autosomal recessive cutis laxa. Mol Genet Metab. 2013 Nov;110(3):352–61.

44. D'Orazio J, Jarrett S, Amaro-Ortiz A, Scott T. UV radiation and the skin. Vol. 14, International Journal of Molecular Sciences. MDPI AG; 2013. p. 12222–48.

45. Draptchinskaia N, Gustavsson P, Andersson B, Pettersson M, Willig TN, Dianzani I, Ball S, Tchernia G, Klar J, Matsson H, Tentler D, Mohandas N, Carlsson B, Dahl N. The gene encoding ribosomal protein S19 is mutated in Diamond-Blackfan anaemia. Nat Genet. 1999 Feb;21(2):169–75.

46. Dunker AK, Silman I, Uversky VN, Sussman JL. Function and structure of inherently disordered proteins. Vol. 18, Current Opinion in Structural Biology. 2008. p. 756–64.

47. Dyson HJ, Wright PE. Intrinsically unstructured proteins and their functions. Vol. 6, Nature Reviews Molecular Cell Biology. 2005. p. 197–208.

48. Dziembowski A, Ventura AP, Rutz B, Caspary F, Faux C, Halgand F, Laprévote O, Séraphin B. Proteomic analysis identifies a new complex required for nuclear pre-mRNA retention and splicing. EMBO J. 2004 Dec 8;23(24):4847–56.

49. Eakin GS, Hadjantonakis AK. Production of chimeras by aggregation of embryonic stem cells with diploid or tetraploid mouse embryos. Nat Protoc. 2006 Aug;1(3):1145–53.

50. Egerer J, Emmerich D, Fischer-Zirnsak B, Chan WL, Meierhofer D, Tuysuz B, Marschner K, Sauer S, Barr FA, Mundlos S, Kornak U. GORAB Missense Mutations Disrupt RAB6 and ARF5 Binding and Golgi Targeting. J Invest Dermatol. 2015 Oct 14;135(10):2368–76.

51. Ehmke N, Graul-Neumann L, Smorag L, Koenig R, Segebrecht L, Magoulas P, Scaglia F, Kilic E, Hennig AF, Adolphs N, Saha N, Fauler B, Kalscheuer VM, Hennig F, Altmüller J, Netzer C, Thiele H, Nürnberg P, Yigit G, Jäger M, Hecht J, Krüger U, Mielke T, Krawitz PM, Horn D, Schuelke M, Mundlos S, Bacino CA, Bonnen PE, Wollnik B, Fischer-Zirnsak B, Kornak U De Novo Mutations in SLC25A24 Cause a Craniosynostosis Syndrome with Hypertrichosis, Progeroid Appearance, and Mitochondrial Dysfunction. Am J Hum Genet. 2017 Nov 2;101(5):833–43.

52. Eriksson M, Brown WT, Gordon LB, Glynn MW, Singer J, Scott L, Erdos MR, Robbins CM, Moses TY, Berglund P, Dutra A, Pak E, Durkin S, Csoka AB, Boehnke M, Glover TW, Collins FS. Recurrent de novo point mutations in lamin A cause Hutchinson-Gilford progeria syndrome. Nature. 2003 May 15;423(6937):293–8.

53. Evangelisti C, Cenni V, Lattanzi G. Potential therapeutic effects of the MTOR inhibitors for preventing ageing and progeria-related disorders. British Journal of Clinical Pharmacology. Blackwell Publishing Ltd; 2016. p. 1229–44.

54. Farag AAM, Fadel M. Optical absorption and dispersion analysis of nanocrystalline perylene-3,4,9,10-tetracarboxylic-3,4,9,10-dianhydride film prepared by dip coating and its optoelectronic application. Opt Laser Technol. 2013 Feb;45(1):356–63.

55. Faustino NA, Cooper TA. Pre-mRNA splicing and human disease. Vol. 17, Genes and Development. 2003. p. 419–37.

56. Fernandez JP, Moreno-Mateos MA, Gohr A, Miao L, Chan SH, Irimia M, Giraldez AJ. RES complex is associated with intron definition and required for zebrafish early embryogenesis. PLoS Genet. 2018 Jul 1;14(7).

57. Finley J. Alteration of splice site selection in the LMNA gene and inhibition of progerin production via AMPK activation. Med Hypotheses. 2014 Nov 1;83(5):580–7.

58. Finley J. Cellular stress and AMPK activation as a common mechanism of action linking the effects of metformin and diverse compounds that alleviate accelerated aging defects in Hutchinson-Gilford progeria syndrome. Med Hypotheses. 2018 Sep 1;118:151–62.

59. Fischer B, Callewaert B, Schröter P, Coucke PJ, Schlack C, Ott CE, Morroni M, Homann W, Mundlos S, Morava E, Ficcadenti A, Kornak U. Severe congenital cutis laxa with cardiovascular manifestations due to homozygous deletions in ALDH18A1. Mol Genet Metab. 2014;112(4):310–6.

60. Fischer B, Dimopoulou A, Egerer J, Gardeitchik T, Kidd A, Jost D, Kayserili H, Alanay Y, Tantcheva-Poor I, Mangold E, Daumer-Haas C, Phadke S, Peirano RI,

Heusel J, Desphande C, Gupta N, Nanda A, Felix E, Berry-Kravis E, Kabra M, Wevers RA, van Maldergem L, Mundlos S, Morava E, Kornak U. Further characterization of ATP6V0A2-related autosomal recessive cutis laxa. Hum Genet. 2012 Nov;131(11):1761–73.

61. Fischer-Zirnsak B, Koenig R, Alisch F, Güneş N, Hausser I, Saha N, Beck-Woedl S, Haack TB, Thiel C, Kamrath C, Tüysüz B, Henning S, Mundlos S, Hoffmann K, Horn D, Kornak U. SOPH syndrome in three affected individuals showing similarities with progeroid cutis laxa conditions in early infancy. J Hum Genet. 2019 Jul 1;64(7):609–16.

62. Folgueras AR, Freitas-Rodríguez S, Velasco G, López-Otín C. Mouse models to disentangle the hallmarks of human aging. Circ Res. 2018;123(7):905–24.

63. Fontana L, Partridge L, Longo VD. Extending healthy life span-from yeast to humans. Vol. 328, Science. 2010. p. 321–6.

64. Fox-Walsh KL, Hertel KJ. Splice-site pairing is an intrinsically high fidelity process. Proc Natl Acad Sci U S A. 2009 Feb 10;106(6):1766–71.

65. Fradet-Turcotte A, Canny MD, Escribano-Díaz C, Orthwein A, Leung CC, Huang H, Landry MC, Kitevski-LeBlanc J, Noordermeer SM, Sicheri F, Durocher D. 53BP1 is a reader of the DNA-damage-induced H2A Lys 15 ubiquitin mark. Nature. 2013;499(7456):50–4.

66. Frankiw L, Majumdar D, Burns C, Vlach L, Moradian A, Sweredoski MJ, Baltimore D. BUD13 Promotes a Type I Interferon Response by Countering Intron Retention in Irf7. Mol Cell. 2019 Feb 21;73(4):803-814.e6.

67. Freund A, Laberge RM, Demaria M, Campisi J. Lamin B1 loss is a senescence-associated biomarker. Mol Biol Cell. 2012 Jun 1;23(11):2066–75.

68. Friedrich K, Lee L, Leistritz DF, Nürnberg G, Saha B, Hisama FM, Eyman DK, Lessel D, Nürnberg P, Li C, Garcia-F-Villalta MJ, Kets CM, Schmidtke J, Cruz VT, Van den Akker PC, Boak J, Peter D, Compoginis G, Cefle K, Ozturk S, López N, Wessel T, Poot M, Ippel PF, Groff-Kellermann B, Hoehn H, Martin GM, Kubisch C,

Oshima J. WRN mutations in Werner syndrome patients: Genomic rearrangements, unusual intronic mutations and ethnic-specific alterations. Hum Genet. 2010 Jul;128(1):103–11.

69. Fumagalli M, Rossiello F, Clerici M, Barozzi S, Cittaro D, Kaplunov JM, Bucci G, Dobreva M, Matti V, Beausejour CM, Herbig U, Longhese MP, d'Adda di Fagagna F. Telomeric DNA damage is irreparable and causes persistent DNA-damage-response activation. Nat Cell Biol. 2012 Apr;14(4):355–65.

70. Gabryšová L, Alvarez-Martinez M, Luisier R, Cox LS, Sodenkamp J, Hosking C, Pérez-Mazliah D, Whicher C, Kannan Y, Potempa K, Wu X, Bhaw L, Wende H, Sieweke MH, Elgar G, Wilson M, Briscoe J, Metzis V, Langhorne J, Luscombe NM, O'Garra A. C-Maf controls immune responses by regulating disease-specific gene networks and repressing IL-2 in CD4 + T cells article. Nat Immunol. 2018 May 1;19(5):497–507.

71. Gasch AP, Payseur BA, Pool JE. The Power of Natural Variation for Model Organism Biology. Vol. 32, Trends in Genetics. Elsevier Ltd; 2016. p. 147–54.

72. Goldman RD, Shumaker DK, Erdos MR, Eriksson M, Goldman AE, Gordon LB, Gruenbaum Y, Khuon S, Mendez M, Varga R, Collins FS. Accumulation of mutant lamin A progressive changes in nuclear architecture in Hutchinson-Gilford progeria syndrome. Proc Natl Acad Sci U S A. 2004 Jun 15;101(24):8963–8.

73. Goldring MB. Chondrogenesis, chondrocyte differentiation, and articular cartilage metabolism in health and osteoarthritis. Ther Adv Musculoskelet Dis. 2012;4(4):269–85.

74. Goldsmith TC. Theories of biological aging and Implications for Public Health: Executive Summary. Vol. 20, Experimental gerontology. 2009 Jan.

75. Graul-Neumann LM, Hausser I, Essayie M, Rauch A, Kraus C. Highly variable cutis laxa resulting from a dominant splicing mutation of the elastin gene. Am J Med Genet Part A. 2008 Apr 15;146(8):977–83.

76. Graziotto JJ, Cao K, Collins FS, Krainc D. Rapamycin activates autophagy in Hutchinson-Gilford progeria syndrome: Implications for normal aging and age-dependent neurodegenerative disorders. Vol. 8, Autophagy. Taylor and Francis Inc.; 2012. p. 147–51.

77. Green DR, Galluzzi L, Kroemer G. Mitochondria and the autophagy-inflammation-cell death axis in organismal aging. Vol. 333, Science. 2011. p. 1109–12.

78. Gruosso T, Mieulet V, Cardon M, Bourachot B, Kieffer Y, Devun F, Dubois T, Dutreix M, Vincent-Salomon A, Miller KM, Mechta-Grigoriou F. Chronic oxidative stress promotes H2 AX protein degradation and enhances chemosensitivity in breast cancer patients . EMBO Mol Med. 2016 May;8(5):527–49.

79. Guillard M, Dimopoulou A, Fischer B, Morava E, Lefeber DJ, Kornak U, Wevers RA. Vacuolar H+-ATPase meets glycosylation in patients with cutis laxa. Vol. 1792, Biochimica et Biophysica Acta - Molecular Basis of Disease. 2009. p. 903–14.

80. Hamamy H. Consanguineous marriages preconception consultation in primary health care settings. Vol. 3, Journal of Community Genetics. 2012. p. 185–92.

81. Hansen L, Eiberg H, Rosenberg T. Novel MAF mutation in a family with congenital cataract-microcornea syndrome. Mol Vis. 2007 Oct 18;13:2019–22.

82. Harhouri K, Frankel D, Bartoli C, Roll P, De Sandre-Giovannoli A, Lévy N. An overview of treatment strategies for hutchinson-gilford progeria syndrome. Vol. 9, Nucleus. Taylor and Francis Inc.; 2018. p. 265–76.

83. HARMAN D. THE FREE RADICAL THEORY OF AGING: EFFECT OF AGE ON SERUM COPPER LEVELS. J Gerontol. 1965;20:151–3.

84. Harris E. Review: On the Origin of Species by Charles Darwin. New Sci. 2009 Feb;201(2694):49.

85. Hayflick L, Moorhead PS. The serial cultivation of human diploid cell strains. Exp Cell Res. 1961;25(3):585–621.

86. Hebbar P, Elkum N, Alkayal F, John SE, Thanaraj TA, Alsmadi O. Genetic risk variants for metabolic traits in Arab populations. Sci Rep. 2017 Jan 20;7.

87. Hennies HC, Kornak U, Zhang H, Egerer J, Zhang X, Seifert W, Kühnisch J, Budde B, Nätebus M, Brancati F, Wilcox WR, Müller D, Kaplan PB, Rajab A, Zampino G, Fodale V, Dallapiccola B, Newman W, Metcalfe K, Clayton-Smith J, Tassabehji M, Steinmann B, Barr FA, Nürnberg P, Wieacker P, Mundlos S. Gerodermia osteodysplastica is caused by mutations in SCYL1BP1, a Rab-6 interacting golgin. Nat Genet. 2008 Dec;40(12):1410–2.

88. Hernandez-Segura A, de Jong T V., Melov S, Guryev V, Campisi J, Demaria M. Unmasking Transcriptional Heterogeneity in Senescent Cells. Curr Biol. 2017 Sep 11;27(17):2652-2660.e4.

89. Hunt SE, McLaren W, Gil L, Thormann A, Schuilenburg H, Sheppard D, Parton A, Armean IM, Trevanion SJ, Flicek P, Cunningham F. Ensembl variation resources. Database (Oxford). 2018 Jan 1;2018.

90. Jacquinet A, Verloes A, Callewaert B, Coremans C, Coucke P, de Paepe A, Kornak U, Lebrun F, Lombet J, Piérard GE, Robinson PN, Symoens S, Van Maldergem L, Debray FG. Neonatal progeroid variant of Marfan syndrome with congenital lipodystrophy results from mutations at the 3' end of FBN1 gene. Eur J Med Genet. 2014;57(5):230–4.

91. Javadiyan S, Craig JE, Sharma S, Lower KM, Casey T, Haan E, Souzeau E, Burdon KP. Novel missense mutation in the bZIP transcription factor, MAF, associated with congenital cataract, developmental delay, seizures and hearing loss (Aymé-Gripp syndrome). BMC Med Genet. 2017 May 8;18(1).

92. Johnson AA, Shokhirev MN, Shoshitaishvili B. Revamping the evolutionary theories of aging. Vol. 55, Ageing Research Reviews. Elsevier Ireland Ltd; 2019.

93. Kamphans T, Krawitz PM. GeneTalk: An expert exchange platform for assessing rare sequence variants in personal genomes. Bioinformatics. 2012;28(19):2515–6.

94. Kasper D, Planells-Cases R, Fuhrmann JC, Scheel O, Zeitz O, Ruether K, Schmitt A, Poët M, Steinfeld R, Schweizer M, Kornak U, Jentsch TJ. Loss of the chloride channel CIC-7 leads to lysosomal storage disease and neurodegeneration. EMBO J. 2005 Mar 9;24(5):1079–91.

95. Kelly DP. Cell biology: Ageing theories unified. Vol. 470, Nature. 2011. p. 342–3.

96. Kenyon CJ. The genetics of ageing. Vol. 464, Nature. 2010. p. 504–12.

97. Kim HK, Anwar MA, Choi S. Association of BUD13-ZNF259-APOA5-APOA1-SIK3 cluster polymorphism in 11q23.3 and structure of APOA5 with increased plasma triglyceride levels in a Korean population. Sci Rep. 2019 Dec 1;9(1).

98. Kim, J. I., Li, T., Ho, I. C., Grusby, M. J., & Glimcher, L. H. (1999). Requirement for the c-Maf transcription factor in crystallin gene regulation and lens development. *Proceedings of the National Academy of Sciences of the United States of America*, *96*(7), 3781–3785.

99. Knierim E, Hirata H, Wolf NI, Morales-Gonzalez S, Schottmann G, Tanaka Y, Rudnik-Schöneborn S, Orgeur M, Zerres K, Vogt S, van Riesen A, Gill E, Seifert F, Zwirner A, Kirschner J, Goebel HH, Hübner C, Stricker S, Meierhofer D, Stenzel W, Schuelke M Mutations in Subunits of the Activating Signal Cointegrator 1 Complex Are Associated with Prenatal Spinal Muscular Atrophy and Congenital Bone Fractures. Am J Hum Genet. 2016 Mar 3;98(3):473–89.

100. Kornak U, Reynders E, Dimopoulou A, van Reeuwijk J, Fischer B, Rajab A, Budde B, Nürnberg P, Foulquier F; ARCL Debré-type Study Group, Lefeber D, Urban Z, Gruenewald S, Annaert W, Brunner HG, van Bokhoven H, Wevers R, Morava E, Matthijs G, Van Maldergem L, Mundlos S. Impaired glycosylation and cutis laxa caused by mutations in the vesicular H+-ATPase subunit ATP6V0A2. Nat Genet. 2008 Jan;40(1):32–4.

101. Korneta I, Bujnicki JM. Intrinsic Disorder in the Human Spliceosomal Proteome. PLoS Comput Biol. 2012 Aug;8(8).

102. Koruyucu M, Kang J, Kim YJ, Seymen F, Kasimoglu Y, Lee ZH, Shin TJ, Hyun HK, Kim YJ, Lee SH, Hu JCC, Simmer JP, Kim JW. Hypoplastic AI with Highly Variable Expressivity Caused by ENAM Mutations. J Dent Res. 2018 Aug 1;97(9):1064–9.

103. Kraft K, Geuer S, Will AJ, Chan WL, Paliou C, Borschiwer M, Harabula I, Wittler L, Franke M, Ibrahim DM, Kragesteen BK, Spielmann M, Mundlos S, Lupiáñez DG, Andrey G. Deletions, inversions, duplications: Engineering of structural variants using CRISPR/Cas in mice. Cell Rep. 2015 Feb 10;10(5):833–9.

104. Kurogi Y, Matsuo Y, Mihara Y, Yagi H, Shigaki-Miyamoto K, Toyota S, Azuma Y, Igarashi M, Tani T. Identification of a chemical inhibitor for nuclear speckle formation: Implications for the function of nuclear speckles in regulation of alternative pre-mRNA splicing. Biochem Biophys Res Commun. 2014 Mar 28;446(1):119–24.

105. Kwon SM, Min S, Jeoun UW, Sim MS, Jung GH, Hong SM, Jee BA, Woo HG, Lee C, Yoon G. Global spliceosome activity regulates entry into cellular senescence. FASEB J. 2021 Jan;35(1): e21204.

106. Lander ES, Linton LM, Birren B, Nusbaum C, Zody MC, Baldwin J, Devon K, Dewar K, Doyle M, FitzHugh W, Funke R, Gage D, Harris K, Heaford A, Howland J, Kann L, Lehoczky J, LeVine R, McEwan P, McKernan K, Meldrim J, Mesirov JP, Miranda C, Morris W, Naylor J, Raymond C, Rosetti M, Santos R, Sheridan A, Sougnez C, Stange-Thomann Y, Stojanovic N, Subramanian A, Wyman D, Rogers J, Sulston J, Ainscough R, Beck S, Bentley D, Burton J, Clee C, Carter N, Coulson A, Deadman R, Deloukas P, Dunham A, Dunham I, Durbin R, French L, Grafham D, Gregory S, Hubbard T, Humphray S, Hunt A, Jones M, Lloyd C, McMurray A, Matthews L, Mercer S, Milne S, Mullikin JC, Mungall A, Plumb R, Ross M, Shownkeen R, Sims S, Waterston RH, Wilson RK, Hillier LW, McPherson JD, Marra MA, Mardis ER, Fulton LA, Chinwalla AT, Pepin KH, Gish WR, Chissoe SL, Wendl MC, Delehaunty KD, Miner TL, Delehaunty A, Kramer JB, Cook LL, Fulton RS, Johnson DL, Minx PJ, Clifton SW, Hawkins T, Branscomb E, Predki P, Richardson P, Wenning S, Slezak T, Doggett N, Cheng JF, Olsen A, Lucas S, Elkin C, Uberbacher E, Frazier M, Gibbs RA, Muzny DM, Scherer SE, Bouck JB, Sodergren EJ, Worley KC, Rives CM, Gorrell JH, Metzker ML, Naylor SL, Kucherlapati RS,

Nelson DL, Weinstock GM, Sakaki Y, Fujiyama A, Hattori M, Yada T, Toyoda A, Itoh T, Kawagoe C, Watanabe H, Totoki Y, Taylor T, Weissenbach J, Heilig R, Saurin W, Artiguenave F, Brottier P, Bruls T, Pelletier E, Robert C, Wincker P, Smith DR, Doucette-Stamm L, Rubenfield M, Weinstock K, Lee HM, Dubois J, Rosenthal A, Platzer M, Nyakatura G, Taudien S, Rump A, Yang H, Yu J, Wang J, Huang G, Gu J, Hood L, Rowen L, Madan A, Qin S, Davis RW, Federspiel NA, Abola AP, Proctor MJ, Myers RM, Schmutz J, Dickson M, Grimwood J, Cox DR, Olson MV, Kaul R, Raymond C, Shimizu N, Kawasaki K, Minoshima S, Evans GA, Athanasiou M, Schultz R, Roe BA, Chen F, Pan H, Ramser J, Lehrach H, Reinhardt R, McCombie WR, de la Bastide M, Dedhia N, Blöcker H, Hornischer K, Nordsiek G, Agarwala R, Aravind L, Bailey JA, Bateman A, Batzoglou S, Birney E, Bork P, Brown DG, Burge CB, Cerutti L, Chen HC, Church D, Clamp M, Copley RR, Doerks T, Eddy SR, Eichler EE, Furey TS, Galagan J, Gilbert JG, Harmon C, Hayashizaki Y, Haussler D, Hermjakob H, Hokamp K, Jang W, Johnson LS, Jones TA, Kasif S, Kaspryzk A, Kennedy S, Kent WJ, Kitts P, Koonin EV, Korf I, Kulp D, Lancet D, Lowe TM, McLysaght A, Mikkelsen T, Moran JV, Mulder N, Pollara VJ, Ponting CP, Schuler G, Schultz J, Slater G, Smit AF, Stupka E, Szustakowki J, Thierry-Mieg D, Thierry-Mieg J, Wagner L, Wallis J, Wheeler R, Williams A, Wolf YI, Wolfe KH, Yang SP, Yeh RF, Collins F, Guyer MS, Peterson J, Felsenfeld A, Wetterstrand KA, Patrinos A, Morgan MJ, de Jong P, Catanese JJ, Osoegawa K, Shizuya H, Choi S, Chen YJ, Szustakowki J. Initial sequencing and analysis of the human genome. Nature. 2001 Feb 15;409(6822):860–921.

107. Kunen LCB, Fontes LHS, Moraes-Filho JP, Assirati FS, Navarro-Rodriguez T. Esophageal motility patterns are altered in older adult patients. Rev Gastroenterol Mex. 2020 Jul-Sep;85(3):264-274.

108. Leventhal EQA. Ageing and health. In: Cambridge Handbook of Psychology, Health and Medicine, Second Edition. Cambridge University Press; 2014. p. 20–2.

109. Li M, Khambu B, Zhang H, Kang JH, Chen X, Chen D, Vollmer L, Liu PQ, Vogt A, Yin XM. Suppression of lysosome function induces autophagy via a feedback down-regulation of MTOR complex 1 (MTORC1) activity. J Biol Chem. 2013 Dec 13;288(50):35769–80.

110. Li X, Manley JL. Inactivation of the SR protein splicing factor ASF/SF2 results in genomic instability. Cell. 2005 Aug 12;122(3):365–78.

111. Lin DS, Chang JH, Liu HL, Wei CH, Yeung CY, Ho CS, Shu CH, Chiang MF, Chuang CK, Huang YW, Wu TY, Jian YR, Huang ZD, Lin SP. Compound heterozygous mutations in PYCR1 further expand the phenotypic spectrum of De Barsy syndrome. Am J Med Genet Part A. 2011 Dec;155(12):3095–9.

112. Loaiza N, Demaria M. Cellular senescence and tumor promotion: Is aging the key? Vol. 1865, Biochimica et Biophysica Acta - Reviews on Cancer. Elsevier B.V.; 2016. p. 155–67.

113. Löbrich M, Shibata A, Beucher A, Fisher A, Ensminger M, Goodarzi AA, Barton O, Jeggo PA. γH2AX foci analysis for monitoring DNA double-strand break repair: Strengths, limitations and optimization. Vol. 9, Cell Cycle. Taylor and Francis Inc.; 2010. p. 662–9.

114. Loi M, Cenni V, Duchi S, Squarzoni S, Lopez-Otin C, Foisner R, Lattanzi G, Capanni C. Barrier-to-autointegration factor (BAF) involvement in prelamin a-related chromatin organization changes. Oncotarget. 2016 Mar 29;7(13):15662–77.

115. López-Otín C, Blasco MA, Partridge L, Serrano M, Kroemer G. The hallmarks of aging. Vol. 153, Cell. Cell Press; 2013. p. 1194.

116. Magnuson B, Ekim B, Fingar DC. Regulation and function of ribosomal protein S6 kinase (S6K) within mTOR signalling networks. Vol. 441, Biochemical Journal. 2012. p. 1–21.

117. Makarov EM, Makarova OV, Urlaub H, Gentzel M, Will CL, Wilm M, Lührmann R. Small nuclear ribonucleoprotein remodeling during catalytic activation of the spliceosome. Science (80-). 2002 Dec 13;298(5601):2205–8.

118. Mariño G, Ugalde AP, Salvador-Montoliu N, Varela I, Quirós PM, Cadiñanos J, van der Pluijm I, Freije JM, López-Otín C. Premature aging in mice activates a systemic

metabolic response involving autophagy induction. Hum Mol Genet. 2008;17(14):2196–211.

119. Mariotti LG, Pirovano G, Savage KI, Ghita M, Ottolenghi A, Prise KM, Schettino G. Use of the γ-H2AX assay to investigate DNA repair dynamics following multiple radiation exposures. PLoS One. 2013 Nov 29;8(11).

120. Marteijn JA, Lans H, Vermeulen W, Hoeijmakers JHJ. Understanding nucleotide excision repair and its roles in cancer and ageing. Vol. 15, Nature Reviews Molecular Cell Biology. Nature Publishing Group; 2014. p. 465–81.

121. Martin GM, Oshima J. Lessons from human progeroid syndromes. Vol. 408, Nature. 2000. p. 263–6.

122. Mazin P, Xiong J, Liu X, Yan Z, Zhang X, Li M, He L, Somel M, Yuan Y, Phoebe Chen YP, Li N, Hu Y, Fu N, Ning Z, Zeng R, Yang H, Chen W, Gelfand M, Khaitovich P. Widespread splicing changes in human brain development and aging. Mol Syst Biol. 2013;9.

123. McCauley L. K. (2010). c-Maf and you won't see fat. *The Journal of clinical investigation*, *120*(10), 3440–3442.

124. McClintock D, Ratner D, Lokuge M, Owens DM, Gordon LB, Collins FS, Djabali K. The mutant form of Lamin A that causes Hutchinson-Gilford progeria is a biomarker of cellular aging in human skin. PLoS One. 2007 Dec 5;2(12).

125. Meierhofer D, Wang X, Huang L, Kaiser P. Quantitative analysis of global ubiquitination in HeLa cells by mass spectrometry. J Proteome Res. 2008 Oct;7(10):4566–76.

126. Meister G, Bühler D, Pillai R, Lottspeich F, Fischer U. A multiprotein complex mediates the ATP-dependent assembly of spliceosomal U snRNPs. Nat Cell Biol. 2001;3(11):945–9.

127. Mesquita A, Weinberger M, Silva A, Sampaio-Marques B, Almeida B, Leão C, Costa V, Rodrigues F, Burhans WC, Ludovico P. Caloric restriction or catalase

inactivation extends yeast chronological lifespan by inducing H2O2 and superoxide dismutase activity. Proc Natl Acad Sci U S A. 2010 Aug 24;107(34):15123–8.

128. Miyamoto MI, Djabali K, Gordon LB. Atherosclerosis in ancient humans, accelerated aging syndromes and normal aging: Is lamin a protein a common link? Vol. 9, Global Heart. Elsevier; 2014. p. 211–8.

129. Mohamed M, Kouwenberg D, Gardeitchik T, Kornak U, Wevers RA, Morava E. Metabolic cutis laxa syndromes. Vol. 34, Journal of Inherited Metabolic Disease. 2011. p. 907–16.

130. Monnerat G, Evaristo GPC, Evaristo JAM, Dos Santos CGM, Carneiro G, Maciel L, Carvalho VO, Nogueira FCS, Domont GB, Campos de Carvalho AC. Metabolomic profiling suggests systemic signatures of premature aging induced by Hutchinson–Gilford progeria syndrome. Metabolomics. 2019 Jul 1;15(7).

131. Morava E, Guillard M, Lefeber DJ, Wevers RA. Autosomal recessive cutis laxa syndrome revisited. Eur J Hum Genet [Internet]. 2009;17(9):1099–110

132. Moulson CL, Go G, Gardner JM, van der Wal AC, Smitt JH, van Hagen JM, Miner JH. Homozygous and compound heterozygous mutations in ZMPSTE24 cause the laminopathy restrictive dermopathy. J Invest Dermatol. 2005;125(5):913–9.

133. Na I, Meng F, Kurgan L, Uversky VN. Autophagy-related intrinsically disordered proteins in intra-nuclear compartments. Mol Biosyst. 2016 Sep 1;12(9):2798–817.

134. Narla A, Ebert BL. Ribosomopathies: Human disorders of ribosome dysfunction. Vol. 115, Blood. 2010. p. 3196–205.

135. Navarro CL, Cadiñanos J, De Sandre-Giovannoli A, Bernard R, Courrier S, Boccaccio I, Boyer A, Kleijer WJ, Wagner A, Giuliano F, Beemer FA, Freije JM, Cau P, Hennekam RC, López-Otín C, Badens C, Lévy N. Loss of ZMPSTE24 (FACE-1) causes autosomal recessive restrictive dermopathy and accumulation of Lamin A precursors. Hum Mol Genet. 2005 Jun 1;14(11):1503–13.

136. Navarro CL, De Sandre-Giovannoli A, Bernard R, Boccaccio I, Boyer A, Geneviève D, Hadj-Rabia S, Gaudy-Marqueste C, Smitt HS, Vabres P, Faivre L, Verloes A,

Van Essen T, Flori E, Hennekam R, Beemer FA, Laurent N, Le Merrer M, Cau P, Lévy N. Lamin A and ZMPSTE24 (FACE-1) defects cause nuclear disorganization and identify restrictive dermopathy as a lethal neonatal laminopathy. Hum Mol Genet. 2004 Oct 15;13(20):2493–503.

137. Navas Tejedor P, Palomino Doza J, Tenorio Castaño JA, Enguita Valls AB, Rodríguez Reguero JJ, Martínez Meñaca A, Hernández González I, Bueno Zamora H, Lapunzina Badía PD, Escribano Subías P. Variable Expressivity of a Founder Mutation in the EIF2AK4 Gene in Hereditary Pulmonary Veno-occlusive Disease and Its Impact on Survival. Rev Española Cardiol (English Ed. 2018 Feb;71(2):86–94.

138. Ni L, Snyder M. A genomic study of the bipolar bud site selection pattern in Saccharomyces cerevisiae. Mol Biol Cell. 2001;12(7):2147–70.

139. Nishikawa, K., Nakashima, T., Takeda, S., Isogai, M., Hamada, M., Kimura, A., Kodama, T., Yamaguchi, A., Owen, M. J., Takahashi, S., & Takayanagi, H. (2010). Maf promotes osteoblast differentiation in mice by mediating the age-related switch in mesenchymal cell differentiation. *The Journal of clinical investigation*, *120*(10), 3455–3465.

140. Nussbacher JK, Yeo GW. Systematic Discovery of RNA Binding Proteins that Regulate MicroRNA Levels. Mol Cell. 2018 Mar 15;69(6):1005-1016.e7.

141. Orchard S, Ammari M, Aranda B, Breuza L, Briganti L, Broackes-Carter F, Campbell NH, Chavali G, Chen C, del-Toro N, Duesbury M, Dumousseau M, Galeota E, Hinz U, Iannuccelli M, Jagannathan S, Jimenez R, Khadake J, Lagreid A, Licata L, Lovering RC, Meldal B, Melidoni AN, Milagros M, Peluso D, Perfetto L, Porras P, Raghunath A, Ricard-Blum S, Roechert B, Stutz A, Tognolli M, van Roey K, Cesareni G, Hermjakob H. The MIntAct project - IntAct as a common curation platform for 11 molecular interaction databases. Nucleic Acids Res. 2014 Jan 1;42(D1).

142. Palm W, de Lange T. How Shelterin Protects Mammalian Telomeres. Annu Rev Genet. 2008 Dec;42(1):301–34.

143. Panier S, Boulton SJ. Double-strand break repair: 53BP1 comes into focus. Vol. 15, Nature Reviews Molecular Cell Biology. 2014. p. 7–18.

144. Parra EJ, Mazurek A, Gignoux CR, Sockell A, Agostino M, Morris AP, Petty LE, Hanis CL, Cox NJ, Valladares-Salgado A, Below JE, Cruz M. Admixture mapping in two Mexican samples identifies significant associations of locus ancestry with triglyceride levels in the BUD13/ ZNF259/APOA5 region and fine mapping points to rs964184 as the main driver of the association signal. PLoS One. 2017 Feb 1;12(2).

145. Pellizzoni L, Kataoka N, Charroux B, Dreyfuss G. A novel function for SMN, the spinal muscular atrophy disease gene product, in pre-mRNA splicing. Cell. 1998 Nov 25;95(5):615–24.

146. Peng Y, Clark KJ, Campbell JM, Panetta MR, Guo Y, Ekker SC. Making designer mutants in model organisms. Vol. 141, Development (Cambridge). Company of Biologists Ltd; 2014. p. 4042–54.

147. Pervouchine D, Popov Y, Berry A, Borsari B, Frankish A, Guigó R. Integrative transcriptomic analysis suggests new autoregulatory splicing events coupled with nonsense-mediated mRNA decay. *Nucleic Acids Res*. 2019;47(10):5293-5306

148. Plomp RG, van Lieshout MJ, Joosten KF, Wolvius EB, van der Schroeff MP, Versnel SL, Poublon RM, Mathijssen IM. Treacher collins syndrome: A systematic review of evidence-based treatment and recommendations. Plast Reconstr Surg. 2016 Jan 1;137(1):191–204.

149. Puente XS, Quesada V, Osorio FG, Cabanillas R, Cadiñanos J, Fraile JM, Ordóñez GR, Puente DA, Gutiérrez-Fernández A, Fanjul-Fernández M, Lévy N, Freije JM, López-Otín C. Exome sequencing and functional analysis identifies BANF1 mutation as the cause of a hereditary progeroid syndrome. Am J Hum Genet. 2011 May 13;88(5):650–6.

150. Puffenberger EG, Jinks RN, Sougnez C, Cibulskis K, Willert RA, Achilly NP, Cassidy RP, Fiorentini CJ, Heiken KF, Lawrence JJ, Mahoney MH, Miller CJ, Nair DT, Politi KA, Worcester KN, Setton RA, Dipiazza R, Sherman EA, Eastman JT,

Francklyn C, Robey-Bond S, Rider NL, Gabriel S, Morton DH, Strauss KA. Genetic mapping and exome sequencing identify variants associated with five novel diseases. PLoS One. 2012 Jan 17;7(1).

151. Ramanathan N, Tan E, Loh LJ, Soh BS, Yap WN. Tocotrienol is a cardioprotective agent against ageing-associated cardiovascular disease and its associated morbidities. Vol. 15, Nutrition and Metabolism. BioMed Central Ltd.; 2018.

152. Reza, H. M., Saleh, R., Jain, P., Rahman, G., & Bepari, A. K. (2020). C-MAF Expression in Adult Human Ocular Surface and its Implication in Pterygium Pathogenesis. *Reports of biochemistry & molecular biology*, *8*(4), 419–423.

153. Rivera-Torres J, Acín-Perez R, Cabezas-Sánchez P, Osorio FG, Gonzalez-Gómez C, Megias D, Cámara C, López-Otín C, Enríquez JA, Luque-García JL, Andrés V. Identification of mitochondrial dysfunction in Hutchinson-Gilford progeria syndrome through use of stable isotope labeling with amino acids in cell culture. J Proteomics. 2013 Oct 8;91:466–77.

154. Robinson P, Krawitz P, Mundlos S. Strategies for exome and genome sequence data analysis in disease-gene discovery projects. Clin Genet. 2011;80(2):127–32.

155. Romero-Bueno, de la Cruz Ruiz, Artal-Sanz, Askjaer, Dobrzynska. Nuclear Organization in Stress and Aging. Cells. 2019 Jul 1;8(7):664.

156. Ruzzi L, Pas H, Posteraro P, Mazzanti C, Didona B, Owaribe K, Meneguzzi G, Zambruno G, Castiglia D, D'Alessio M. A homozygous nonsense mutation in type XVII collagen gene (COL17A1) uncovers an alternatively spliced mRNA accounting for an unusually mild form of non-Herlitz junctional epidermolysis bullosa. J Invest Dermatol. 2001;116(1):182–7.

157. Salminen A, Kaarniranta K, Kauppinen A. Age-related changes in AMPK activation: Role for AMPK phosphatases and inhibitory phosphorylation by upstream signaling pathways. Vol. 28, Ageing Research Reviews. Elsevier Ireland Ltd; 2016. p. 15–26.

158. Scaffidi P, Misteli T. Lamin A-dependent misregulation of adult stem cells associated with accelerated ageing. Nat Cell Biol. 2008;10(4):452–9.

159. Scheibye-Knudsen M, Mitchell SJ, Fang EF, Iyama T, Ward T, Wang J, Dunn CA, Singh N, Veith S, Hasan-Olive MM, Mangerich A, Wilson MA, Mattson MP, Bergersen LH, Cogger VC, Warren A, Le Couteur DG, Moaddel R, Wilson DM 3rd, Croteau DL, de Cabo R, Bohr VA. A high-fat diet and NAD+ activate sirt1 to rescue premature aging in cockayne syndrome. Cell Metab. 2014 Nov 4;20(5):840–55.

160. Scherrer FW, Spingola M. A subset of Mer1p-dependent introns requires Bud13p for splicing activation and nuclear retention. RNA. 2006;12(7):1361–72.

161. Schmid F, Glaus E, Cremers FPM, Kloeckener-Gruissem B, Berger W, Neidhardt J. Mutation- and tissue-specific alterations of RPGR transcripts. Investig Ophthalmol Vis Sci. 2010 Mar;51(3):1628–35.

161. Schmidlin T, Kaeberlein M, Kudlow BA, MacKay V, Lockshon D, Kennedy BK. Single-gene deletions that restore mating competence to diploid yeast. FEMS Yeast Res. 2008 Mar;8(2):276–86.

162. Schneider C, Agafonov DE, Schmitzová J, Hartmuth K, Fabrizio P, Lührmann R. Dynamic Contacts of U2, RES, Cwc25, Prp8 and Prp45 Proteins with the Pre-mRNA Branch-Site and 3' Splice Site during Catalytic Activation and Step 1 Catalysis in Yeast Spliceosomes. PLoS Genet. 2015;11(9).

163. Schwarz JM, Rödelsperger C, Schuelke M, Seelow D. MutationTaster evaluates disease-causing potential of sequence alterations. [Internet]. Vol. 7, Nature methods. 2010. p. 575–6. Available from: http://dx.doi.org/10.1038/nmeth0810-575

164. Sharma S, Langhendries JL, Watzinger P, Kotter P, Entian KD, Lafontaine DLJ. Yeast Kre33 and human NAT10 are conserved 18S rRNA cytosine acetyltransferases that modify tRNAs assisted by the adaptor Tan1/THUMPD1. Nucleic Acids Res. 2015 Feb 27;43(4):2242–58.

165. Shaw AC, Joshi S, Greenwood H, Panda A, Lord JM. Aging of the innate immune system. Vol. 22, Current Opinion in Immunology. 2010. p. 507–13.

166. Sherr CJ, Roberts JM. CDK inhibitors: Positive and negative regulators of G1-phase progression. Vol. 13, Genes and Development. Cold Spring Harbor Laboratory Press; 1999. p. 1501–12.

167. Si N, Song Z, Meng X, Li X, Xiao W, Zhang X. A novel MAF missense mutation leads to congenital nuclear cataract by impacting the transactivation of crystallin and noncrystallin genes. Gene. 2019 Apr 15;692:113–8.

168. Sievers F, Wilm A, Dineen D, Gibson TJ, Karplus K, Li W, Lopez R, McWilliam H, Remmert M, Söding J, Thompson JD, Higgins DG. Fast, scalable generation of high-quality protein multiple sequence alignments using Clustal Omega. Mol Syst Biol. 2011;7.

169. Sossi V, Giuli A, Vitali T, Tiziano F, Mirabella M, Antonelli A, Neri G, Brahe C. Premature termination mutations in exon 3 of the SMN1 gene are associated with exon skipping and a relatively mild SMA phenotype. Eur J Hum Genet. 2001;9(2):113–20.

170. Spang A. Retrograde traffic from the golgi to the endoplasmic reticulum. Cold Spring Harb Perspect Biol. 2013 Jun;5(6).

171. Spingola M, Armisen J, Ares M. Mer1p is a modular splicing factor whose function depends on the conserved U2 snRNP protein Snu17p. Nucleic Acids Res. 2004;32(3):1242–50.

172. Spitz F, Herkenne C, Morris MA, Duboule D. Inversion-induced disruption of the Hoxd cluster leads to the partition of regulatory landscapes. Nat Genet. 2005 Aug;37(8):889–93.

173. Sprenger S, Yumlu geborene, Kurreck J, Uwe Kornak T-B, Roland Lauster M, Leif-Alexander Garbe T-B. The Role of in the Pathomechanism of Autosomal Recessive Cutis Laxa Pycr1. 2014;

174. Sterne-Weiler T, Sanford JR. Exon identity crisis: Disease-causing mutations that disrupt the splicing code. Vol. 15, Genome Biology. 2014.

175. Sundararaman B, Zhan L, Blue SM, et al. Resources for the Comprehensive Discovery of Functional RNA Elements. *Mol Cell*. 2016;61(6):903-913

176. Szilard L. ON THE NATURE OF THE AGING PROCESS. Proc Natl Acad Sci. 1959 Jan 1;45(1):30–45.

177. Szklarczyk D, Gable AL, Lyon D, Junge A, Wyder S, Huerta-Cepas J, Simonovic M, Doncheva NT, Morris JH, Bork P, Jensen LJ, Mering CV. STRING v11: Protein-protein association networks with increased coverage, supporting functional discovery in genome-wide experimental datasets. Nucleic Acids Res. 2019 Jan 8;47(D1):D607–13.

178. Takahara K, Schwarze U, Imamura Y, Hoffman GG, Toriello H, Smith LT, Byers PH, Greenspan DS. Order of intron removal influences multiple splice outcomes, including a two-exon skip, in a COL5A1 acceptor-site mutation that results in abnormal pro-α1(V) N-propeptides and Ehlers-Danlos syndrome type I. Am J Hum Genet. 2002;71(3):451–65.

179. Tazi J, Bakkour N, Stamm S. Alternative splicing and disease. Vol. 1792, Biochimica et Biophysica Acta - Molecular Basis of Disease. 2009. p. 14–26.

180. Teslovich TM, Musunuru K, Smith AV, Edmondson AC, Stylianou IM, Koseki M, Pirruccello JP, Ripatti S, Chasman DI, Willer CJ, Johansen CT, Fouchier SW, Isaacs A, Peloso GM, Barbalic M, Ricketts SL, Bis JC, Aulchenko YS, Thorleifsson G, Feitosa MF, Chambers J, Orho-Melander M, Melander O, Johnson T, Li X, Guo X, Li M, Shin Cho Y, Jin Go M, Jin Kim Y, Lee JY, Park T, Kim K, Sim X, Twee-Hee Ong R, Croteau-Chonka DC, Lange LA, Smith JD, Song K, Hua Zhao J, Yuan X, Luan J, Lamina C, Ziegler A, Zhang W, Zee RY, Wright AF, Witteman JC, Wilson JF, Willemsen G, Wichmann HE, Whitfield JB, Waterworth DM, Wareham NJ, Waeber G, Vollenweider P, Voight BF, Vitart V, Uitterlinden AG, Uda M, Tuomilehto J, Thompson JR, Tanaka T, Surakka I, Stringham HM, Spector TD, Soranzo N, Smit JH, Sinisalo J, Silander K, Sijbrands EJ, Scuteri A, Scott J, Schlessinger D, Sanna S, Salomaa V, Saharinen J, Sabatti C, Ruokonen A, Rudan I, Rose LM, Roberts R, Rieder M, Psaty BM, Pramstaller PP, Pichler I, Perola M, Penninx BW, Pedersen NL, Pattaro C, Parker AN, Pare G, Oostra BA, O'Donnell CJ, Nieminen

MS, Nickerson DA, Montgomery GW, Meitinger T, McPherson R, McCarthy MI, McArdle W, Masson D, Martin NG, Marroni F, Mangino M, Magnusson PK, Lucas G, Luben R, Loos RJ, Lokki ML, Lettre G, Langenberg C, Launer LJ, Lakatta EG, Laaksonen R, Kyvik KO, Kronenberg F, König IR, Khaw KT, Kaprio J, Kaplan LM, Johansson A, Jarvelin MR, Janssens AC, Ingelsson E, Igl W, Kees Hovingh G, Hottenga JJ, Hofman A, Hicks AA, Hengstenberg C, Heid IM, Hayward C, Havulinna AS, Hastie ND, Harris TB, Haritunians T, Hall AS, Gyllensten U, Guiducci C, Groop LC, Gonzalez E, Gieger C, Freimer NB, Ferrucci L, Erdmann J, Elliott P, Ejebe KG, Döring A, Dominiczak AF, Demissie S, Deloukas P, de Geus EJ, de Faire U, Crawford G, Collins FS, Chen YD, Caulfield MJ, Campbell H, Burtt NP, Bonnycastle LL, Boomsma DI, Boekholdt SM, Bergman RN, Barroso I, Bandinelli S, Ballantyne CM, Assimes TL, Quertermous T, Altshuler D, Seielstad M, Wong TY, Tai ES, Feranil AB, Kuzawa CW, Adair LS, Taylor HA Jr, Borecki IB, Gabriel SB, Wilson JG, Holm H, Thorsteinsdottir U, Gudnason V, Krauss RM, Mohlke KL, Ordovas JM, Munroe PB, Kooner JS, Tall AR, Hegele RA, Kastelein JJ, Schadt EE, Rotter JI, Boerwinkle E, Strachan DP, Mooser V, Stefansson K, Reilly MP, Samani NJ, Schunkert H, Cupples LA, Sandhu MS, Ridker PM, Rader DJ, van Duijn CM, Peltonen L, Abecasis GR, Boehnke M, Kathiresan S. Biological, clinical and population relevance of 95 loci for blood lipids. Nature. 2010 Aug 5;466(7307):707–13.

181. Truebestein L, Leonard TA. Coiled-coils: The long and short of it. BioEssays. 2016 Sep 1;38(9):903–16.

182. Tuo S, Nakashima K, Pringle JR. Apparent Defect in Yeast Bud-Site Selection Due to a Specific Failure to Splice the Pre-mRNA of a Regulator of Cell-Type-Specific Transcription. PLoS One. 2012 Oct 31;7(10).

183. Uccelli A, Moretta L, Pistoia V. Mesenchymal stem cells in health and disease. Nat Rev Immunol. 2008 Sep;8(9):726-36

184. Vaclavik V, Gaillard MC, Tiab L, Schorderet DF, Munier FL. Variable phenotypic expressivity in a Swiss family with autosomal dominant retinitis pigmentosa due to a T494M mutation in the PRPF3 gene. Mol Vis. 2010; 16:467–75.

185. Van Nostrand EL, Pratt GA, Shishkin AA, Gelboin-Burkhart C, Fang MY, Sundararaman B, Blue SM, Nguyen TB, Surka C, Elkins K, Stanton R, Rigo F, Guttman M, Yeo GW. Robust transcriptome-wide discovery of RNA-binding protein binding sites with enhanced CLIP (eCLIP). Nat Methods. 2016 Jun 1;13(6):508–14.

186. Vijg J, Suh Y. Genome Instability and Aging. Annu Rev Physiol. 2013 Feb 10;75(1):645–68.

187. Viña J, Borrás C, Miquel J. Theories of ageing. In: IUBMB Life. 2007. p. 249–54.

188. Wang H, Yang H, Shivalila CS, Dawlaty MM, Cheng AW, Zhang F, Jaenisch R. One-step generation of mice carrying mutations in multiple genes by CRISPR/cas-mediated genome engineering. Cell. 2013 May 9;153(4):910–8.

189. Wang R, Yoshida K, Toki T, Sawada T, Uechi T, Okuno Y, Sato-Otsubo A, Kudo K, Kamimaki I, Kanezaki R, Shiraishi Y, Chiba K, Tanaka H, Terui K, Sato T, Iribe Y, Ohga S, Kuramitsu M, Hamaguchi I, Ohara A, Hara J, Goi K, Matsubara K, Koike K, Ishiguro A, Okamoto Y, Watanabe K, Kanno H, Kojima S, Miyano S, Kenmochi N, Ogawa S, Ito E. Loss of function mutations in RPL27 and RPS27 identified by whole-exome sequencing in Diamond-Blackfan anaemia. Br J Haematol. 2015 Mar;168(6):854-64

190. Weyemi U, Paul BD, Bhattacharya D, Malla AP, Boufraqech M, Harraz MM, Bonner WM, Snyder SH. Histone H2AX promotes neuronal health by controlling mitochondrial homeostasis. Proc Natl Acad Sci U S A. 2019 Apr 9;116(15):7471–6.

191. Weyemi U, Paul BD, Snowman AM, Jailwala P, Nussenzweig A, Bonner WM, Snyder SH. Histone H2AX deficiency causes neurobehavioral deficits and impaired redox homeostasis. Nat Commun. 2018 Dec 1;9(1).

192. Will CL, Lührmann R. Spliceosomal UsnRNP biogenesis, structure and function. Vol. 13, Current Opinion in Cell Biology. Elsevier Ltd; 2001. p. 290–301.

193. Wood AM, Rendtlew Danielsen JM, Lucas CA, Rice EL, Scalzo D, Shimi T, Goldman RD, Smith ED, Le Beau MM, Kosak ST. TRF2 and lamin A/C interact to facilitate the functional organization of chromosome ends. Nat Commun. 2014;5.

194. Yang Z, Klionsky DJ. Eaten alive: A history of macroautophagy. Vol. 12, Nature Cell Biology. Nature Publishing Group; 2010. p. 814–22.

195. Young SG, Meta M, Yang SH, Fong LG. Prelamin A farnesylation and progeroid syndromes. Vol. 281, Journal of Biological Chemistry. 2006. p. 39741–5.

196. Zealy RW, Wrenn SP, Davila S, Min KW, Yoon JH. microRNA-binding proteins: specificity and function. Wiley Interdiscip Rev RNA. 2017 Sep 1;8(5).

197. Zemojtel T, Köhler S, Mackenroth L, Jäger M, Hecht J, Krawitz P, Graul-Neumann L, Doelken S, Ehmke N, Spielmann M, Oien NC, Schweiger MR, Krüger U, Frommer G, Fischer B, Kornak U, Flöttmann R, Ardeshirdavani A, Moreau Y, Lewis SE, Haendel M, Smedley D, Horn D, Mundlos S, Robinson PN. Effective diagnosis of genetic disease by computational phenotype analysis of the disease-associated genome. Sci Transl Med. 2014;6(252):252ra123.

198. Zhang L, You Y, Wu Y, Zhang Y, Wang M, Song Y, Liu X, Kou C. Association of BUD13 polymorphisms with metabolic syndrome in Chinese population: A case-control study. Lipids Health Dis. 2017 Jun 28;16(1).

199. Zhang X, Yan C, Zhan X, Li L, Lei J, Shi Y. Structure of the human activated spliceosome in three conformational states. Cell Res. 2018 Mar 1;28(3):307–22.

200. Zhou Y, Chen C, Johansson MJO. The pre-mRNA retention and splicing complex controls tRNA maturation by promoting TAN1 expression. Nucleic Acids Res. 2013 Jun;41(11):5669–78.

201. Zhou Y, Johansson MJO. The pre-mRNA retention and splicing complex controls expression of the Mediator subunit Med20. RNA Biol. 2017 Oct 3;14(10):1411–7.

Statutory Declaration

“I, Namrata Saha, by personally signing this document in lieu of an oath, hereby affirm that I prepared the submitted dissertation on the topic ‘’A recurrent homozygous mutation affects the *BUD13* gene whose residual expression correlates with the severity of a novel human progeroid disorder’’, independently and without the support of third parties, and that I used no other sources and aids than those stated.

All parts which are based on the publications or presentations of other authors, either in letter or in spirit, are specified as such in accordance with the citing guidelines. The sections on methodology (in particular regarding practical work, laboratory regulations, statistical processing) and results (in particular regarding figures, charts and tables) are exclusively my responsibility.

My contributions to any publications to this dissertation correspond to those stated in the below joint declaration made together with the supervisor. All publications created within the scope of the dissertation comply with the guidelines of the ICMJE (International Committee of Medical Journal Editors; www.icmje.org) on authorship. In addition, I declare that I am aware of the regulations of Charité – Universitätsmedizin Berlin on ensuring good scientific practice and that I commit to comply with these regulations.

The significance of this statutory declaration and the consequences of a false statutory declaration under criminal law (Sections 156, 161 of the German Criminal Code) are known to me.”

Date Signature

Declaration of your own contribution to any publications

Namrata Saha contributed the following publication as a part of conference appearances as poster/ talk-

Namrata Saha, Björn Fischer- Zirnsak, Boris Keren, Michael Thelen,Mohammed Al-Bughaili, Claire Schlack, Ulrike Krüger, Jochen Hecht, Malte Spielmann ,Lionel Van Maldergem, Christel Depienne, Uwe Kornak.*Corrective alternative splicing events in a novel segmental progeroid disorder.*

The conferences are listed as follows:

I. EMBO Young Scientists' Forum, September 1-2, 2016 in Lisbon, Portugal.
II. BSRT symposium 2016- Regenerate me if you can! Foster success in compromised regenerative processes, November 30-December 2, 2016 in Berlin, Germany.
III. MaxNetAging Conference 2017 Longevity: Future, Present, Past and across the Tree of Life May 16-19, 2017 in Rostock, Germany.
IV. 6th Sardinian International Summer School-From GWAS to function, June 12-16, 2017, Italy.
V. EMBO Conference- Protein Synthesis and Translational Control, September 6-9, 2017, Heidelberg, Germany.
VI. BSRT symposium 2017- Recognize, Repair, Regrow- Personalized biomedicine rises, November 29- December 1, 2017 in Berlin, Germany.

Detailed statement of contributions

Namrata Saha designed and executed the molecular genetic experiments and cellular assays. Björn Fischer-Zirnsak, Michael Thelen, and Claire Schlack contributed towards functional experiments. Mohammed Al-Bughaili carried out sequencing experiments. RNA-seq and associated analysis was carried out by Ulrike Krüger and Jochen Hecht. Exome sequencing was independently performed by Björn Fischer-Zirnsak in Berlin and by Boris Keren in Paris. The generation of the CRISPR/Cas9 mutant for the murine model was performed by Malte Spielmann. Namrata Saha and Björn Fischer-Zirnsak carried out the mouse work. Uwe Kornak, Christel Depienne Lionel van Maldergem and Björn Fischer-Zirnsak designed the study.

Signature, date and stamp of supervising university professor / lecturer

Signature of doctoral candidate

My curriculum vitae does not appear in the electronic version of my paper for reasons of data protection

List of Publications

1. Ehmke N, Graul-Neumann L, Smorag L, Koenig R, Segebrecht L, Magoulas P, Scaglia F, Kilic E, Hennig AF, Adolphs N, Saha N, Fauler B, Kalscheuer VM, Hennig F, Altmüller J, Netzer C, Thiele H, Nürnberg P, Yigit G, Jäger M, Hecht J, Krüger U, Mielke T, Krawitz PM, Horn D, Schuelke M, Mundlos S, Bacino CA, Bonnen PE, Wollnik B, Fischer-Zirnsak B, Kornak U. **De Novo Mutations in SLC25A24 Cause a Craniosynostosis Syndrome with Hypertrichosis, Progeroid Appearance, and Mitochondrial Dysfunction**. Am J Hum Genet. 2017; 101(5),833-843

2. Fischer-Zirnsak B, Koenig R, Alisch F, Güneş N, Hausser I, Saha N, Beck-Woedl S, Haack TB, Thiel C, Kamrath C, Tüysüz B, Henning S, Mundlos S, Hoffmann K, Horn D, Kornak U. **SOPH syndrome in three affected individuals showing similarities with progeroid cutis laxa conditions in early infancy**. J Hum Genet. 2019;64(7), 609-616.

3. Conference presentations-
   Namrata Saha, Björn Fischer- Zirnsak, Boris Keren, Michael Thelen, Mohammed Al-Bughaili, Claire Schlack, Ulrike Krüger, Jochen Hecht, Malte Spielmann , Lionel Van Maldergem, Christel Depienne, Uwe Kornak. **Corrective alternative splicing events in a novel segmental progeroid disorder.**

Acknowledgements

The work presented in this PhD thesis has been carried out in two institutes as a part of two working groups- AG Kornak at the Institute of Medical and Human Genetics at the Charité – Universitätsmedizin Berlin and FG Mundlos at the Development and Disease group of the Max Planck Institute for Molecular Genetics (MPIMG) in Berlin. I attempt here in utmost sincerity to extend my gratitude to each individual and organisation that has been a part of my exciting journey.

I would first like to begin by thanking the very novel graduate program, MaxNetAging of the Max Planck Institute of Demographic Research (MPIDR) for having presented me with the opportunity to carry out my work in some state of the art laboratories at the Charité and MPIMG. I thank profusely Prof. James Vaupel, Dr.Andre Schmandke, Dr.Beatrice Michaelis, Dr.Jutta Gampe and Ms.Annett Doepke for their immense support and understanding beginning right from my time in Rostock in early 2015. The network introduced me to an incredible mix of individuals from various streams pursuing ageing research and provided me the first hand interdisciplinary training in the domain of ageing. In addition, the program and its coordinators took utmost care to help me with all bureaucratic and other essential tasks that I needed to carry out upon my arrival in Germany. I am also thankful to the staff at the MPIDR for the same.

This directly needs to be followed up by thanking my working group of AG Kornak at the Charité where I carried out most of my research. I am immensely thankful to Prof. Dr.Uwe Kornak for having presented me with an opportunity to step into and specialise under his guidance in the field of human progeroid disorders. His knowledge and body of work in the field has been inspirational and encouraged me to develop and appreciate the undying efforts to understand rare progeroid disorders. The discussions with him helped me formulate and chase various hypotheses in understanding the rather complex disease. I am also grateful to my laboratory mentor, Dr. Björn Fischer- Zirnsak for helping me with his constant input and suggestions in tackling laboratory experiments. I am especially indebted to him for being extremely patient with me even when I made the silliest mistakes with his constant reminder that ‘‘We all made such mistakes‘‘ or his ever encouraging demeanour that came along with ‘‘Keep smiling‘‘. I am thankful to Dr.-Ing Sven Geissler for his valuable comments and suggestions in various mentoring committee meetings. I am thankful to all the physicians involved from France and Portugal

who have been involved in the project and have been very spontaneous in responding to all our queries and needs for patient data/ material. My lab mates, including, Miguel Rodriguez, Naji Choubassi, Michael Thelen, Guido Vogt, Uta Roessler, Floriane Henning, Alexej Knaus and Daniela Mau deserve a special applaud for being such wonderful and helpful co-workers, Miguel and Naji especially with their contributions towards my project. I must mention here Miguel Rodriguez for also being a wonderful and patient friend in the lab who probably has made me laugh every single day, thanks to his great sense of humour. His constant presence and lunch discussions were something I always looked forward to and he made work throughly enjoyable for me. I am grateful, additionally, to Gabriele Hilderbrand, Sussane Rothe, Anja Lekaj and Carola Dietrich for their wonderful technical assistance, Gabriele or Gaby especially for always patiently dealing with my incorrect sample sheets for Sanger sequencing. I am also thankful to the members of FG Mundlos, the mouse facility, the proteomics core facility and the confocal and electron microscopy facilities at the MPIMG for helping us organise the mouse work and imaging experiments.

My graduate school, the Berlin-Brandenburg School for Regenerative Therapies or the BSRT has been a supportive and great school to be affiliated to for my PhD thesis. The school with its numerous events and courses enabled me to gain various other additional skills in addition to my research. I am thankful to Dr. Sabine Bartosch and Bianca Kuhn for their support and kind understanding.

Towards the end, I must mention my friends, Shreemoyee, Sebastian, Ugo, Giulia, Suvarsha, Jitin, Arunima, Menemsha, Fiete, Edoardo, and Nupur for always being there for me. I am also greatly indebted to Gokul Mahadev for being there with me as my best friend and making my PhD journey wonderful with his delightful presence and super delicious, mouth-watering biryanis.

Last but definitely not the least, I am very lucky to have such a wonderful and supportive family that has constantly given me the strength to deal with all kinds of adversities. Their constant love and support has been instrumental to help me achieve my goals and to keep going no matter what. I am thankful to my parents, Mr. Ashit Saha and Mrs.Anjana Saha, and my siblings/ mentors- Marco and especially my sister Amrita for inspiring me to strive for my own PhD degree. This journey would have not been possible without their constant support and encouragement.